

THE ATMOSPHERIC ELECTRIC FIELD  
AND ITS MEASUREMENTS

CENTRE FOR NEWFOUNDLAND STUDIES

**TOTAL OF 10 PAGES ONLY  
MAY BE XEROXED**

(Without Author's Permission)

MURDO MURRAY



182740

C.1








THE ATMOSPHERIC ELECTRIC FIELD  
AND ITS MEASUREMENT

by

 Murdo Murray

Submitted in partial fulfilment  
of the requirements for the degree of Master of Science  
Memorial University of Newfoundland

March, 1969.

## ACKNOWLEDGEMENTS

I wish to express my thanks to the following people who have helped in the course of the work described in this thesis.

My supervisor, T. C. Noel, who introduced me to the subject.

Dr. S. W. Breckon, whose continuous encouragement made the completion of this thesis possible. I am also indebted to him for providing the facilities required during the progress of this investigation.

Mr. P. D. P. Smith for numerous discussions regarding the electronic design, and helpful suggestions during all phases of the work.

Mr. W. Gordon of the University's Technical Services Department for the mechanical construction of the instrument.

Mr. T. White of the Physics Department for mechanical modifications and willingness to assist on numerous occasions.

Mr. E. M. Kenny, Instrument Technician, for assistance in the final assembly and testing of the electronic circuits and for many useful suggestions.

The author also wishes to thank:

W. J. Higgins for assistance in the photographic work.

R. Tucker for drawings.

Also, Miss D. Janes for her patience in the typing of the thesis.

I also wish to express my gratitude to Memorial University of Newfoundland for providing financial assistance in the form of a teaching fellowship.

Also to the Provincial Government for providing a graduate fellowship.

## ABSTRACT

The variables encountered in atmospheric electricity are discussed and the theoretical model as proposed by Kawano developed to show that the vertical distribution of the air resistivity is influenced by the eddy diffusion. Using this vertical distribution, the local characteristic of the electric field is derived. Instrumentation for the measurement of the electrical potential gradient was developed and subsequently a series of observations was conducted to measure the electrical phenomena associated with various conditions in the atmosphere. The response time of the instrument is about one millisecond. The use of 30 dB of negative feedback in the main amplifier ensured a stable output with a low noise level. Indication of the polarity of the field was provided by employing a phase sensitive detector.



## PREFACE

This thesis represents the first series of observations and measurements conducted in the field of atmospheric electricity research at the university. An attempt has therefore been made to assess the present state of knowledge in the field. The first chapter is devoted to a review of the historical development, and outlines the earliest theories proposed. The subsequent two chapters deal with the type and quantity of ionized particles existing in the lower layer of the atmosphere and the variable electrical parameters. Recently, the observation of the short-term perturbations of the electric field has received some attention in the literature and it was considered relevant to devote chapter 4 to this effect. Chapter 5 outlines the recent measurements both at the earth's surface and the variations of the electric field with altitude. The author has taken the liberty of drawing freely upon the observations and conclusions arrived at by many workers in their respective fields of investigation.

The mechanical and electronic development of instrumentation designed for the measurement of the atmospheric electric field and the method of utilization is fully discussed in chapter 6. A method for the absolute determination of the electric field is also discussed along with its limitations and an alternative method outlined. The response of the mill to electrical disturbances in the ambient field and the diurnal variation is discussed in the final chapter.



## TABLE OF CONTENTS

CHAPTER		Page
1	HISTORICAL INTRODUCTION	1
2	THE IONIZATION OF ATMOSPHERIC PARTICLES	7
2.1	Introduction	7
2.2	Nature of Small Ions	7
2.3	Nature of Large Ions	9
2.4	Intermediate Ions	9
2.5	Results of Ion Counting	9
2.6	The Ionizing Agencies	10
2.7	The Effect of Radioactive Matter in the Earth's Crust	12
2.8	The Effect of Radioactive Matter in the Air	14
2.9	The Effect of Cosmic Rays	14
2.10	Ionic Equilibrium in the Atmosphere	15
2.11	The Conductivity of the Atmosphere	17
2.12	The Electrode Effect	20
3	THE VARIABLES OF ATMOSPHERIC ELECTRICITY	24
3.1	The Electric Field and Electric Charge in the Atmosphere	24
3.2	Atmospheric Current	31

4	THE LOCAL VARIATIONS OF THE ATMOSPHERIC ELECTRIC FIELD	34
4.1	The Effect of the Vertical Distribution of the Space Charge on the Electric Field	34
4.2	The Vertical Distribution of the Air Resistivity in the Exchange Layer	40
5	RESULTS OF PAST MEASUREMENTS AT THE EARTH'S SURFACE	44
6	EXPERIMENTAL TECHNIQUES	55
6.1	Methods of Measuring the Potential Gradient	55
6.2	The Absolute Determination of the Potential Gradient	58
6.3	The Antenna System	58
6.4	The Quadrant Electrometer	60
6.5	Theory of Operation	61
6.6	The Heterostatic Method	63
6.7	The Idiostatic Method	65
6.8	Method of Setting Up the Electrometer	65
6.9	The M-Type Potential Gradient Mill	67
6.10	Details of Construction	69
6.11	Details of Motor	70
6.12	Details of Screening Rotor Speed	70
6.13	Electrical Measurements on Output	71
6.14	Location of Measurements	71

CHAPTER	Page
6	Cont'd
6.15	Theory of Operation of Field Mill 72
6.16	The Response Time of the Field Mill 74
6.17	Data Requirements for Amplifier 77
6.18	Development and Modifications 77
6.19	The Amplifying Circuit 84
6.20	The Preamplifier 84
6.21	The Main Amplifier 91
6.22	The Phase Sensitive Detector 94
6.23	Measurement Errors 94
7	RESULTS AND DISCUSSION 96
7.1	Measurements of the Potential Gradient 96
7.2	Discussion of Results 100
7.3	The Diurnal Variation 109
	DISCUSSION OF ERRORS 110
	SUGGESTED IMPROVEMENTS 112
	APPENDIX A 114
	APPENDIX B 117
	BIBLIOGRAPHY 120

FIGURE		Page
16	The Antenna System	57
17	Quadrant Electrometer Heterostatic Curves	64
18	Quadrant Electrometer Idiostatic Curves	66
19	Mechanical Layout of Potential Gradient Mill	68
20	Response of Mill to Equal Incremental Negative Voltages Using Diode Detector	78
21	Response of Mill to Equal Incremental Positive Voltages Using Bridge Detector	79
22	Response of Mill to Residual Voltage and Equal Incremental Voltages	80
23a	Response of Mill Using Phase Sensitive Detector	82
23b	Response of Mill to Zero Signal	82
24a	Filter Circuit to Prevent Feedback from Phase Sensitive Circuit to Amplifying Circuit	83
24b	Circuit to Offset Residual Voltage	83
25	Block Diagram of Electronic Circuits	85
26	Circuit Diagram of Electronic Circuits	86
27	Equivalent Circuit of Preamplifier	89
28	Equivalent Circuit of Amplifying Stage	90
29	Phase Relationship between Signal and Reference Voltages	93
30	Potential Gradient Due to Charged Cloud	98
31	Steep, Short Duration Positive Fields During Snow Showers	99



## FIGURE

## Page

32	Gradually Increasing Positive Fields During Snow Showers	101
33	Positive and Negative Fields During Snow Showers	102
34	Negative Field During Rain Showers	103
35	Local Variations of Field During Period of High Wind Velocity	104
36	Effect of Decreasing Wind Velocity on Electric Field	105
37	Fluctuations During Snow Flurry Activity	106
38	Diurnal Variation of the Field	108

## CHAPTER 1

### HISTORICAL INTRODUCTION

The first serious study of atmospheric electricity commenced with the suggestion by Benjamin Franklin (1750) that it might be possible to obtain electricity from thunderclouds by means of a pointed conductor. Two years later, Dalibard in France and Franklin himself in Philadelphia verified this prediction. Dalibard obtained sparks from an iron rod 40 ft. high; Franklin obtained similar results with a kite whose conducting string ended in an insulating silk ribbon. Next year (1753), Franklin collected the charge from his conductors in a Leyden jar and by means of a cork ball suspended on a silk thread he was able to determine the sign of the charge. He found that "the charge from a thundercloud is nearly always negative but sometimes positive".

The interest aroused by these experiments stimulated further research and led Lemonnier in France to discover that dust particles were attracted to the insulated wire attached to the exposed conductor. Lemonnier was the first to observe that the exposed rod also appeared to be charged even during fair weather. This last result was quite unexpected and marks the birth of "fair weather" electricity. Lemonnier also experimented with other methods of collecting electricity and he was the first to use horizontal stretched wires instead of pointed conductors.

During the next twenty years, a series of systematic observations using a stretched horizontal wire led Beccaria in Italy to conclude (1775) that:

- (a) a diurnal variation existed in the fair weather field
- (b) the sign of the fair weather field was always positive.

The next step forward commenced the following year in 1776 with the technical development of new devices by de Saussure in Switzerland. He constructed the first electrometer consisting of two wires carrying balls of elder pith and suspended in a glass vessel with metal casing. This not only provided quantitative measurements but also proved to be much more sensitive than earlier methods. De Saussure also introduced the movable conductor method in which a wire was connected to the electrometer, grounded, and then raised quickly to a height of one meter or so. The electrometer responded in accordance with the electrical state of the atmosphere. His observations led to the discovery of an annual variation in the fair weather field, the field being greater in winter than in summer.

Until the end of the 18th century, it was generally accepted that the phenomenon of fair weather electricity could be explained by supposing that the air carries a positive charge which increases with height above the earth. A theory to satisfy this phenomenon was proposed by Volta in Italy. He proposed the theory that positive electricity as well as latent heat was released when water vapour condensed; this would also impart a negative charge to the earth.



A completely new interpretation was provided by Erman in Germany in 1804. He put forward the theory that the observations of the past half century could be explained by assuming a negative earth with no charge whatsoever being present in the atmosphere. Further corroboration of this theory was provided by Peltier forty years later in 1842 when he accounted for the de Saussure movable conductor method by electrical induction from a negatively charged earth.

In 1850, the investigation of atmospheric electrical phenomena was revitalized by Lord Kelvin who presented an interpretation of all known facts on the subject on the basis of electrostatics, involving, for the first time, the concept of potential. Kelvin also developed new instruments for the study of electrical phenomena and inaugurated a program of continuous recording at Kew Observatory. From these observations and others taken at various locations over the surface of the earth, it was ascertained that:

- (1) the atmosphere is electrically positive with respect to the earth.
- (2) the electric field near the earth is greater in winter than in summer.
- (3) a diurnal variation in the electric field exists at all stations.
- (4) balloon observations recorded a decrease in field intensity with altitude.
- (5) a positive space charge must exist in the lower atmosphere.



(6) the earth must have a negative charge.

The existence of an air-earth current had to await discovery until much later. As early as 1785, Coulomb had concluded that the atmosphere is not a perfect insulator. From this fact and the knowledge of the existence of a potential field, the presence of an electric current could be surmised but the low value of the current enabled it to evade detection. The first evidence for its existence is due to Linns in Germany in 1887 who observed the rate of discharge of an insulated sphere exposed to the air and, thus, showed the conductivity of the air. These observations also showed a diurnal variation.

Elster and Geitel in 1899 reported that:

- (1) the conductivity thus measured was inversely proportional to the field strength.
- (2) the conductivity is reduced by fog and smoke.
- (3) negatively charged bodies lose their charge faster than positively charged bodies.

At the beginning of the 20th century, it was generally accepted that a positive current is flowing to the earth through the conducting atmosphere due to the presence of a world-wide electric field. The problem that now presented itself was how the earth maintained its negative charge.

In 1923, K. Hoffman and S. J. Mauchly, after an examination of the Carnegie observations, independently drew attention to the fact that the variation of the electric field relative to Universal Time

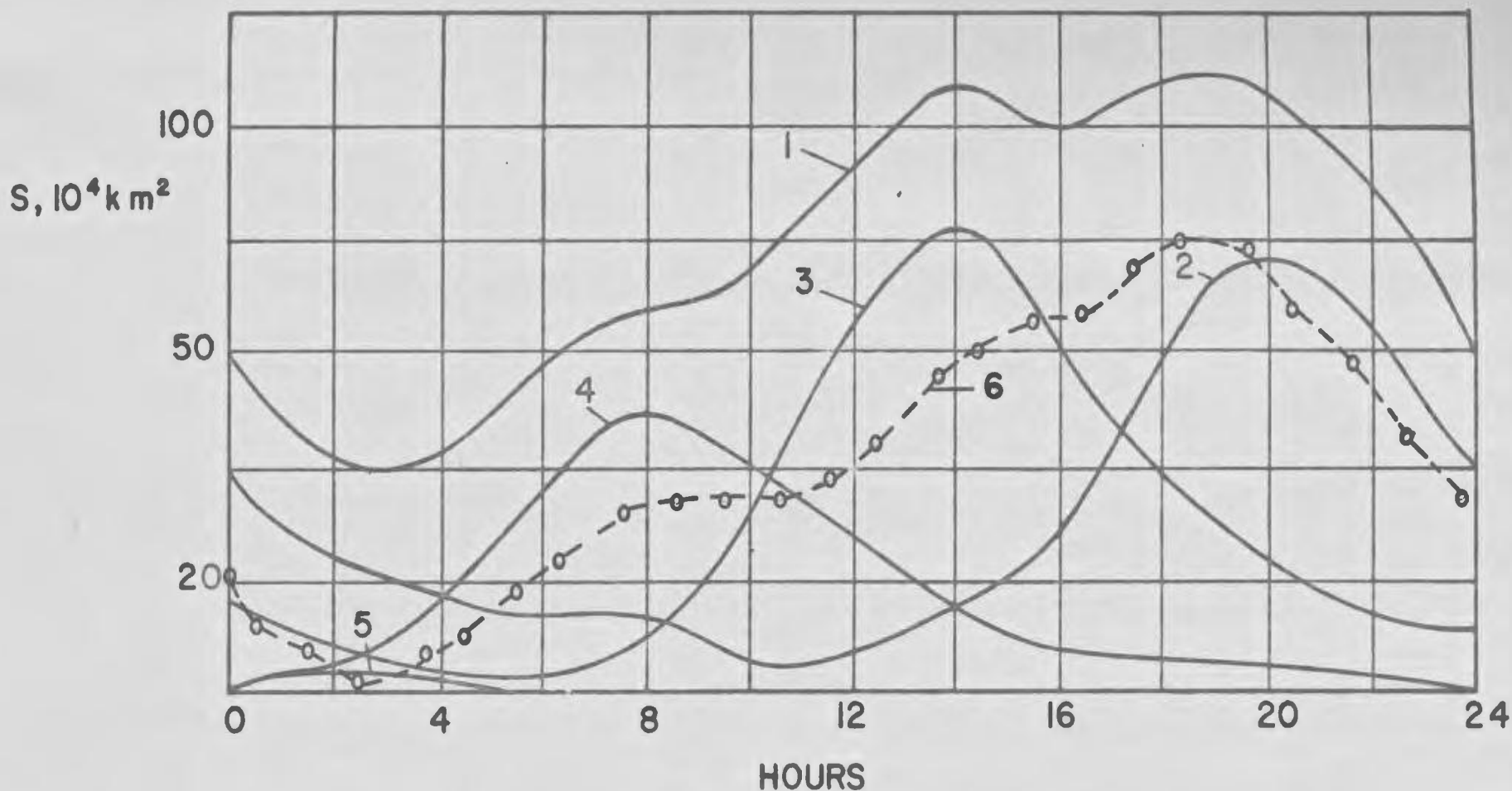


Fig. 1. DAILY COURSE OF THE AREA COVERED BY THUNDERSTORMS (WHIPPLE 1929)

- 1 — FOR THE ENTIRE EARTH'S SURFACE
- 2 — IN AMERICA
- 3 — IN AFRICA AND EUROPE
- 4 — IN ASIA AND AUSTRALIA
- 5 — IN NEW ZEALAND

6 — DIURNAL VARIATION OF POTENTIAL GRADIENT (CARNEGIE 1928-29 CRUISE)

occurred at approximately the same hour and was independent of local time. This discovery led Whipple in 1929, following a suggestion by C. T. R. Wilson, to study the association of the diurnal variation of electric potential field in fair weather with the distribution of thunderstorms over the globe. Further study carried out (1950) by O. H. Gish and G. R. Wait, who studied the flow of air-earth current above thunderstorms, supported the generally accepted theory that thunderstorms are the generators which maintain the earth's negative charge. The diurnal variation of the electric field and world-wide thunderstorm activity is shown in Fig. 1.

Between 1915 and 1920, C. T. R. Wilson was led to the conclusion, through study of the earth's charge underneath thunderclouds, that a thunderstorm cell is essentially bipolar with the base charged negatively. However, the search for the fundamental mechanism which initiates and maintains the charge separation in clouds, particularly thunderstorms, is probably the most elusive goal in the modern investigation of atmospheric electricity.

## CHAPTER 2

### IONIZATION OF ATMOSPHERIC PARTICLES

#### 2.1 Introduction

Under normal conditions, gases are among the best insulators known. From the first studies of electricity, it was known that a gold leaf electroscope or other charged body gradually loses its charge regardless of the precautions taken to insure good insulation.

Coulomb was the first to conclude that, after allowing for the charge lost by a body due to conductivity, there remained an additional loss of charge which must be attributed to leakage through the surrounding air. Later, Elster and Geitel, and Wilson, independently were led through experimental observations to conclude the existence of ions in the atmosphere, and these may be classified as follows:

- (1) small ions
- (2) intermediate ions
- (3) large ions.

In addition, the atmosphere carries uncharged particles which serve as nuclei for the initiation of condensation. These are called

- (4) Aitken or condensation nuclei.

#### 2.2 Nature of Small Ions

Through the effect of some primary ionizing agency, neutral molecules in the atmosphere are dissociated into positive ions and free electrons. In the lower atmosphere, the mean lifetime of the



electron is of the order of a few microseconds due to the fact that it combines with a neutral oxygen atom to form a negative ion. Experimental evidence derived from the study of ionic motions indicates that these ions have a very short lifetime also. Since water molecules are easily polarized, it is probable that where they exist in large numbers, they are readily attached to ionized molecules. Thus, the negative apex of the water molecule attracts positive ions and forms a cluster of molecules with a positive charge.

Similarly, the negative ions form a cluster of molecules. These small ions, which appear to consist of one single ionized molecule with other molecules clustered around it, are kept together by the charge and this is the distinguishing feature of the small ions. When an electric field is established in the air, it superimposes on the random molecular motion of the ions, a drift velocity. The average ionic drift velocity in unit field is called the mobility. Small ions have a mobility ranging from 1 to 2 cm/sec per V/cm. The mobility varies with pressure and temperature according to the equation

$$(1) \quad K(p, t) = K_o(p_o, t_o) \frac{p_o}{p} \frac{T}{T_o} \quad .$$

Under similar conditions, it is found that the negative ions have mobilities rather greater than positive ions.

When the charge is neutralized or removed, the cluster of molecules dissociates into its constituent components since it is the charge itself that is the mechanism holding the molecules together.

### 2.3 Nature of Large Ions

Whereas the small ions are not much larger than molecular size, the large ions are considerably larger. These are probably suspended particles of evaporated sea salts, dust, water or other substances mostly derived from industrial smoke. The large ions have mobilities ranging from  $3 \times 10^{-4}$  to  $8 \times 10^{-4}$ , cm/sec per v/cm. Large ions are distinguished from small ions by their tendency to remain attached after the charge has been removed.

### 2.4 Intermediate Ions

Intermediate ions have mobilities ranging from  $10^{-1}$  to  $10^{-2}$  cm/sec per v/cm. The existence of these was reported by Pollock (1915) under conditions of low humidity, and disappear at higher humidity. These were identified as particles of  $H_2SO_4$  and, consequently, are detectable near industrial areas. Condensation (Aitken) nuclei are uncharged particles and consist of water soluble substances.

### 2.5 Results of Ion Counting

The accepted normal concentration of small ions is about 100 per  $cm^3$ , though a low of 40 per  $cm^3$  and a maximum of 1500 per  $cm^3$  have been recorded.

The concentration of large ions is dependent upon the locality and varies from a minimum of 200 per  $cm^3$  to 80,000 per  $cm^3$  in the vicinity of large towns. The concentration of large ions increases at the expense of small ions, thus explaining the lower conductivity in fog and smoke as reported by Elster and Geitel in 1899.

Experimental evidence has also established the fact that the number of positive ions slightly exceeds the number of negative ions. This discrepancy may be due to

- (1) the electrode effect
- (2) the greater diffusion coefficient of negative ions.

At higher altitudes, the number of small ions per  $\text{cm}^3$  increases, values of over  $2000/\text{cm}^3$  having been found. The excess of positive ions also becomes more marked, implying an increase in conductivity. Above the austausch region, the number of large ions becomes very small.

## 2.6 The Ionizing Agencies

Three principal agencies are responsible for the ionization of the lower atmosphere. These are:

- (1) Radiation from radioactive substances in the crust of the earth.
- (2) Radiation from radioactive matter present in the air itself.
- (3) Cosmic rays.

To a lesser degree, ionization is also produced by

- (4) The photo-electric effect - effective in the higher regions of the atmosphere.
- (5) Breaking of water drops.
- (6) Lightning flashes.
- (7) Dust and snow storms.

FROM E. PIERCE:  
RECENT ADVANCES  
IN ATMOSPHERIC  
ELECTRICITY.

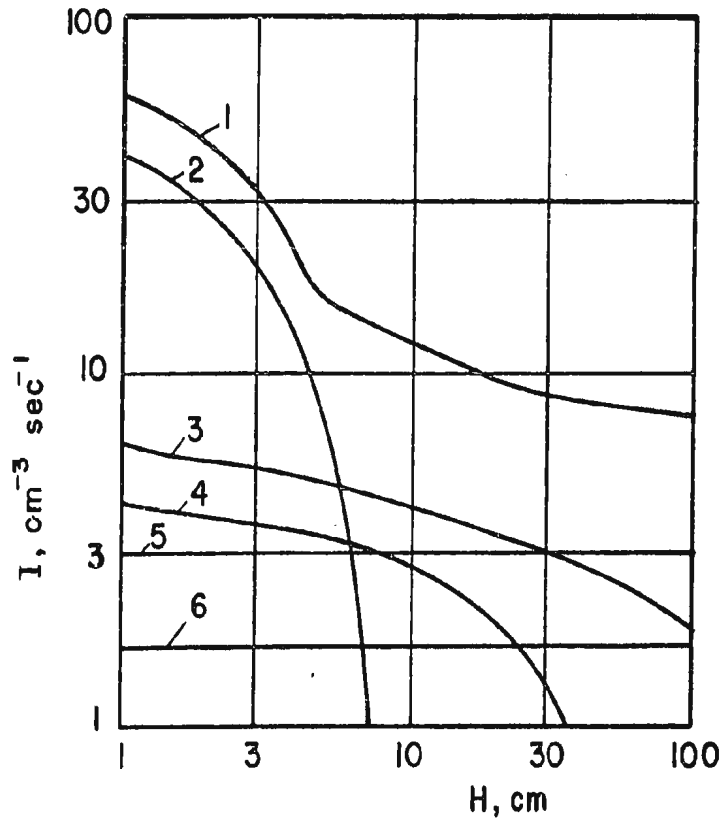


FIG. 2. CHANGE IN INTENSITY OF IONIZATION AT THE EARTH'S SURFACE WITH ALTITUDE

- 1 - Total Ionization.
- 2 - Ionization by  $\alpha$  Radiation from Earth
- 3 - " " " " " Radioactive Gases
- 4 - " " " " " Earth
- 5 - " " " " " " "
- 6 - " " " " " Cosmic Rays.



## 2.7 The Effect of Radioactive Matter in the Earth's Crust

Only in the immediate vicinity of the earth is the effect of the radioactive elements of the earth's crust of primary importance. The elements of thorium and uranium and their daughter products emit  $\alpha$ ,  $\beta$  and  $\gamma$  rays into the atmosphere. The  $\alpha$  particles are only effective for the first few cm and their contribution is consequently negligible in their effect on atmospheric ionization. The  $\beta$  rays can come from still greater depths and can penetrate to a greater height in the atmosphere.

Let  $I$  represent the number of pairs of ions produced per  $\text{cm}^3$  per sec. in air at N.T.P. Calculations based upon average values for the measured concentration of radioactive matter in the air indicate that an effect ranging from 1  $I$  at the surface to 0.1  $I$  at 10 meters is due to  $\beta$  rays from the earth.

The  $\gamma$  rays can come from still greater depths and, consequently, from a larger volume of radioactive material. The  $\gamma$  rays are estimated to produce approximately 3  $I$  at the surface, 1.5  $I$  at 150 meters and 0.3  $I$  at a height of 3 km.

More recent measurements seem to indicate that the radioactive contribution of potassium due to its high percentage in the earth's crust may contribute even more than the combined uranium-radium and thorium families. Local crustal geochemical conditions will have a controlling effect on the atmospheric ionization. The average values range from 2  $I$  to about 10  $I$ . Fig. 2 shows the effect of the various ionizing agencies with altitude.

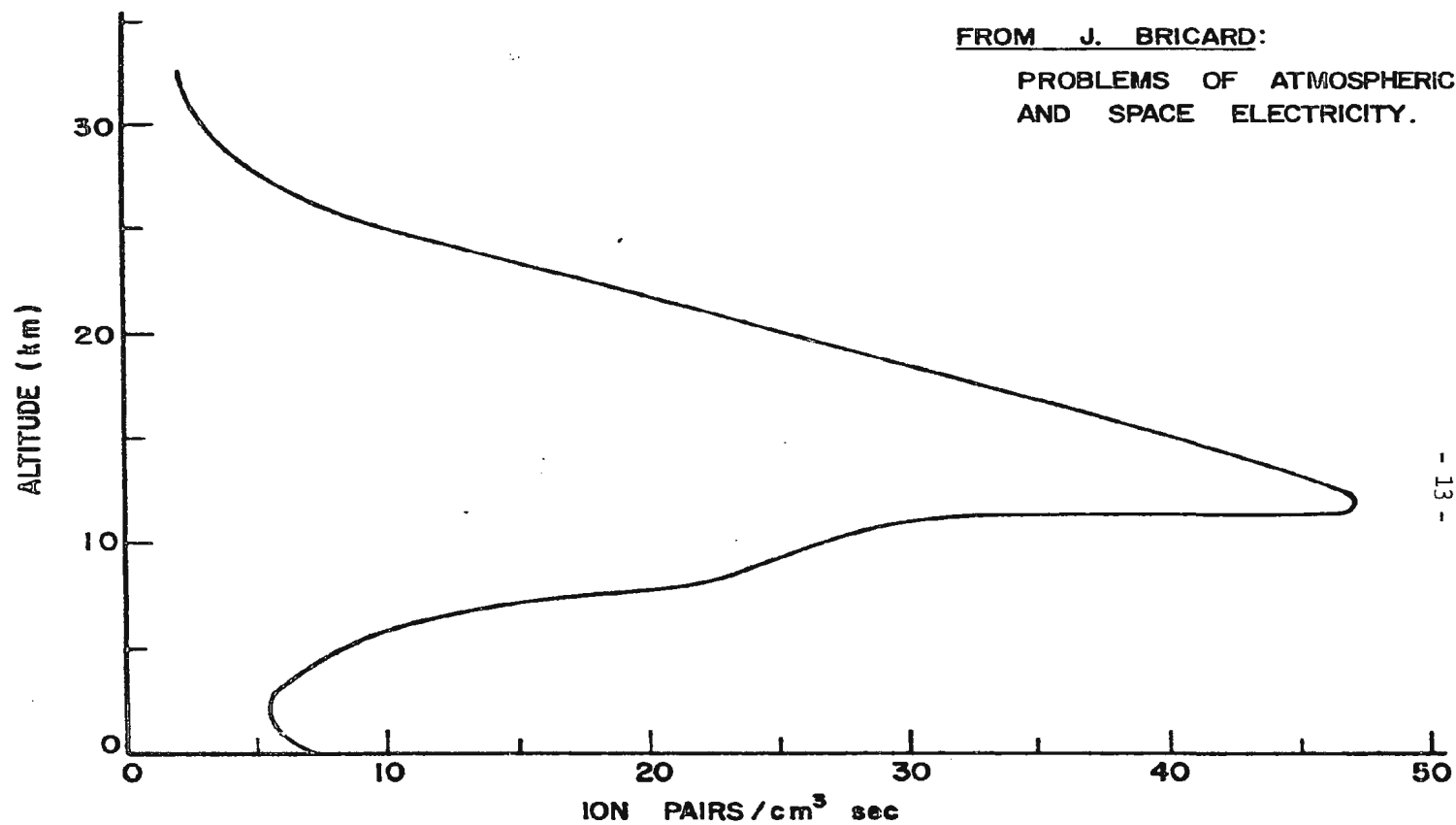


Fig. 3. INTENSITY of IONIZATION

The radioactive content of sea water is found to be very small in comparison with that of the soil and rocks, and over the oceans the earth radiation effects are negligible.

#### 2.8 The Effect of Radioactive Matter in the Air

The gases, radon and thoron, are produced in the earth's crust from the radioactive decay of radium and thorium and diffuse into the atmosphere. These gases are very effective in producing ionization due to their emission of  $\alpha$  rays which is directly incident on atmospheric particles. Estimates place the air radiation effect at 2 I in the neighbourhood of the earth's surface. The effect, like that of the earth-radiation, is extremely small over the oceans where the emanation content of the air is only about 1% of its value over land.

#### 2.9 The Effect of Cosmic Rays

Cosmic ray primaries are deflected by the earth's magnetic field so that only the most energetic reach the earth near the equator while the less energetic enter the atmosphere at higher geomagnetic latitudes. Cosmic ray ionization over both land and sea varies from about 2.0 I in high geomagnetic latitudes to about 1.5 I near magnetic equator. Over the surface of the oceans and polar regions, about 95% of the ionization is due to cosmic radiation, while most of the remaining 5% is believed due to radioactive materials of continental origin.

A graph showing intensity of ionization with altitude is shown in Fig. 3.

## 2.10 Ionic Equilibrium in the Atmosphere

The processes involving the equilibrium of ionization in the atmosphere may be summarized thus:

- (1) Production of small ions directly by radioactivity, cosmic rays and other causes.
- (2) Combination of small ions and uncharged nuclei to form large ions.
- (3) Recombination of small ions.
- (4) Combination of large ions with small ions of opposite signs.
- (5) Recombination of large ions of opposite signs.

The recombination rate of small ions is usually negligible, which is also true for the recombination rate of large ions.

The following symbols will be used in further discussion:

$n_1$  = number of small positive ions.

$n_2$  = number of small negative ions.

$N_1$  = number of large positive ions.

$N_2$  = number of large negative ions.

$N_0$  = number of uncharged nuclei.

$Z = N_0 + N_1 + N_2$  = total number of nuclei.

$q$  = rate of production of small ions.

$\alpha$  = recombination rate of small ions.

$\eta_{12}$  = recombination rate of positive small ions and negative large ions.

These symbols represent the number per unit volume.

$\eta_{21}$  = recombination rate of negative small ions and positive large ions.

$\eta_{10}$  = recombination rate of positive small ions and uncharged nuclei.

$\eta_{20}$  = recombination rate of negative small ions and uncharged nuclei.

$\gamma$  = recombination rate of large ions.

The concentration of any ion group per unit volume under equilibrium conditions depends upon a balance between their rate of formation and their rate of recombination.

Thus, for small positive ions, the ionization-recombination equation has the form

$$(2) \quad \frac{dn_1}{dt} = q - \alpha n_1 n_2 - \eta_{12} n_1 N_2 - \eta_{10} n_1 N_0$$

Analogous equations can be written for  $n_2$ ,  $N_1$ ,  $N_2$  and  $N_0$ .

In a state of equilibrium and in quiet air  $dn_1/dt = 0$ , and we have

$$(3) \quad n_1 = \frac{q}{\alpha n_2 + \eta_{12} N_2 + \eta_{10} N_0}$$

Thus, the concentration of small positive ions will decrease as the concentration of heavy ions and uncharged particles increases.

If  $\eta_{12} N_2 + \eta_{10} N_0$  is much greater than  $\alpha n_2$  and, if we assume that  $\eta_{12}$  is approximately equal to  $\eta_{10}$  and put  $N_0 + N_2 = N$ , then using



these approximations, we see that the concentration of small positive ions is inversely proportional to the non-radioactive particles in the air,

$$(4) \quad \text{i.e., } n_1 \propto N^{-1}.$$

#### 2.11 The Conductivity of the Atmosphere

The conductivity is defined as the current density produced by a unit field. If there are several groups of ions present in the air, the total current density is given by

$$(5) \quad i = \sum_r n_r e_r \omega_r E$$

where  $n_r$  = number of ions with the same charge

$e_r$  = charge on ion

$\omega_r$  = mobility of ions

$E$  = electric field.

The conductivity ( $\lambda$ ) is then given by

$$(6) \quad \lambda = \frac{i}{E} = \sum_r n_r e_r \omega_r.$$

Because of the relatively high mobilities, only the small ions make a significant contribution to atmospheric conductivity, so that we can write

$$(7) \quad \lambda = n_1 e \omega_1 + n_2 e \omega_2.$$

The two expressions on the right are called polar conductivities.

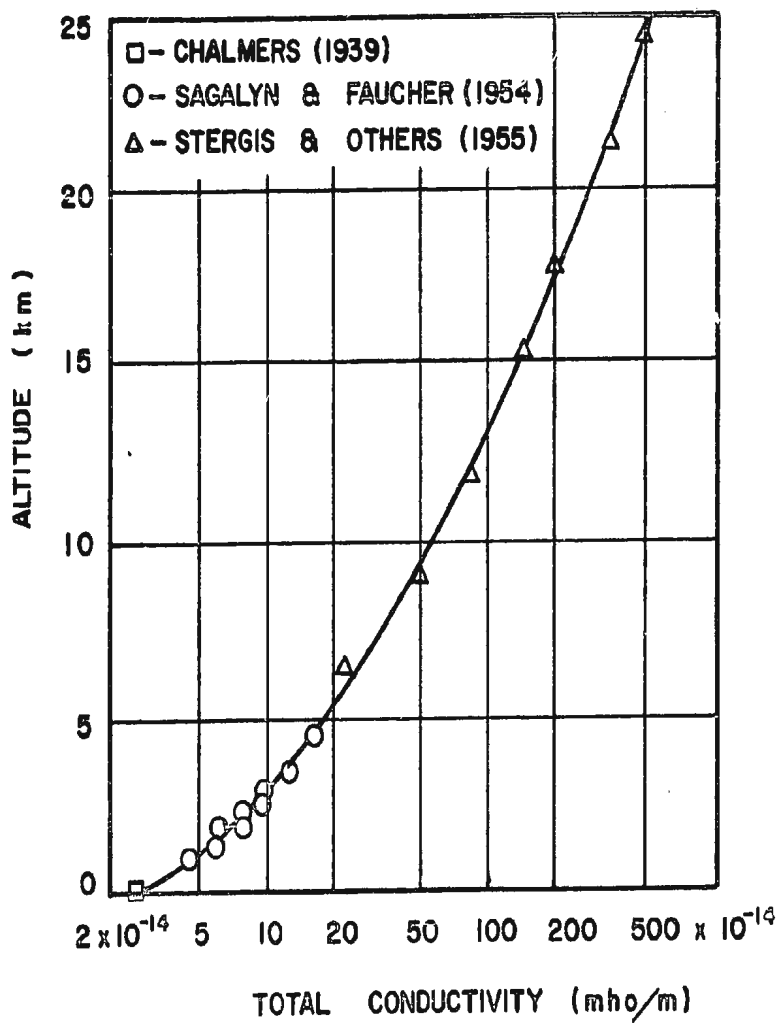


Fig. 4. ATMOSPHERIC CONDUCTIVITY VARIATION WITH ALTITUDE

The daily and annual variations of the conductivity at the earth's surface are influenced by the daily and annual variations determining the conductivity, namely the ionization intensity and the atmospheric pollution. The conductivity usually decreases during the daytime when pollution of the atmosphere increases. In northern latitudes, the conductivity decreases in the winter due to the enveloping snow cover reducing the radioactive emission from the earth. The conductivity has been found to increase nearly exponentially with increasing altitude (Fig. 4) because of a corresponding increase in cosmic ray ionization and ionic mobility, and a decrease in concentration of large nuclei with height. This explains Elster and Geitel's observation in 1899 that the conductivity of the atmosphere is reduced by fog and smoke.

The vertical conductivity profile consists of two parts:

- (1) The turbulent or austausch region where  $N$  is large and the conductivity is given by

$$(8) \quad \lambda \propto N^{-1}.$$

- (2) The region above the turbulent layer and which extends to a height of about 30 km. The conductivity in this region is a function of pressure and temperature and can be expressed by

$$(9) \quad \lambda(h) = \lambda(0) \left[ \frac{p_0}{p_h} \right]^r \left[ \frac{T_h}{T_0} \right]^s$$

where  $r = 0.5$

$s = 1.5$  are approximate values.

The existence of such an altitude variation of conductivity above the continents was investigated by Sagaly and Faucher (1954), and Stergis et al (1955). Since the solid and liquid impurities in the atmosphere usually accumulate in the turbulent region between the earth's surface and temperature inversion layers, there exists a minimum value of  $\lambda$  in this region and in consequence a maximum value of  $E$  under such inversion layers. A lower value of conductivity is observed over the oceans than over land areas in spite of a lower large ion content over the oceans. This is attributed to the greater ionization over land due to the emission of radioactive gases from the decay of radioactive decay of elements in the crust. Experiments to determine polar conductivities have also shown that the conductivity due to the negative ions exceeds that due to the positive ions. This ratio is at present accepted as being in the region

$$(10) \quad \frac{\lambda_1}{\lambda_2} = 1.05 \quad .$$

## 2.12 The Electrode Effect

In the layer of air near the surface of the earth, the positive conductivity has been found to exceed the negative conductivity by 10 to 20 per cent. In this region, the excess of positive ions over negative ions is also more pronounced. This effect is called the electrode effect.

This effect can be explained if we consider a column of air bounded at its base by a negative electrode (the earth's surface) and at its upper limit by a positive charge extending upwards. Then positive

ions can enter the lower region from above and are removed from it by transfer to the negatively charged earth. Negative ions, on the other hand, are removed from this lower region by transfer upwards and this loss is not replenished by a corresponding flow of negative ions from the earth. Thus, the layer of air next to the earth's surface is depleted in negative ions, thus acquiring a positive space charge. Another factor enhancing this effect was proposed by Nolan and De Sachy in 1927. They made the assumption that the rate of combination of positive ions and oppositely charged nuclei  $\eta_{12}$  to the rate of combination of positive ions and uncharged nuclei  $\eta_{10}$  is the same as the combination ratio for negative ions,

$$\text{i.e., } \frac{\eta_{12}}{\eta_{10}} = \frac{\eta_{21}}{\eta_{20}} ,$$

(11)

$$\therefore \frac{\eta_{21}}{\eta_{12}} = \frac{\eta_{20}}{\eta_{10}} .$$

The larger the value of this ratio, the more readily do the negative, rather than positive, small ions combine with oppositely charged or neutral nuclei. The process of combination of small ions with uncharged nuclei must involve the accidental collision of these particles, and the difference between  $\eta_{10}$  and  $\eta_{20}$  must be mainly due to the difference in the speeds of the small ions.

If we measure the conduction current at ground level and at a height  $h$  (of the order of 1 m) in still air, the values obtained should



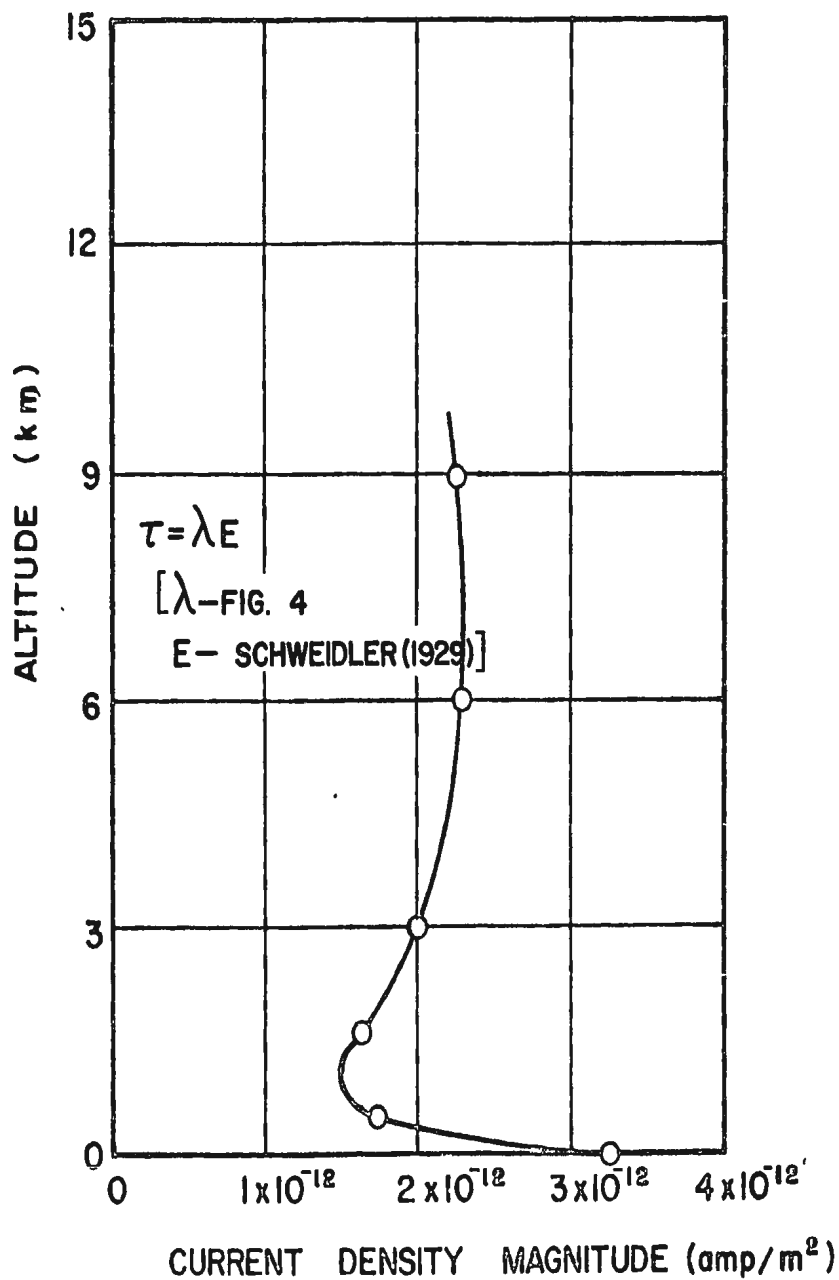


Fig. 5. CONDUCTION CURRENT DENSITY MAGNITUDE

be nearly equal as is proved by observation (see Fig. 5).

Let  $E^1$  = electric field at height  $h$ .

$E$  = electric field at ground level.

$\lambda_+^1$  = positive conductivity at height  $h$ .

$\lambda_-^1$  = negative conductivity at height  $h$ .

$\lambda_+$  = positive conductivity at ground level.

Then it must follow that

$$(12) \quad E^1(\lambda_+^1 + \lambda_-^1) = E\lambda_+.$$

This equation shows that either  $E$  varies with altitude or  $\lambda_+$  varies with altitude.

According to Hogg (1939), the local effect of  $\alpha$  and  $\beta$  rays from radioactive matter in the soil is sufficient to make  $\lambda^+$  equal to  $(\lambda_+^1 + \lambda_-^1)$  and  $E^1$  is approximately equal to  $E$  for the altitude considered.

### CHAPTER 3

#### THE VARIABLES OF ATMOSPHERIC ELECTRICITY

##### 3.1 The Electric Field and Electric Charge in the Atmosphere

In this section, the variables of atmospheric electricity will be treated, the sequence adopted being considered most appropriate but entirely arbitrary.

The most important world-wide variable is the potential  $V$  of the ionosphere relative to the earth. The most recent value of this potential (Chalmers 1954) was estimated in the range 3 to 4 hundred kilovolts. In the same report, Chalmers quotes:

"There seems now no reason to doubt that it is thunderstorms which maintain the earth's fine weather field against the conduction current, and it may be safely said that this problem can be regarded as solved."

The zero potential in electrostatics is arbitrary and in theory is usually chosen as a point far removed from any electrostatic charges. It is not known whether the outer surface of the ionosphere is charged or not, and this cannot be determined from measurements conducted within the ionosphere. By convention, the potential of the earth is assumed to be zero, despite its known surface charge. The variable most directly dependent upon the spatial distribution of  $V$  is the vector potential gradient,  $\text{grad } V$ .

$$(13) \quad \text{grad } V = - \vec{E} \quad .$$

The horizontal components of  $E$  are negligible compared to the vertical,

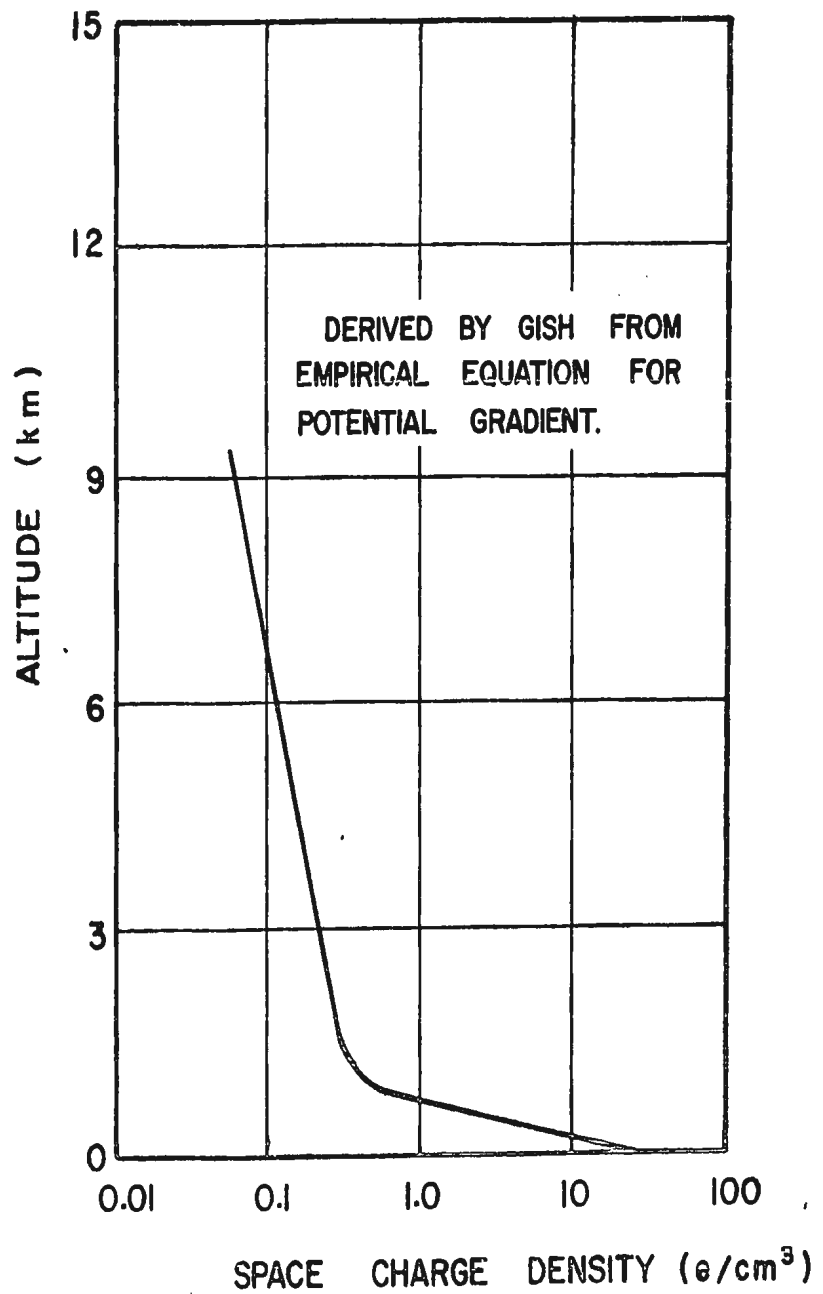


Fig. 6. SPACE CHARGE DENSITY DISTRIBUTION



so equation (13) is reduced to

$$(14) \quad \frac{\partial V}{\partial z} = - \vec{E}_z$$

where the positive direction of the z-axis is upward.

The potential as a function of altitude may be obtained by direct integration.

$$(15) \quad V(z) = - \int_0^z \vec{E}_z \cdot dz$$

The space charge density  $\rho$  (Fig. 6) may also be obtained from an altitude variation of  $E$  by means of Maxwell's relation

$$(16) \quad \text{div } E = \frac{\rho}{\epsilon}$$

where  $\epsilon$  is the permittivity of the atmosphere. Although  $\epsilon$  is a function of humidity, pressure and temperature, its range of variation in the lower atmosphere is so small that it may be assumed as a constant.

Equation (16) may also be simplified to give

$$(17) \quad \frac{\partial E_z}{\partial z} = \frac{\rho}{\epsilon}$$

Since  $E_z$  usually becomes negative as the altitude increases, the resultant atmospheric space charge density is usually positive.

We have already discussed the conductivity of the air and showed it to be given by the expression

$$(6) \quad \lambda = e \Sigma \omega \frac{n}{r} r$$

so that the total conductivity is given by the sum of the two conductivities, namely

$$\lambda = e[\omega_1 n_1 + \omega_2 n_2] \quad .$$

The columnar resistance  $R(z)$ , which is the resistance of a column of air of  $1 \text{ m}^2$  cross-section extending from the earth's surface to a given height  $z$ , is given by

$$(18) \quad R(z) = \int_0^z \frac{dz}{\lambda} \quad .$$

Stergis (1955) estimated  $R$  to be equal to about  $10^{17}$  ohms up to the ionospheric layer. The conductivity from an altitude of 15 km upwards is so high that this region contributes only a small fraction of the total resistance. Gish estimated half of the total resistance is contributed by the lowest 2 km.

It is thus evident that potential gradient measurements over land and, in particular, near centres of industrial activity or urban areas, where local atmospheric pollution has a dominating effect on the resistivity, cannot be expected to yield information which can be directly correlated with the question of the total difference of potential between the earth and upper layers of the atmosphere.

In the case of observations over the oceans and over polar regions, practically all the ionization throughout the whole column is due to cosmic radiation. The only local effect which can influence the fine weather gradient is a change in the number of nuclei available for the capture of small ions.

Since a potential difference  $V$  exists across a columnar resistance  $R$ , a current density

$$(19) \quad j_z = \frac{V}{R}$$

exists, flowing downward to the earth. This current may also be measured directly at the earth's surface from the relationship

$$(20) \quad \vec{j}_z = \lambda \vec{E} .$$

The average value of  $j$  is approximately  $3 \times 10^{-12}$  amp/m<sup>2</sup>.

From equations (19) and (20), we get

$$(21) \quad \frac{V}{R} = \lambda E .$$

Equation (21) is useful in that it relates the potential  $V$ , which is the same over the entire ionosphere, with the characteristic  $R$  of an air column above the point of measurement, and with the local characteristics  $\lambda$  and  $E$ , measured at any altitude and in a particular locality near the earth's surface.

The question arises as to the maximum rate at which  $V$  or  $R$  may vary and still have a sensibly constant  $\vec{j}$  at all altitudes.

The equation of continuity,

$$(22) \quad \text{div } \vec{j} + \frac{\partial \rho}{\partial t} = 0 ,$$

depends only on the conservation of charge. From equations (16) and (21), equation (22) becomes

$$(23) \quad \frac{\lambda}{\epsilon} \rho + \frac{\partial \rho}{\partial t} = 0 .$$



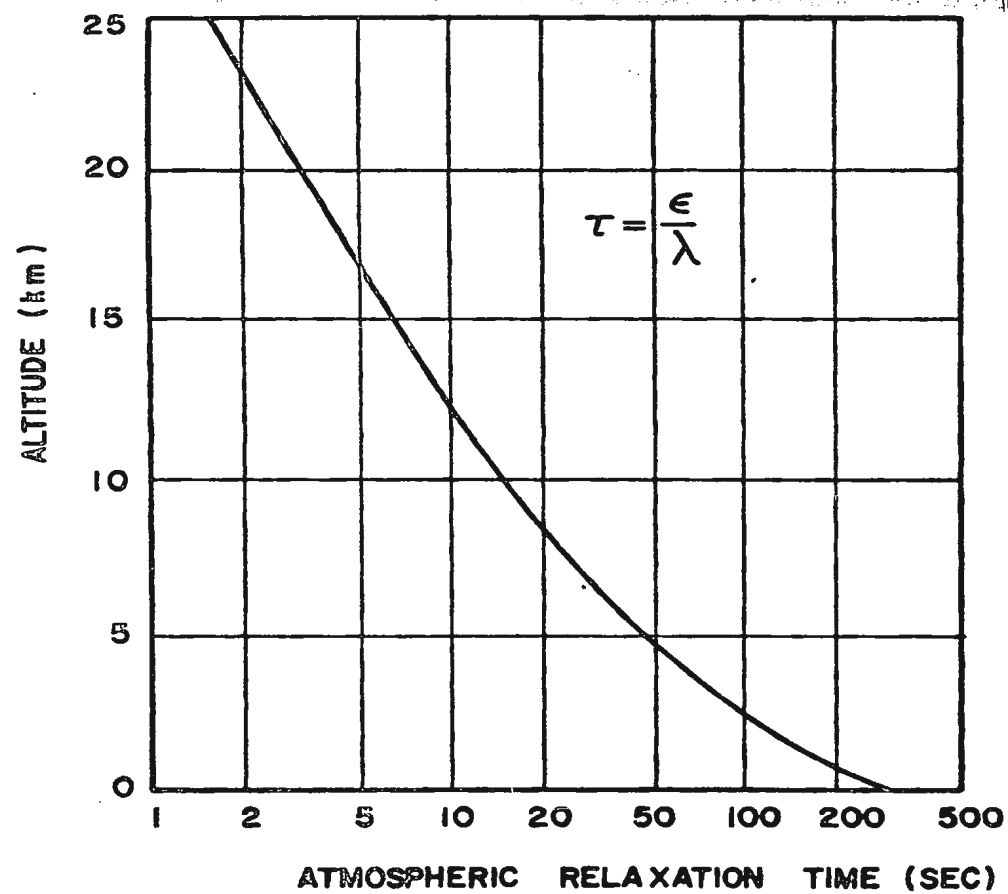


Fig. 7. ATMOSPHERIC RELAXATION TIME VARIATION WITH ALTITUDE



The solution of this equation is

$$(24) \quad \rho = \rho_0 e^{-\frac{\lambda}{\epsilon} t}.$$

The ratio  $\frac{\epsilon}{\lambda}$  is known as the atmospheric relaxation time  $\tau$ . It is a function of altitude and is inversely proportional to the conductivity. A graph of  $\tau$  against altitude is shown in Fig. 7.  $\tau$  gives the time required for the charge on a conductor to diminish to  $1/e$  of its initial value. Only when significant field changes occur in intervals substantially greater than  $\tau$  can it be assumed that a steady state is approximated. At the earth's surface, this time is of the order of 500 sec.

The average value of the "fair weather" field intensity at the earth's surface is about 120 volts/meter. Therefore, the charge on the earth's surface given by

$$(25) \quad \sigma = \epsilon E$$

amounts to about  $10^{-9}$  coulombs per meter<sup>2</sup>.

Israel (1953) quotes:

"With a sudden change in the atmospheric electrical field the new equilibrium state is again 99 per cent attained in about one half hour; and that variations, which happen in time periods which are large in comparison with this time span - for example, diurnal processes - may be regarded as quasi-stationary."

### 3.2 Atmospheric Current

The current flowing between the atmosphere and the earth may be considered as the sum of the parallel components composed of

- (1) the diffusion current.
- (2) the conduction current.
- (3) the convection current.

Each of these is treated separately below.

#### (1) The diffusion current

Since the space charge is unevenly distributed in the atmosphere, and the turbulent diffusion coefficient  $K$  in the atmosphere is quite large, a diffusion current given by

$$(26) \quad i_{\text{diff}} = \frac{dN}{dt} = -K \frac{\partial \rho}{\partial z}$$

flows in the atmosphere.

$\frac{dN}{dt}$  gives the number of charged particles crossing unit cross-sectional area in unit time.

$K$  is the diffusion coefficient and is derived from the formula:

$$K = \frac{kT\omega}{e}$$

where  $k$  = Boltzmann's constant

$\omega$  = mobility

$T$  = absolute temperature

$e$  = electric charge

$\frac{d\rho}{dz}$  = space charge concentration gradient.

(2) The conduction current

The conduction current in the atmosphere, as we have seen, is carried almost entirely by the small ions in an electric field  $E$ . Thus, the conduction current is given by

$$(6) \quad i_{\text{cond}} = \lambda E$$

$$\text{where } \lambda = \lambda_1 + \lambda_2$$

and  $\lambda_1 = n_1 e_1 \omega_1$  is the conductivity of the positive ions.

A similar equation can be written for  $\lambda_2$ , the conductivity of negative ions.

(3) The convection current

When the air contains, at any given point, an excess of ions of one sign (i.e. a space charge), movement due to wind or ordinary turbulence will give rise to a mechanical transference of electric charge. This constitutes the convection current and is given by

$$(27) \quad i_{\text{conv}} = \rho v$$

where  $v$  = vertical component of wind velocity

$\rho$  = charge density.

Thus, the total current in the atmosphere in good weather zones is given by

$$(28) \quad i_t = \lambda E - K \frac{d\rho}{dz} + \rho v$$

I. Kraakevik observed that the conduction current above the mixing layer remains constant within  $\pm 10\%$ , while in the mixing layer, it may be on the average 30% and sometimes even 200% larger than the conduction current at considerable altitude (see Fig. 5). If it is assumed that the total current remains constant, then the observed effect can be ascribed only to the turbulent diffusion produced by the upward moving positive space charge in the mixing layer.

Also, according to Kraakevik, the conduction current density above the oceans amounts to  $2.7 \times 10^{-12}$  amp/m<sup>2</sup> and is constant with altitude to within 2%. Assuming this estimate to be correct for the earth as a whole, an estimated total current of 1400 amps. flows from the ionosphere to the earth in regions of good weather.

CHAPTER 4

THE LOCAL VARIATIONS OF THE ATMOSPHERIC ELECTRIC FIELD

4.1 The Effect of the Vertical Distribution of the Space Charge on the Electric Field

Several workers have investigated the local anomalies of the atmospheric electric field and have made comparisons of the diurnal variations observed at various stations over the earth's surface. Muhleisen (1956) concluded that the complicated variations in urban environments were caused by the positive space charge which is produced profusely by the industrial activity in such conditions.

Israel (1952) reported that the diurnal variation at three different stations in the Alps varied with the season, and the height of the exchange layer. Sagalyn and Faucher (1956) carried out observations from an aircraft and investigated the vertical distribution of the several electrical parameters in the exchange layer and compared the results with those obtained in the region above the exchange layer. These results confirmed the conclusion arrived at by Israel. According to the results obtained, it appeared that the local anomaly of the electric field seemed to be mainly controlled by the vertical distribution of the air resistivity and the space charge in the lower atmosphere.

Kawano (1958) discussed the local anomaly of the atmospheric electric field on the basis of the ionization equilibrium process.

In order to determine the local atmospheric electric parameters on the basis of the ionization equilibrium process, Kawano

first ascertained the vertical distribution of ionic densities by introducing the eddy diffusion coefficient (K) into the equilibrium equations. K is the rate of diffusion of ions per unit area per unit concentration gradient.

The variation of the concentration of small positive ions with altitude on account of eddy diffusion can be expressed by the formula

$$(29) \quad \frac{dn}{dt} = \frac{d}{dz} \left( \frac{Kdn}{dz} \right) .$$

The contribution of ions, coming from lower altitudes, adds to the production of ions by the various ionizing agents, and the process of ionization equilibrium especially near centres of pollution can be expressed by the formula

$$(30) \quad \frac{d}{dz} \left( \frac{Kdn}{dz} \right) + q + \frac{Kd(nE)}{dz} = \beta Nn + \alpha n^2$$

where  $\beta$  is the coefficient of attachment between small ions and nuclei. The left-hand side of the equation gives the rate of change of positive space charge with respect to height, the production  $q$  of small ions and the contribution due to the flow of a conduction current of positive ions. The right-hand side gives the rate of the combination of small positive ions with large ions and the rate of recombination of small ions. The last term on each side produces insignificant results and the final equation may be simplified to give

$$(31) \quad \frac{d}{dz} \left( \frac{Kdn}{dz} \right) + q = \beta Nn .$$



This is assuming that the quantities of radiation of cosmic rays and the penetrating radiation from the earth's crust are not affected by air motions. However, the distribution of the radioactive gases and their decay products in the atmosphere is directly affected by air motions. The quantity  $q$  may thus be subdivided into three classes, namely,

$q_1$ : which is the radiation by the radioactive gases and their decay products in the atmosphere, and which is affected by air motion, and

$q_2$ : which is the penetrating radiations by the radioactive substances in the earth's crust, and

$q_3$ : radiation due to cosmic rays.

Hence, we may write

$$(32) \quad q = q_1 + q_2 + q_3 \quad .$$

The intensity of  $q_2$  and  $q_3$  is independent of air motions.

The radioactive substance in the atmosphere is due to the diffusion of radioactive gases (mostly thoron and radon) from the disintegration of radioactive elements in the earth's crust. It may, therefore, be assumed that the vertical distribution of the radioactive substance in the atmosphere is controlled by the eddy diffusivity. The quantity  $Q$  of radioactive substance present at a given altitude in the exchange layer may therefore be expressed by the formula

$$(33) \quad Q = Q_h e^{-\frac{\sqrt{T}}{\sqrt{K}}(z-h)}$$

where  $Q_h$  = amount of radioactive material at a given height  $h$ .

$\tau$  = decay constant of radon =  $2.09 \times 10^{-6}/\text{sec}^{-1}$ .

$K$  = coefficient of eddy diffusivity (here assumed to remain constant with altitude, though strictly speaking, it is a function of height).

$z$  = altitude.

The ionizing effect of the radioactive material in the atmosphere is mainly due to the  $\alpha$ -radiation, and the intensity of this radiation may be considered as directly proportional to the quantity  $Q$  of the radioactive gases present. Consequently, the rate of ion pair production ( $q_1$ ) due to the radioactive substances in the atmosphere is proportional to the quantity  $Q$ ,

$$(34) \quad \text{i.e., } q_1 = k_1 Q$$

Substituting for  $Q$  in this equation, we get

$$(35) \quad q_1 = q_{1h} e^{-\frac{\tau}{\sqrt{K}}(z-h)}$$

where  $q_{1h}$  = the value of the rate of ion pair production at  $z = h$ .

$$(36) \quad \therefore q = q_{1h} e^{-\frac{\tau}{\sqrt{K}}(z-h)} + q_2 + q_3,$$

from equation (32).

Substituting in equation (31), we get

$$(37) \quad K \frac{d^2 n}{dz^2} + q_{1h} e^{-\sqrt{\frac{\tau}{K}} (z-h)} + q_2 + q_3 = \beta N n$$

The solution of this equation is derived in Appendix 1 and is given by

$$(38) \quad n = \left[ n_h - \left( \frac{q_{1h}}{\beta N - \tau} + \frac{q_2}{\beta N} \right) e^{-\sqrt{\frac{\beta N}{K}} (z-h)} + \frac{q_{1h}}{\beta N - \tau} e^{-\sqrt{\frac{\tau}{K}} (z-h)} + \frac{q_2 + q_3}{\beta N} \right]$$

We can express the electrical conductivity of the atmosphere by

$$\lambda = n e \omega$$

where  $n$  = number of small ions.

$e$  = electronic charge.

$\omega$  = mobility of small ions.

Substituting for  $n$ , we now get

$$(39) \quad \lambda = \left[ n_h - \left( \frac{q_{1h}}{\beta N - \tau} + \frac{q_2}{\beta N} \right) e^{-\sqrt{\frac{\beta N}{K}} (z-h)} + \frac{q_{1h}}{\beta N - \tau} e^{-\sqrt{\frac{\tau}{K}} (z-h)} + \frac{q_2 + q_3}{\beta N} \right] e \omega$$

From Poisson's equation

$$\nabla \cdot \mathbf{E} = \frac{\rho}{\epsilon}$$

and Ohm's law

$$i = \lambda E$$

we can now derive an expression for the space charge, thus,

$$(40) \quad \rho = i \epsilon \frac{d}{dz} \left( \frac{1}{\lambda} \right)$$

assuming only a vertical variation in E.

Differentiating equation (39) to obtain  $\frac{d}{dz}\left(\frac{1}{\lambda}\right)$  and substituting  $\lambda E = n\omega E$  for the current i, and substituting these expressions in equation (40), we get

$$(41) \quad \rho = \frac{n_h E \epsilon \left(\frac{\beta N}{K}\right)^{\frac{1}{2}} \left\{ n_h - \left( \frac{q_{1h}}{\beta N - \tau} + \frac{q_2}{\beta N} \right) \right\} e^{-\sqrt{\frac{\beta N}{K}}(z-h)} + \left(\frac{\tau}{K}\right)^{\frac{1}{2}} \frac{q_{1h}}{\beta N - \tau} e^{-\sqrt{\frac{\tau}{K}}(z-h)}}{\left[ \left\{ n_h - \left( \frac{q_{1h}}{\beta N - \tau} + \frac{q_2}{\beta N} \right) \right\} e^{-\sqrt{\frac{\beta N}{K}}(z-h)} + \frac{q_{1h}}{\beta N - \tau} e^{-\sqrt{\frac{\tau}{K}}(z-h)} + \frac{q_2}{\beta N} \right]^2}$$

When  $z = h$ , this expression reduces to

$$(42) \quad \rho_h = \frac{\epsilon E_h}{n_h} \left(\frac{\beta N}{K}\right)^{\frac{1}{2}} \left\{ n_h - \left( \frac{q_{1h}}{\beta N - \tau} + \frac{q_2 + q_3}{\beta N} \right) \right\} + \frac{\tau}{K} \frac{q_{1h}}{\beta N - \tau}.$$

Since  $\tau$  equals  $2.09 \times 10^{-6} \text{ sec}^{-1}$  for radon (which is the major  $\alpha$ -ray source in the atmosphere) and  $\beta N$  is  $10^{-2} \text{ sec}^{-1}$  on land, this relation reduces to

$$(43) \quad \rho_h = \frac{\epsilon E_h}{n_h} \left(\frac{\beta N}{K}\right)^{\frac{1}{2}} \left( n_h - \frac{q_{1h} + q_2 + q_3}{\beta N} \right)$$

$$(44) \quad \therefore E_h = \frac{\rho_h n_h}{\epsilon \left(\frac{\beta N}{K}\right)^{\frac{1}{2}} \left( n_h - \frac{q_{1h} + q_2 + q_3}{\beta N} \right)}$$

This formula expresses the value of the electric field considering the influence of the eddy diffusion on the vertical distribution of the electrical conductivity of the atmosphere.

At zero altitude, the quantities on the right-hand side of the equation have been separately investigated by various workers and the following values are substituted in the equation:

$$n = 10^9/\text{m}^3$$

$$\rho = ne = 1.6 \times 10^{-10} \text{ Coul}/\text{m}^3$$

$$\epsilon = 8.8 \times 10^{-12} \text{ Coul/newton-m}^2$$

$$K = 4 \text{ m}^2/\text{sec.}$$

$$\beta N = 10^{-2}/\text{sec.}$$

$$q_h = 10^7 \text{ pI}/\text{m}^3$$

Hence, according to equation (44), the value of E is about 100 V/m.

The fluctuations in the atmospheric field can thus be assumed to be caused by the fluctuations in the density of the space charge and its distribution with respect to height.

#### 4.2 The Vertical Distribution of the Air Resistivity in the Exchange Layer

Local agitation of the electric field can also be attributed to the columnar resistivity. Kawano investigated the vertical distribution of the air resistivity and the columnar resistance by taking into account the influence of the eddy diffusion on the ionization equilibrium. At the lower levels of the exchange layer,  $q_2$  has a dominant effect. In this case, we will consider the variation of the earth radiation effect with altitude, and can express  $q_2$  as

$$(45) \quad q_2 = q_{20} e^{-\mu z}$$

where  $\mu$  is the absorption coefficient for air of  $\gamma$ -rays of RaC which is the emitter of the highest energy in the earth's crust.  $q_{20}$  is the absorption coefficient of RaC at the earth's surface.

The ionization equilibrium equation may now be written

$$(46) \quad K \frac{d^2 n}{dh^2} + q_{1h} e^{-\sqrt{\frac{\tau}{K}}(z-h)} + q_2 e^{-\mu z} + q_3 = \beta N n$$

Solving this equation for the same boundary conditions as before, we get

$$(47) \quad n = \left( n_h - \frac{q_{1h}}{\beta N - \tau} + \frac{q_{20} e^{-\mu h}}{\beta N - K\mu^2} + \frac{q_3}{\beta N} \right) e^{-\sqrt{\frac{\beta N}{K}}(z-h)} + \frac{q_{1h}}{\beta N - \tau} e^{-\sqrt{\frac{\tau}{K}}(z-h)} + \frac{q_{20}}{\beta N - K\mu^2} e^{-\mu z} + \frac{q_3}{\beta N}$$

This formula expresses the vertical distribution of the ion concentration under conditions of ionization equilibrium in the lower atmosphere.

$$\text{Now } \mu = 1.06 \times 10^{-5} \text{ cm}^{-1}.$$

$$\tau = \text{decay constant of Rn} = 2.09 \times 10^{-6} \text{ sec}^{-1}.$$

$$\beta N = 10^{-2} \text{ sec}^{-1}.$$

Hence, terms involving  $\mu$  and  $\tau$  are many orders of magnitude less than those containing  $\beta N$  and the expression may now be simplified to give

$$(48) \quad n = \left( n_h - \frac{q_{1h} + q_{20} + q_3}{\beta N} \right) e^{-\sqrt{\frac{\beta N}{K}}(z-h)} + \frac{1}{\beta N} \left\{ q_{1h} e^{-\sqrt{\frac{\tau}{K}}(z-h)} + q_{20} e^{-\mu z} + q_3 \right\}.$$

The expression for  $r_1$ , the resistivity of the atmosphere in the exchange layer, can now be expressed,



since  $r_1 = \frac{1}{\lambda_1} = \frac{1}{\text{new}}$ , by the formula

$$(49) \quad r_1 = \frac{1}{\left[ \left( n_h - \frac{q_{1h} + q_{20} + q_3}{\beta N} \right) e^{-\sqrt{\frac{\beta N}{K}}(z-h)} + \frac{1}{\beta N} \left\{ q_{1h} e^{-\sqrt{\frac{T}{K}}(z-h)} + q_{20} e^{-\mu z} + q_3 \right\} \right] e u}$$

The first term in the denominator in the right-hand side depends on the distribution of the air resistivity up to a height of about 20 meters above the ground. The second term expresses the distribution of the air resistivity above this level.

From the above equation, the value of the electrical resistance ( $R_1$ ) of the air column within the exchange layer can be estimated. Thus,

$$(50) \quad R_1 = \int_0^{H_1} r_1 dz = \int_0^{H_1} \frac{dz}{\left[ \left( n_h - \frac{q_{1h} + q_{20} + q_3}{\beta N} \right) e^{-\sqrt{\frac{\beta N}{K}}(z-h)} + \frac{1}{\beta N} \left\{ q_{1h} e^{-\sqrt{\frac{T}{K}}(z-h)} + q_{20} e^{-\mu z} + q_3 \right\} \right] e u}$$

where  $H_1$  is the height of the exchange layer.

Stergis et al (1955) made measurements on the conductivity in the stratosphere and were able to assess the resistance ( $R_2$ ) of the air column in this region by the relation

$$(51) \quad R_2 = \int_{H_1}^{H_2} r_2 dz$$

where  $H_2$  is the height of the upper conducting layers of the atmosphere.

The columnar resistance of the exchange layer thus represents a significant variable contribution to the total columnar resistance  $R$ . Results indicate that the total resistance of a column of air of cross-section one square meter is about  $10^{17}$  ohms. The conductivity from an altitude of 15 km upwards is so high that this region contributes only a small fraction of the total resistance. It is thus evident that potential gradient measurements over land and, in particular, near cities are susceptible to large and continuous fluctuations. In the case of observations over the oceans and in polar regions, practically all the ionization is directly due to cosmic radiation and the only local effect which can influence the potential gradient is the number of nuclei available for the capture of small ions. Atmospheric electric properties at the earth's surface are so sensitive to weather factors and pollution that it is not possible to determine with certainty from such measurements alone what proportion of their day-to-day variation is the result of fluctuations of the world-wide potential.

The accepted extent of the exchange layer extends from ground level up to about 800 to 1400 meters. The potential of the conducting layer which is variously placed at 40 to 60 kilometers is uniform throughout the globe and it has been estimated at about  $3 \text{ to } 4 \times 10^5$  volts. Given that  $R$  amounts to  $10^{17}$  ohms, then

$$i = 3 \text{ to } 4 \times 10^{-16} \text{ amps}$$

which agrees with the experimental values of the air-earth current.

## CHAPTER 5

### RESULTS OF PAST MEASUREMENTS AT THE EARTH'S SURFACE

The three atmospheric electric variables which have been measured with the greatest regularity at the earth's surface are the conductivity  $\lambda$ , the electric field intensity  $E$ , and the current density  $j$ . The atmospheric conductivity has usually been obtained by a study of the current-voltage characteristic slope curve of a discharging electrode. The electric field has been determined directly in two ways:

- (1) By determination of the voltage difference between vertically separated collectors, each in equilibrium with the atmospheric potential in its immediate vicinity.

- (2) By electric induction effects on moving conductors.

The current density has been obtained either directly by using an insulated plate mounted flush with the ground to collect the current, or indirectly from the product  $\lambda E$ .

Chalmers (1957) gives a table of the average values for all stations on land, and the results of the same measurements over the oceans. The table is produced below.

FROM I. M. IMYANITOV & K. S. SHIFRIN  
(SOVIET PHYSICS USPEKH 1962)

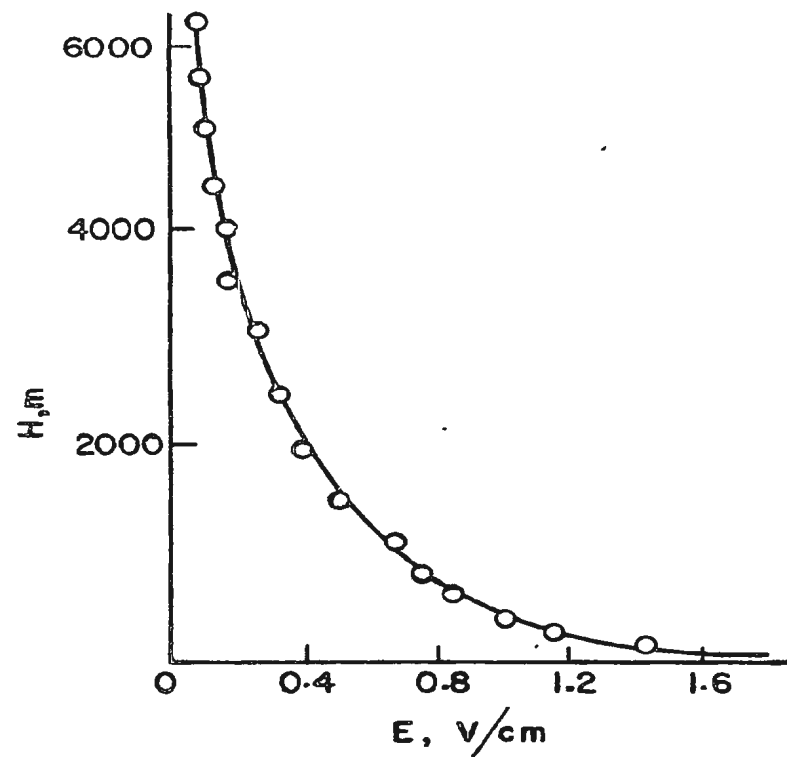
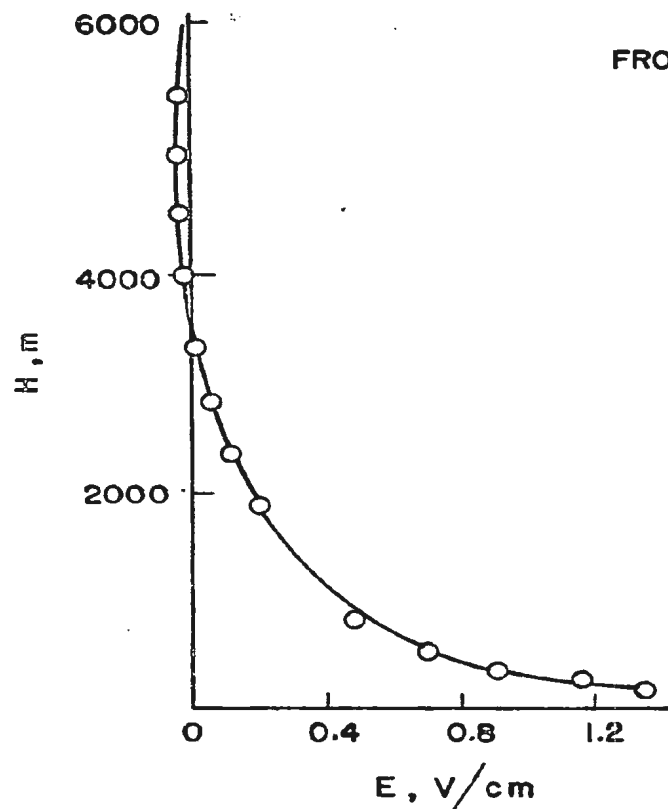


Fig. 8. VARIATION OF FIELD INTENSITY  $E$  WITH ALTITUDE  $H$   
GROUP I Leningrad

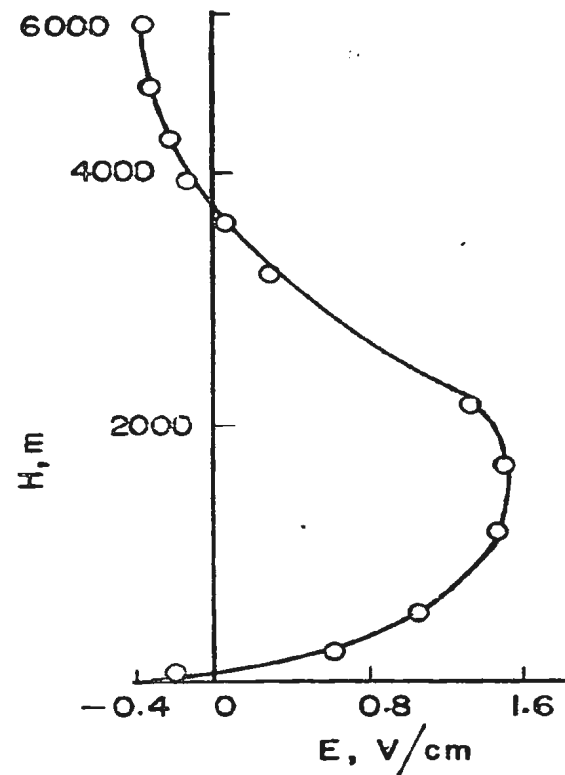


FROM I. M. IMYANITOV & K. S. SHIFRIN  
(SOVIET PHYSICS USPEKH 1962)

- 97 -

Fig. 9. VARIATION OF FIELD INTENSITY "E" WITH ALTITUDE "H"

GROUP II. LENINGRAD



FROM I. M. IMYANITOV & K. S. SHIFRIN  
(SOVIET PHYSICS USPEKH 1962)

Fig. 10. VARIATION OF INTENSITY  $E$  WITH ALTITUDE  $H$

GROUP III. TASHKENT



<u>QUANTITY</u>	<u>UNITS</u>	<u>LAND STATIONS</u>	<u>OCEANS</u>
Potential gradient	V/m	130	126
Air-earth current	A/m <sup>2</sup>	$2.4 \times 10^{-12}$	$3.7 \times 10^{-12}$
Conductivity	ohm <sup>-1</sup> m <sup>-1</sup>	$1.8 \times 10^{-14}$	$2.8 \times 10^{-14}$
Columnar resistance	ohm/m <sup>2</sup>	$1.9 \times 10^{17}$	$1.2 \times 10^{14}$
No. of nuclei	cm <sup>-3</sup>	4000	4500 (?)
No. of +ve small ions	cm <sup>-3</sup>	750	640
No. of -ve small ions	cm <sup>-3</sup>	680	575
Rate of production of ions	cm <sup>-3</sup> sec <sup>-1</sup>	9.5	1.5
Space charge	C/m <sup>3</sup>	$10^{-11}$	?

Further work was carried out to determine the variation of the electric field with increasing altitude. During the IGY, the field variation with altitude was observed at three Russian stations. It was found that even in days of good weather the electric field profiles can be quite varied. It was found convenient to classify the profiles into three groups (Figs. 8, 9, 10). The first group includes profiles which decrease exponentially with increasing altitude. This accounts for 40% of the altitude profiles. This profile can be expressed by the relation

$$(52) \quad E = E_n e^{-az}$$

where  $E_n$  = electric field at a given level

$a$  = constant.

(See Fig. 8.)

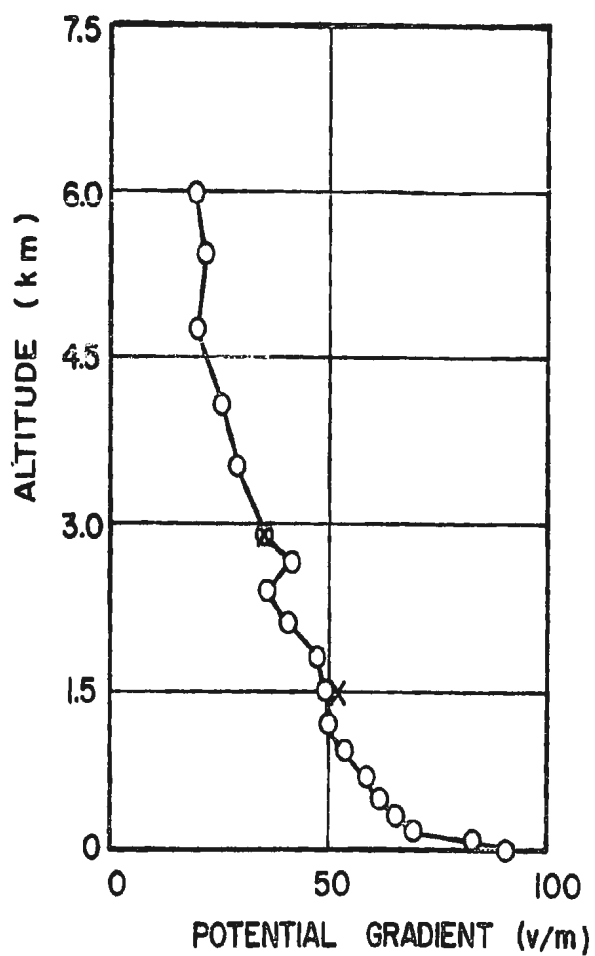


Fig. 11. POTENTIAL GRADIENT DISTRIBUTION ABOVE GREENLAND FJORD

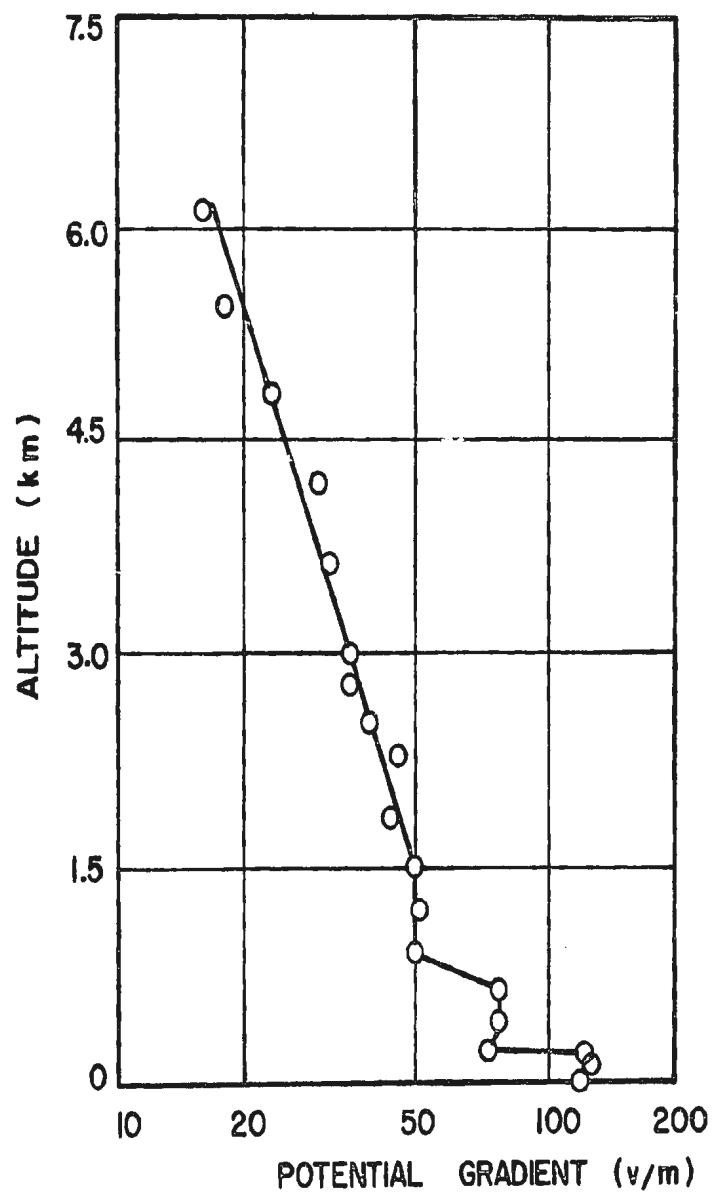


Fig. 12. VARIATION OF POTENTIAL GRADIENT DISTRIBUTION ABOVE GREENLAND

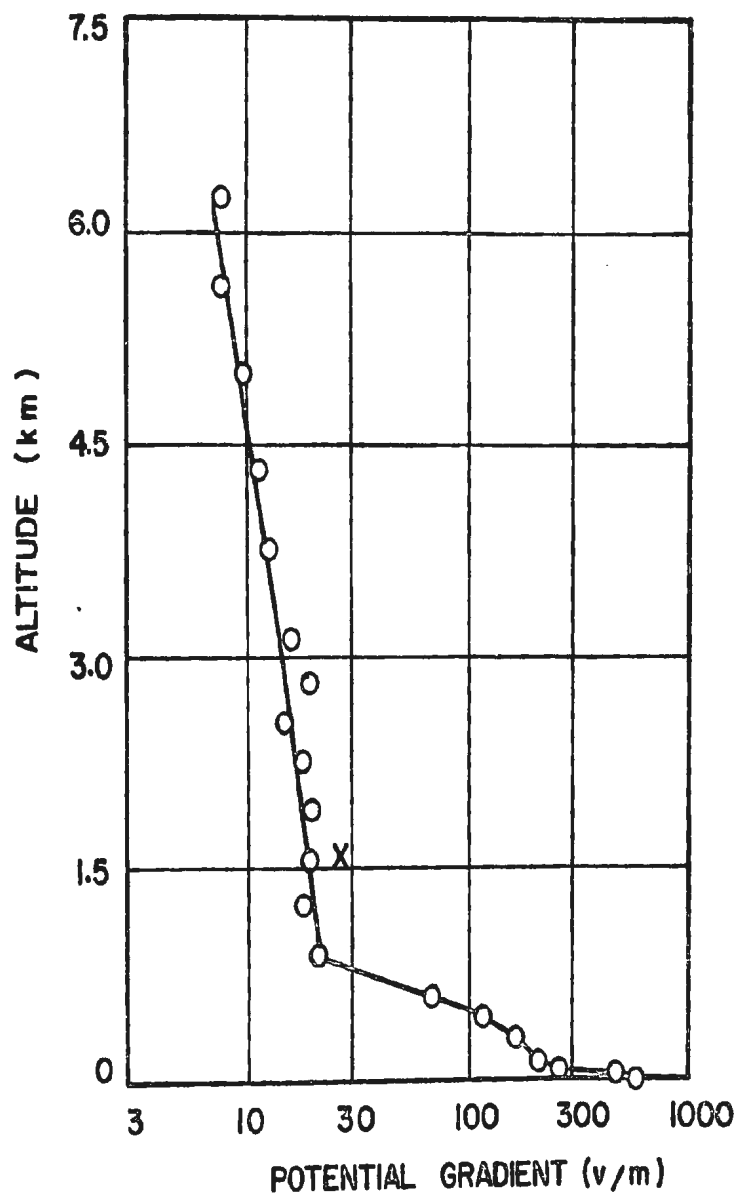


Fig. 13. POTENTIAL GRADIENT DISTRIBUTION OFF CALIFORNIA COAST

In many cases, the field intensity was found to decrease with height at first in accordance with equation (52), and then to reverse sign at an altitude of about 3500 to 4000 meters. This comprised the second group. Finally, in the third group which comprised more than 40% of the profiles, the field first increases with altitude and then starts decreasing. Usually the field was found to change direction around 3500 to 4000 km but, in some cases, it remained positive up to the maximum sounding height. These changes are closely connected with the changes in humidity, air turbulence and dust content.

In 1956, J. F. Clark carried out similar measurements of the electric field profiles over the north American continent. He also classifies the profiles into three groups. Thus, Group A approximates very nearly an exponential decrease with altitude (see Fig. 11). Group B showed an anomaly at around 2 km, at which the potential gradient was 1.5 larger than the exponential approximation value (see Fig. 12). This anomaly coincided with the base of an inversion layer.

Group C is characterized by a maximum value near the surface and which is several times as large as that of the A profile. Group C gradient decreases rapidly until at an altitude of about 1 km the gradient is smaller than that of type A profile (see Fig. 13).

The contrast between Group A and Group C profiles was borne out by the ratio of the maximum surface gradient to the minimum (6 km) gradient encountered. Thus, near Newfoundland, this ratio was found to be of the order of 5.8, while off the San Francisco shore the ratio was

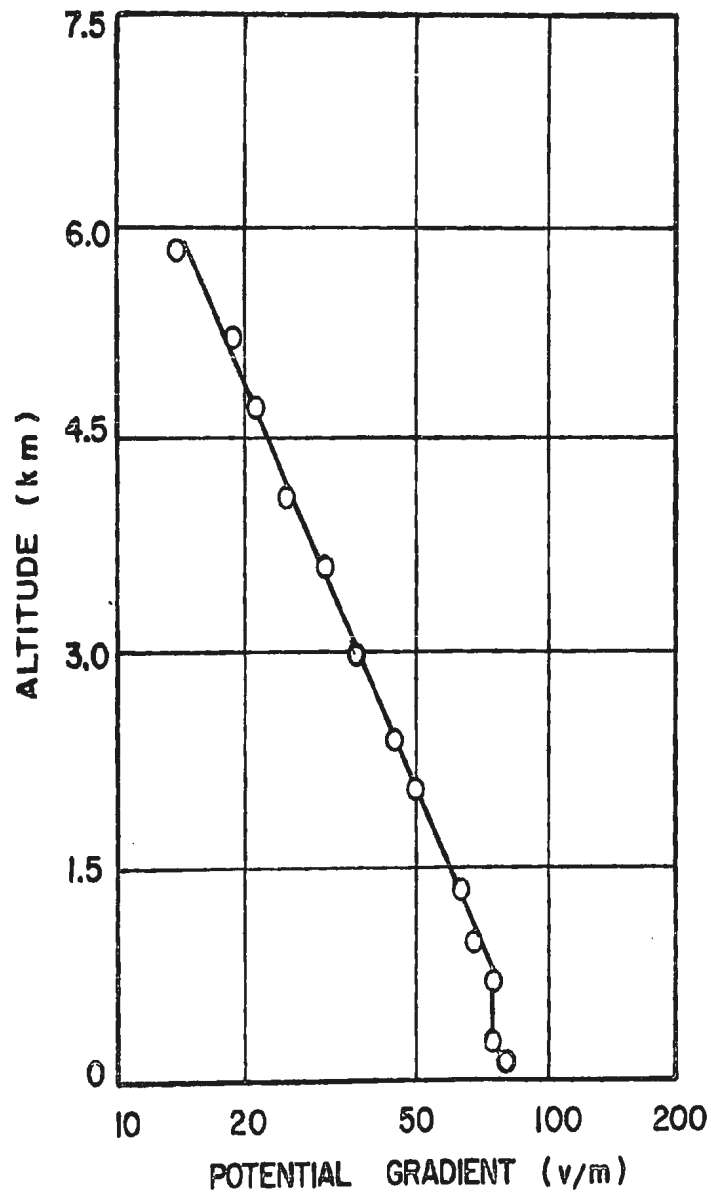


Fig. 14. POTENTIAL GRADIENT DISTRIBUTION OFF NEWFOUNDLAND COAST

found to be 67. The profile obtained off the Newfoundland coast is shown in Fig. (14).

Continuous recording of the potential field is carried out at the Brebeuf College Geophysical Observatory in Montreal. For 1955, they give a value of 73.5 V/m for days with "maritime Atlantic air". Quoting from one of their reports

"For reasons yet debatable, the potential gradient is smaller in pure Maritime air than in pure polar air. It might be useful to remember that continental polar air is mostly subsiding while the Maritime air is mostly convective. Would the consideration of the resistance of the air column and its conductivity help to find the physical reason of the levels of confidence."



## CHAPTER 6

### EXPERIMENTAL TECHNIQUES

#### 6.1 Methods of Measuring the Potential Gradient

The methods of measuring the electric field may be divided into two types:

- (1) those employing probes or collectors and
- (2) those depending on the induction of charge.

The collector may be considered as an arrangement in which an insulated metal probe is located at a convenient position in the atmosphere. If its potential initially differs from the surrounding atmosphere, it will collect ions of the appropriate sign until it acquires the same potential as the atmosphere. The potential thus acquired is measured by an instrument with a high input impedance. Various forms of collectors that have been used are classified below.

- (1) Probe with glowing fuse.
- (2) Probe with radioactive source.
- (3) Water dropper (Kelvin).
- (4) Two vertically displaced horizontal wires (Scraser).

Induction meters depend upon the basic fact that, when a conductor is placed in an electric field, the density of charge ( $\sigma$ ) induced on its surface is proportional to the field intensity at that point, that is,

$$(25) \quad \sigma = \epsilon E \quad .$$



Fig. 15. LOCATION OF MEASURING APPARATUS



Fig. 16. THE ANTENNA SYSTEM

The first of these types was described by Russelveldt in 1926. In the same year, a similar form was described by Mathias.

#### 6.2 The Absolute Determination of the Potential Gradient

It is necessary to have means to calibrate potential gradient field mills. In this case, an attempt was made to use one of the earlier methods employed in the determination of the electric field. The arrangement consisted of two wires stretched horizontally between two antenna masts separated by a distance of 120 ft. A small ratchet winch made it possible to adjust the sag in the wires so that they were separated by a vertical distance of one meter. A polonium source Po 210 attached to a copper strip was fixed to the midpoint of the antenna. Two conductors with polyvinyl insulation were attached to the midpoints of the antennae and led through metal conduits to the room below where they were connected to a quadrant electrometer.

#### 6.3 The Antenna System (Photos 15, 16)

An antenna system of symmetrical form and suspended far enough above the ground so that the mirror effect can be neglected will develop an open circuit voltage ( $v$ ) proportional to the electric field ( $E$ ) and the height ( $h$ ) above the ground, i.e.,

$$(53) \quad v = Eh \quad .$$

When a change occurs in the potential field, the antenna will respond in such a way as to equalize its potential with the new field. Thus,

a charge is gradually dissipated or acquired by ionic conduction and the rate at which this occurs depends on the relaxation time for electrical phenomena in the atmosphere.

If  $Q$  is the charge and  $S$  the surface area of the antenna, the potential field close to the antenna is given by

$$(54) \quad E = \frac{QS}{\epsilon_0}$$

A total current

$$(55) \quad i = \frac{\lambda QS}{\epsilon_0}$$

consisting of ions of one sign flows until the antenna is in equilibrium with its surroundings. Thus, for unit area,

$$(56) \quad \frac{dQ}{dt} = \frac{\lambda Q}{\epsilon_0}$$

$$(57) \quad Q = Q_0 e^{-\frac{\lambda t}{\epsilon_0}}$$

Actual relaxation times are shown below.

Air near the earth, 5 - 40 minutes.

(The actual value near the earth's surface depends on the amount of pollution in the air.)

Air at 18 km., 4 sec.

Air at 70 km.,  $10^{-8}$  sec.

The earth as a whole,  $10^{-5}$  sec.

It is thus seen that the relaxation time is inversely proportional to the conductivity  $\lambda$  of the atmosphere.  $\lambda$  is a very variable quantity. It increases after rain and is decreased in fog, clouds, dust and heavy atmospheric pollution.

In calculating the conductivity of the air, the effect of the positive and the negative ions is taken into account. However, for charging or discharging the antenna, only one class of ions is effective according to the sign of the field. Therefore, when determining the relaxation time for a positive field from the relationship  $\tau = \epsilon/\lambda$ , only the positive conductivity should be taken into consideration. Consequently, the average relaxation time is increased to double its value. The same reasoning leads to the fact that the antenna acquires the potential of the surrounding air by the flow of ions of the same sign. When fog is prevalent, this would explain the delay between a change in the field and the acquisition by the antenna of the same potential.

#### 6.4 The Quadrant Electrometer

The principal part of the instrument consists of a low metal cylinder divided into quadrants by two diameters at right angles to each other. The quadrants are insulated from each other and mounted separately on amber insulating stands.

The inside of the cylinder is hollow and inside this a light aluminum symmetrical vane (needle) is free to rotate in a horizontal plane. The needle is suspended by a delicate fibre of quartz so that

it can rotate without touching the quadrants. Provision is made for the quadrants to slide open to allow visual inspection of the needle. Screws are provided on the instrument to adjust the alignment of the needle in the centre of the quadrants. To begin with, the fibre is adjusted so that, in the neutral position, the needle rests in a symmetrical position with respect to the quadrants. In this state, either surface of the needle and the opposite face of the quadrants may be regarded as forming a parallel plate capacitor.

#### 6.5 Theory of Operation

Let  $v$  be the potential of the needle,

$V_1$  the potential of one pair of quadrants - the A-quadrants,  
say,

$V_2$  the potential of the other pair of quadrants - the B-quadrants, say.

Suppose that when the needle has turned through an angle  $\theta$ , the total area  $A$  of the needle is placed such that a fraction  $S$  of the area is inside the pair of quadrants at potential  $V_1$ , and an area  $A - S$  inside the pair of quadrants at potential  $V_2$ . Let  $d$  be the perpendicular distance from either face of the needle to the opposite face of the quadrants.

The system may now be regarded as two parallel plate capacitors of area  $S$ , the distance apart of plates being equal to  $d$  and difference of potential  $v - V_1$ , together with two parallel plate capacitors of area  $A - S$ , the distance apart of plates being equal to  $d$  and difference of potential  $v - V_2$ . There are two capacitors of each kind, since there is

an upper and a lower surface to the needle.

The electrostatic energy ( $W$ ) stored in a parallel plate capacitor is expressed as

$$(58) \quad W = \frac{\epsilon_0}{2} \frac{(\Delta V)^2}{d} S$$

In this formula,  $S$  denotes the overlapping area of the plates. Therefore, in the case of the quadrant electrometer, we may write an expression for energy thus,

$$(59) \quad W = \frac{\epsilon_0 (v-V_1)^2}{d} S + \frac{\epsilon_0 (v-V_2)^2}{d} (A-S)$$

The mechanical force tending to turn the needle in the direction of increasing  $\theta$  is given by

$$(60) \quad \frac{dW}{d\theta} = \frac{\epsilon_0}{d} \left[ (v-V_1)^2 - (v-V_2)^2 \right] \frac{dS}{d\theta}$$

since  $S$  is the only term which varies with  $\theta$ . If  $r$  is the radius of the needle and is adjusted so as to lie symmetrically under the intersection of the diameters forming the quadrants, then we have

$$(61) \quad \frac{dW}{d\theta} = \frac{\epsilon_0 r^2}{d} \left[ (V_2 - V_1)(2v - V_2 - V_1) \right]$$

In equilibrium, this torsion is balanced by the torsion couple of the fibre, which tends to decrease  $\theta$ . This couple may be expressed as  $k\theta$ , where  $k$  is a constant depending on the nature of the fibre. The equation of the quadrant electrometer may now be expressed as

$$(62) \quad k\theta = \frac{\epsilon_0 r^2}{d} \left[ (V_2 - V_1)(2v - V_2 - V_1) \right]$$



There are two ways of employing the quadrant electrometer as a device for measuring potential.

#### 6.6 The Heterostatic Method

In this method,  $V_2 > V_1$  and the needle is given a high potential such that

$$2v > V_1 + V_2 .$$

The unknown potential to be measured is applied to one pair of quadrants, while the other pair is grounded. If  $v$  is very large compared to  $V_2$ , and  $V_1$  equals ground potential, equal to zero, then we can write

$$(63) \quad k\theta = \frac{\epsilon_0 r^2}{d} \cdot V_2 \cdot 2v$$

$$\text{or } \theta = CV_2 v$$

where  $C$  is a constant and equal to  $\frac{2\epsilon_0 r^2}{kd}$  .

However, if  $V_2$  is large compared to  $v$ , then the relationship approaches a square law proportionality, since the value of  $\theta$  is now given by

$$\theta = C.V_2.(2v - V_2) .$$

Thus, the deflection of the needle is dependent on three factors. It was found necessary to draw various sizes of quartz fibre to accommodate the readings required. The heterostatic method has the advantage that the polarity of the applied voltage can be determined from the deflection of the needle. Graphs for calibration are shown

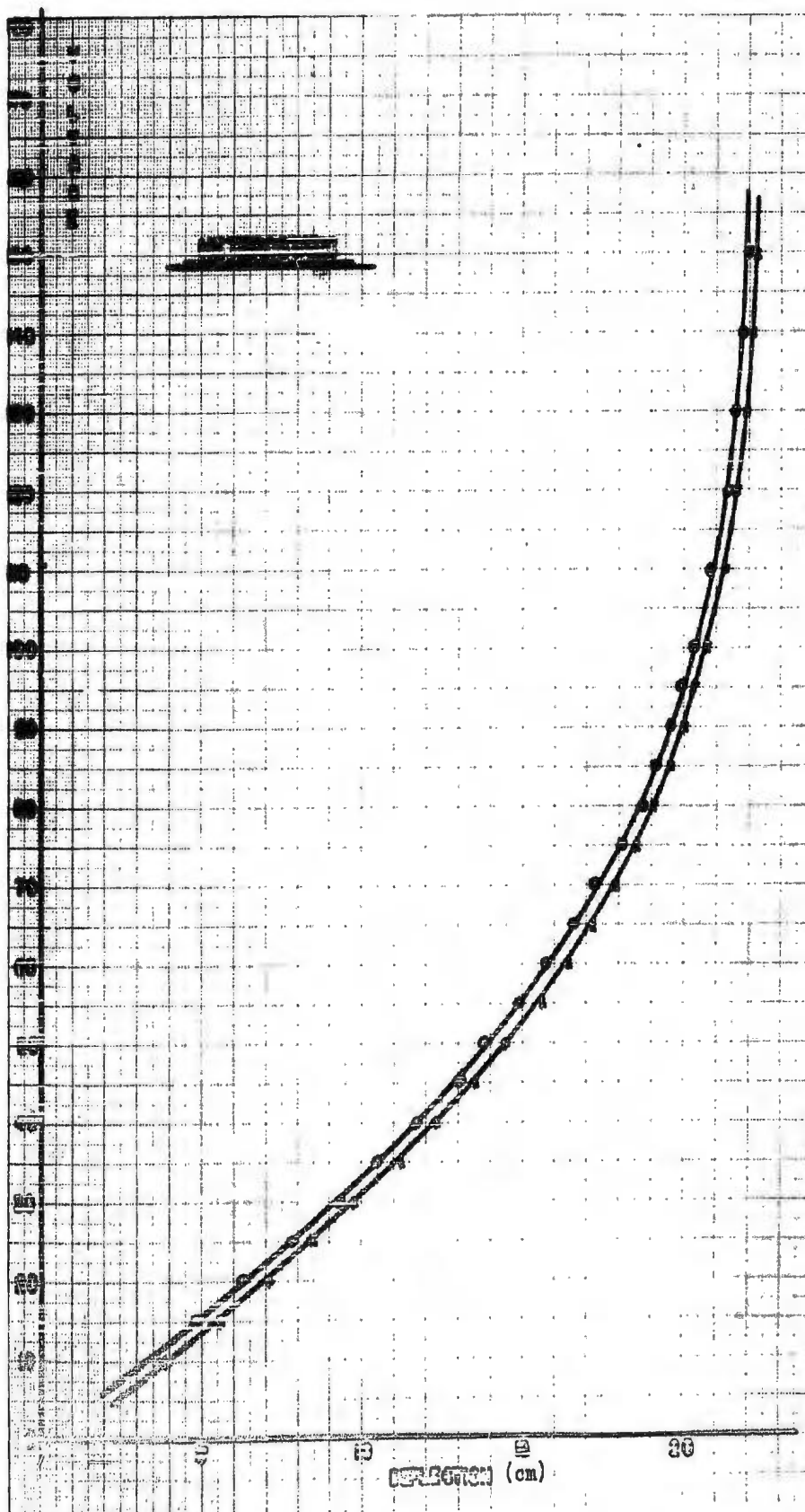


Fig. 17. Quadrant Electrometer Heterostatic Curves

in Fig. (17). This method had the disadvantage, however, that it was difficult to obtain the same potential on the needle on every occasion and, also, the necessity of recharging the needle every time before use.

#### 6.7 Idiostatic Method

In this method, the needle and one pair of quadrants are maintained at the same potential, while the other pair may be grounded. Thus, if  $v = V_2$  and  $V_1 = 0$ , then

$$\theta = C(V_2 - V_1)^2 .$$

The needle will thus be deflected in the same direction for both positive and negative potentials. It is thus impossible to detect the polarity of the potential to be measured from this method. The idiostatic method has the advantage that only one calibration is necessary and no recharging of the needle is required and, consequently, no leakage of charge which would affect the calibration.

#### 6.8 Method of Setting Up the Electrometer

The first requirement was to mount the electrometer on a stable platform to eliminate as much vibration as possible. The vane was then adjusted visually to rest in a horizontal plane spaced midway between the upper and lower surfaces of the hollow quadrants. At the same time, adjustment was made so that the needle rested symmetrically between two sets of quadrants.

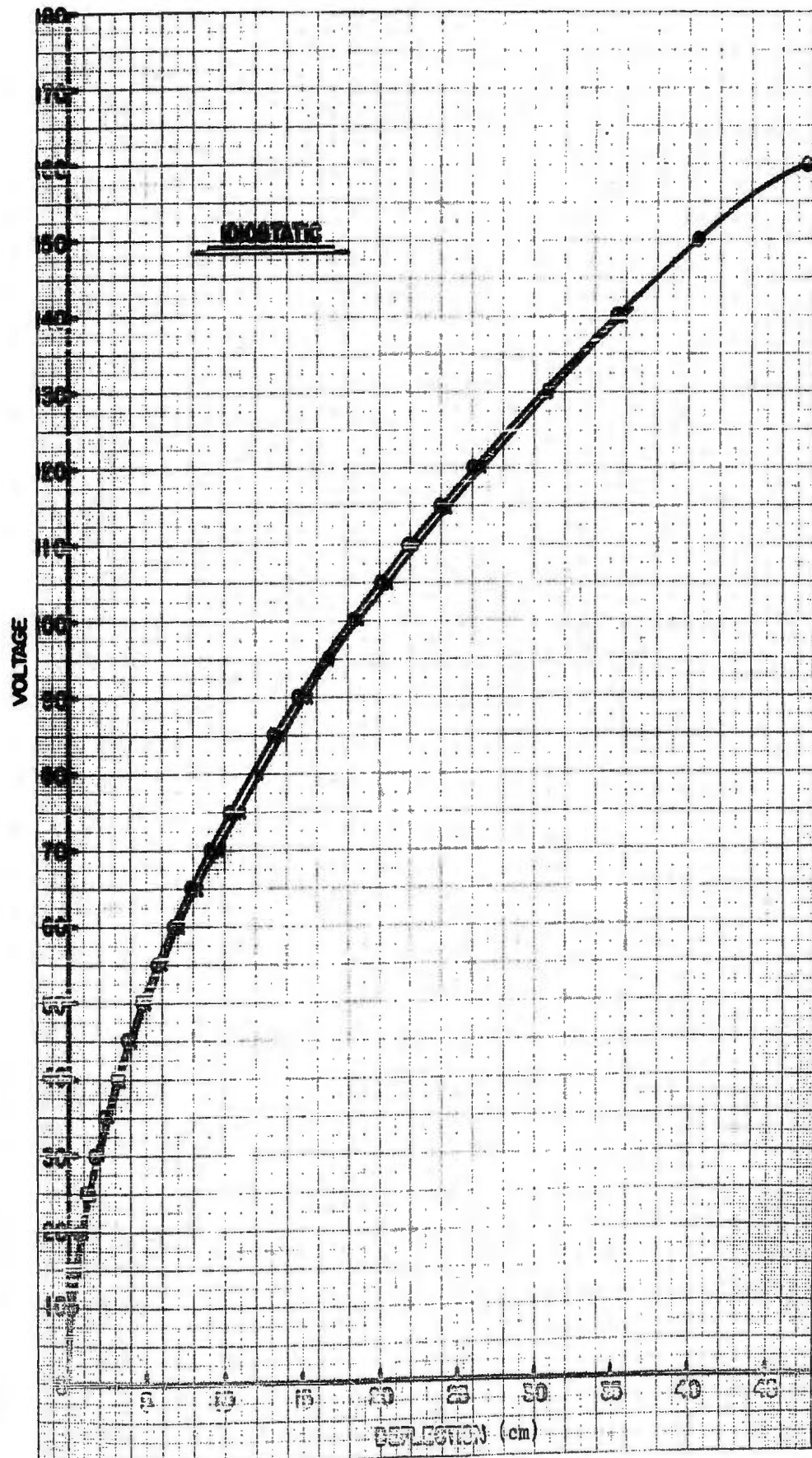


Fig. 18. Quadrant Electrometer Idiostatic Curves

In the idiostatic method of employment, in order to maintain the needle and one set of quadrants at the same potential, the quartz fibre was dipped in a solution of calcium chloride, thus rendering the fibre electrically conductive. The needle was then connected to one set of quadrants - the A quadrants, while the other set - the B quadrants, was connected to a good ground system.

Calibration of the electrometer was obtained by applying known voltages to the needle and the A quadrants. A light beam directed onto a mirror attached to the quartz fibre formed a light spot on a metric scale located about one meter from the electrometer. The graph thus obtained is shown in Fig. (18). This graph of deflection versus voltage provides a quick method of obtaining the potential at any instant, thus ensuring a quick check on the calibration of the potential gradient meter.

#### 6.9 The M-Type Potential Gradient Mill

The M-type mill was the term used by Mapleson and Whitlock to distinguish between mills producing sinusoidal waveform outputs from mills producing triangular waveform outputs. The latter types were classified under the term S-type mills. The first forms of these types of instruments were originally designed by Russelveldt (1926) and Mathias (1926). The M-type mill described here consists essentially of a conducting system of small capacity which is alternately and regularly exposed to, and then screened from the electric field by the movement of a rapidly rotating earthed metal screen.





#### 6.10 Details of Construction (Fig. 19)

The construction is essentially similar to that used by Malen and Schonland (1950). The stator consists of a tufnol disc 23.5 cm in diameter. The conducting system is embedded in this disc and consists of 18 metal studs with diameter 6.5 mm and arranged in a circle of 20 cm diameter. The metal discs are connected electrically below the disc. The charge on these discs given by

$$(25) \quad \sigma = \epsilon E$$

is thus directly proportional to the atmospheric field  $E$ . During the screening period, the charge leaks to earth through a high impedance. The screening rotor disc is 23.5 cm in diameter, 1.3 thick and provided with 18 equally spaced holes of diameter 2.0 cm, and arranged such that their centres lie directly above the centres of the studs in the conducting system. The spacing between the two discs was set at 2 mm. This spacing between the stator and rotor discs is not critical but the effects of various spacing distances is considered in the theory of the field mills (see later).

The screening disc is driven by a 3-phase induction motor. A pulley and belt reduction drive of ratio 2 : 1 resulted in a screening rotor angular velocity of 1600 RPM. This gave rise to a pulsating signal output at a frequency of 480 c/s. An essential requirement is a good grounding connection to the rotating shaft to which the screening disc is attached. This proved to be a source of trouble at the

beginning of the experiment as the noise level increased substantially with deterioration in the electrical contact between the shaft and the connecting grounding contact. This trouble was finally eliminated by constructing a spring loaded carbon brush device which maintained constant pressure against the rotating shaft and thus provided good electrical contact. The framework supporting the device is built of angle iron with welded joints. The whole framework is enclosed in a rectangular metal box which has a good ground connection.

#### 6.11 Details of Motor

Type - 3-phase induction synchronous  
Speed - 3200 RPM  
Voltage - 208 volts  
Power - 1/4 horsepower.

#### 6.12 Details of Screening Rotor Speed

Diameter of motor shaft pulley - 5 in.  
Diameter of screening disc shaft pulley - 2½ in.  
Speed of screening disc - 1600 RPM  
Frequency of output signal - 480 c/s.

A frequency of 480 c/s is sufficiently high to be free from mains interference. This signal frequency is also easily amplified by standard electronic circuits. The output waveform approximated very nearly to a pure sinusoidal waveform. The output amplitude varies with



the applied field and, in the laboratory with artificial fields applied to a cover plate over the meter, this amplitude varied from 2 to 8 mV.

#### 6.13 Electrical Measurements on Output

Insulation resistance (running)	- 75 kohms.
Insulation resistance (stationary)	- 78 kohms.
Capacitance (running)	- 110 - 120 pf.
Dissipation factor	- 0.02.

#### 6.14 Location of Measurements

The measurements were made at Memorial University, St. John's, Newfoundland, at a location situated  $47^{\circ} 34.3' \text{ N}$  and  $52^{\circ} 44.0' \text{ W}$ . The meter was located on top of the Physics/Chemistry Building at a height of 89.5 ft. above ground level and 279.5 ft. above sea level. Due to the nature of the weather, it was found necessary to protect the meter inside a wooden box, which also acted as an anchoring device. Originally, the top of the box was removed when measurements were being taken. Later it was found that the wooden box was quite transparent to the electric field and continuous recording was commenced on the 1st of October 1968. The top of the Physics/Chemistry Building is by no means an ideal site for potential gradient measurements. The location is shown in Fig. (16). There are numerous metal outlets for the air ventilation system of the building. What is more troublesome is the fact that the outlets for chemical fumes are located on this roof, also. Furthermore, the power

distribution station is located only about 300 ft. from the site of measurements.

#### 6.15 Theory of Operation of Field Mill

Let  $C$  = capacitance of stator to earth.

$R$  = resistance of stator to earth.

$E$  = electric field.

$a$  = area of stator studs exposed to atmosphere.

$A$  = maximum area of stator studs.

$\omega$  = angular velocity.

The charge induced on the stator studs when an area  $a$  is exposed to a field  $E$  is given by

$$(64) \quad q = \epsilon_0 E a$$

and the maximum value of the induced charge is given by

$$(65) \quad Q = \epsilon_0 E A$$

Since the waveform is sinusoidal, it can be expressed by the expression,

$$(66) \quad A/2 (1 + \sin \omega t)$$

$$(67) \quad q = \epsilon_0 E A/2 (1 + \sin \omega t)$$

$$(68) \quad = Q/2 (1 + \sin \omega t)$$

Now the current  $i$  is given by

$$(69) \quad i = dq/dt$$
$$= \omega Q/2 \cos \omega t$$

The peak value of  $q$  is given by

$$\begin{aligned} (70) \quad I &= \omega Q/2 \\ &= \omega \epsilon_0 EA/2 \end{aligned}$$

The peak voltage across  $C$  and  $R$  is given by

$$\begin{aligned} (71) \quad V &= IZ \\ &= \omega \epsilon_0 EAZ/2 \end{aligned}$$

$$(72) \quad \text{where } Z = R/(\omega^2 C^2 R^2 + 1)^{1/2}$$

$$(73) \quad \therefore V = (\omega \epsilon_0 EA/2) \cdot R/(\omega^2 C^2 R^2 + 1)^{1/2}$$

This relation will be true only if  $a$  varies sinusoidally.  $C$  will vary somewhat in synchronism with  $a$  and this will introduce a slight error.

However, if these effects are small and  $\omega^2 C^2 R^2 \gg 1$ , then

$$(74) \quad V = \epsilon_0 EA/2C$$

Thus, the output voltage is

- (1) proportional to the electric field  $E$ .
- (2) proportional to the area of the plates exposed.
- (3) inversely proportional to the stator-ground capacitance.

According to the above expression, the signal output is independent of the frequency, and the resistance of the stator to the ground.

The position of the rotor relative to the stator is somewhat of a compromise, since both output voltage and Volta effects decrease with increasing rotor-stator spacing. The existence of Volta potentials on the exposed surfaces of the measuring system gives rise to apparent fields called the residual field.

### 6.16 The Response Time of the Field Mill

The response time of potential gradient meters has been defined differently by two authorities on the subject, namely,

- (1) time required for  $(V_n - V_f)/V_f$  to become equal to  $1/e$

where  $V_n$  = voltage after  $n$  half cycles

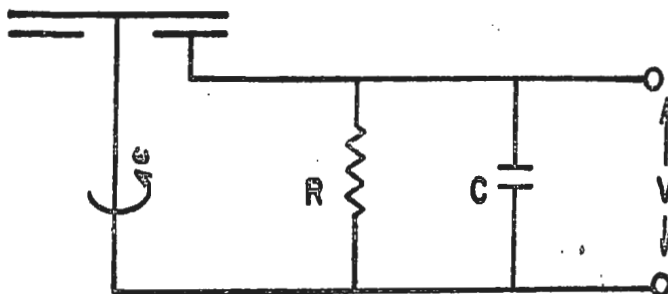
and  $V_f$  = voltage ultimately attained.

This method was used by K. N. Groom (1965).

- (2) number of half-cycles before the amplitude reaches 99% of its final steady value.

This method was used by Malan and Schonland (1950).

The equivalent circuit of the stator-rotor arrangement as far as the resistive and capacitive effects are concerned, and including the input circuit of the field effect transistor is shown in the diagram below.



When a change  $\Delta E$  occurs in the electric field, a corresponding change  $\Delta \sigma$  takes place in the bound charge on the upper surfaces of the conducting studs. Thus,

$$(70) \quad \Delta \sigma = \epsilon_0 \Delta E$$

where A is the area of the exposed surfaces of the studs. This change takes place instantaneously and, provided it occurs when the studs are exposed, the initial response of the instrument is instantaneous. However, the final steady value of the amplitude is less than the initial response.

Let T sec. be the duration of either the screening or exposure interval and, for simplicity, let us assume that they both start and stop instantaneously.

C is the capacity of the system including the input circuit.

R is the total resistance.

Then the rate of discharge of the system during the screening interval is proportional to

$$(71) \quad \alpha = e^{-\frac{T}{CR}} .$$

Successive half-cycles of exposure and screening result in changes in the charge on the studs. These changes can be expressed by the terms of the convergent series

$$(72) \quad \Delta\sigma \sum_0^n (-\alpha)^n .$$

The final steady amplitude is thus given by

$$(73) \quad \frac{\Delta\sigma}{1 + \alpha}$$

which is attained when n is very large.



The output signal frequency of the mill is 480 c/s and, therefore, this gives a value of approximately one millisec. for the screening or exposure interval. The capacitance of the mill and the input circuit of the field effect transistor is about 100 pf.

The resistance between the stator and ground is approximately  $10^7$  ohms.

$$\text{Since } T = .001 \text{ sec.}$$

$$C = 10^{-10} \text{ F}$$

$$R = 10^7 \text{ ohms}$$

$$\therefore T/CR = 1.$$

Thus, the amplitude is equal to  $1/e$  of its final value in about one millisec., which is the time of exposure of the studs.

Alternately, if we define the response time as the number of half-cycles ( $N$ ) required until the amplitude attains 99% of its final steady value, we can proceed in the following manner.

The nth expression of equation (72) can be written as

$$(74) \quad \left[ 1 + (-1)^n \alpha^{n+1} \right] \frac{\Delta \sigma}{1 + \alpha} .$$

Hence, the required number  $N$  is given by

$$(75) \quad (.37)^{N+1} = .01$$

$$\therefore N = 3.6 .$$

Thus, the signal output amplitude is 99% of its final value after about 4 half-cycles.

A sudden change in the field is thus manifested by an equally sudden response of the field mill. This initial response decreases to  $\frac{1}{1 + \alpha}$  of its initial value, i.e., the final steady value will be  $\frac{1}{1 + 0.37} = 70\%$  of its initial peak value. In the design of the amplifying circuit, the time constant was chosen so as to be within this limit also.

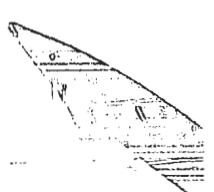
#### 6.17 Design Requirements for Amplifier

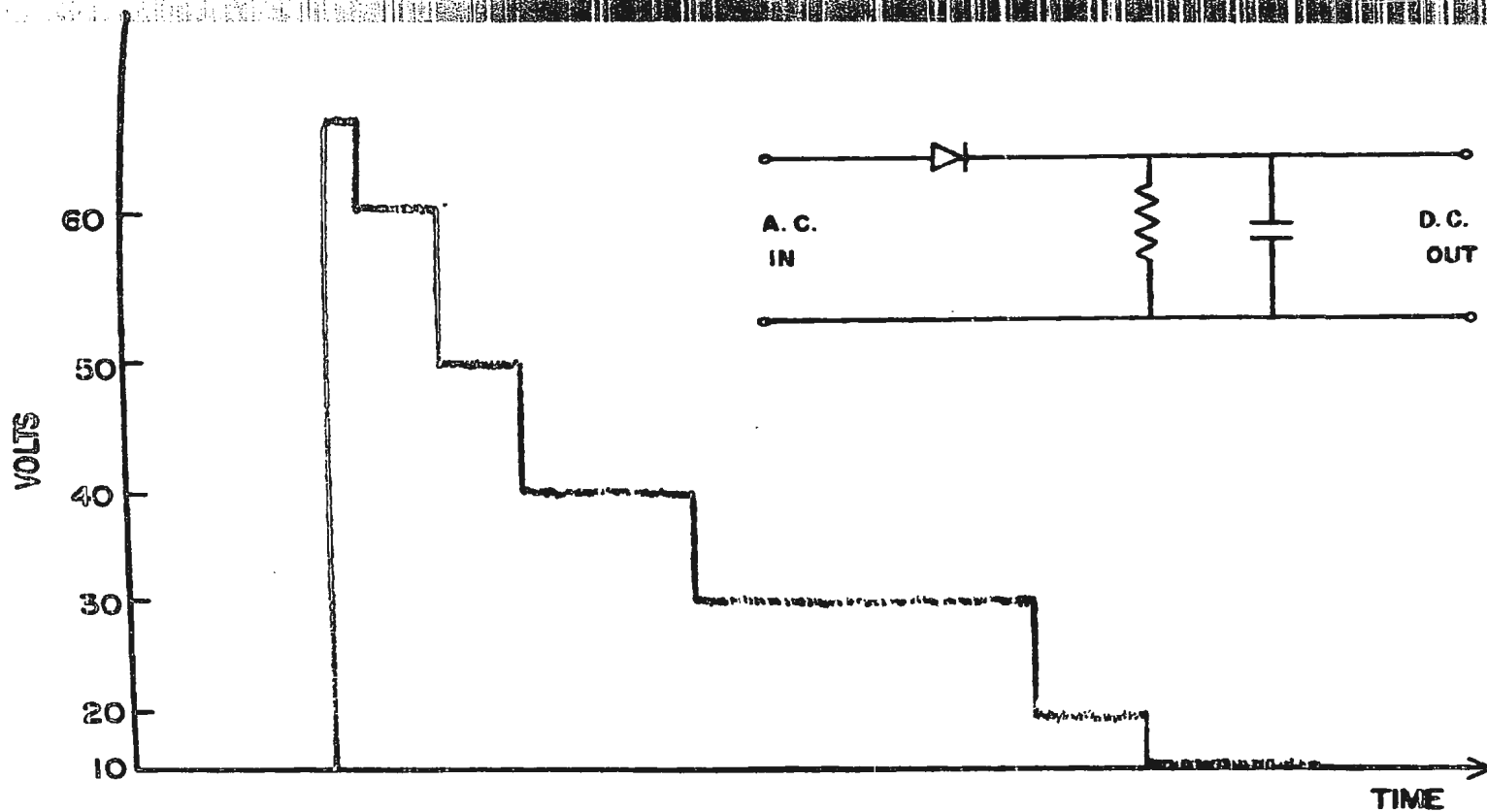
It was found desirable to design an amplifier with the following characteristics:

- (1) Gain of at least 30 db.
- (2) Stability of the zero level.
- (3) Low noise level.
- (4) Insensitive to variations in the supply voltage.
- (5) Provision to alter the phase of the signal.
- (6) Provide a good sine wave output to the phase sensitive detector.
- (7) Provision to control the zero setting of the output.
- (8) Operate on low power d.c. currents to eliminate interference between the various circuits.
- (9) Have a high input impedance and a low output impedance.

#### 6.18 Development and Modifications

In the original instrument designed by Malen and Schonland (1950), the output of the mill was fed by a cathode follower circuit to





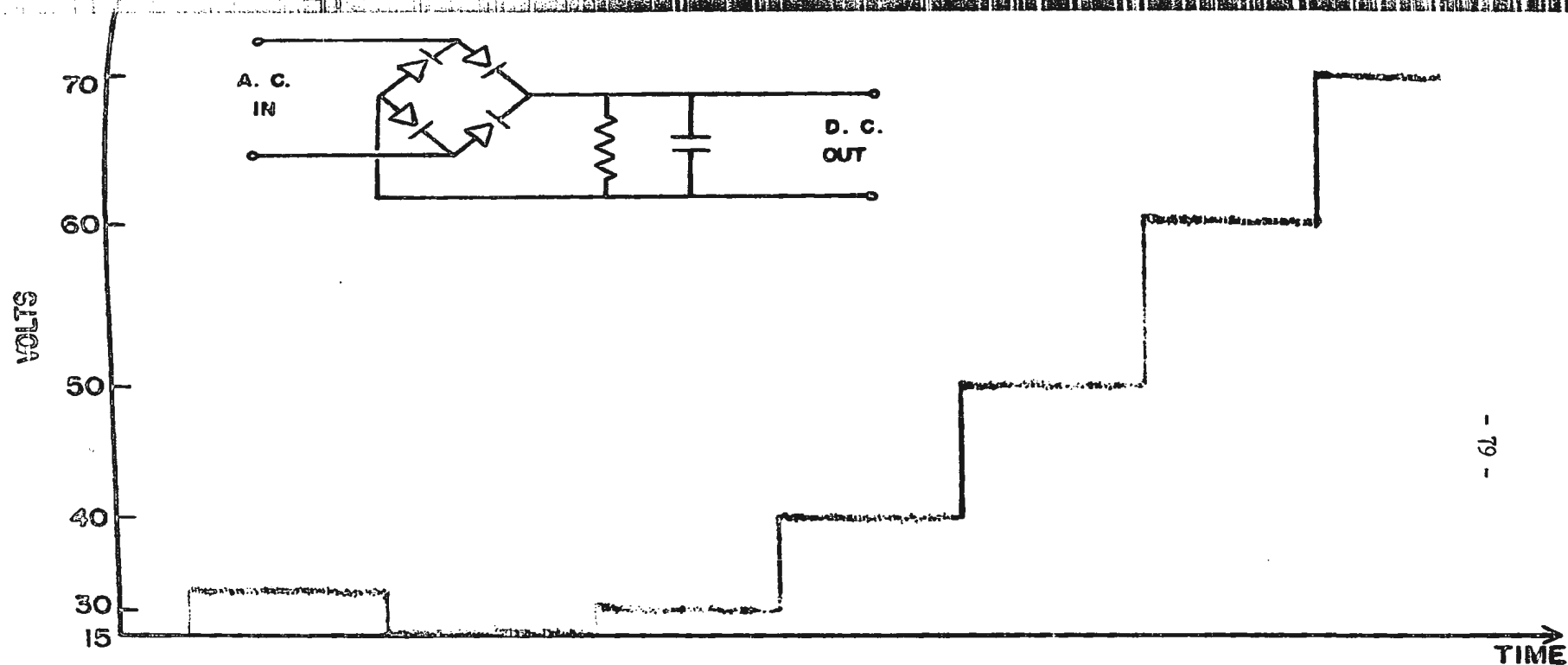
- 78 -

Fig. 20. RESPONSE OF MILL TO EQUAL INCREMENTS OF NEGATIVE VOLTAGE ON COVER PLATE

A SINGLE CRYSTAL DIODE DETECTOR USED.







- 79 -

Fig. 21. RESPONSE TO EQUAL INCREMENTS OF + VOLTAGE ON COVER PLATE

USING A 4-CRYSTAL BRIDGE DETECTOR. TRACE ON LEFT SHOWS RESPONSE OF METER IN LAB WITH COVER PLATE GROUNDING.

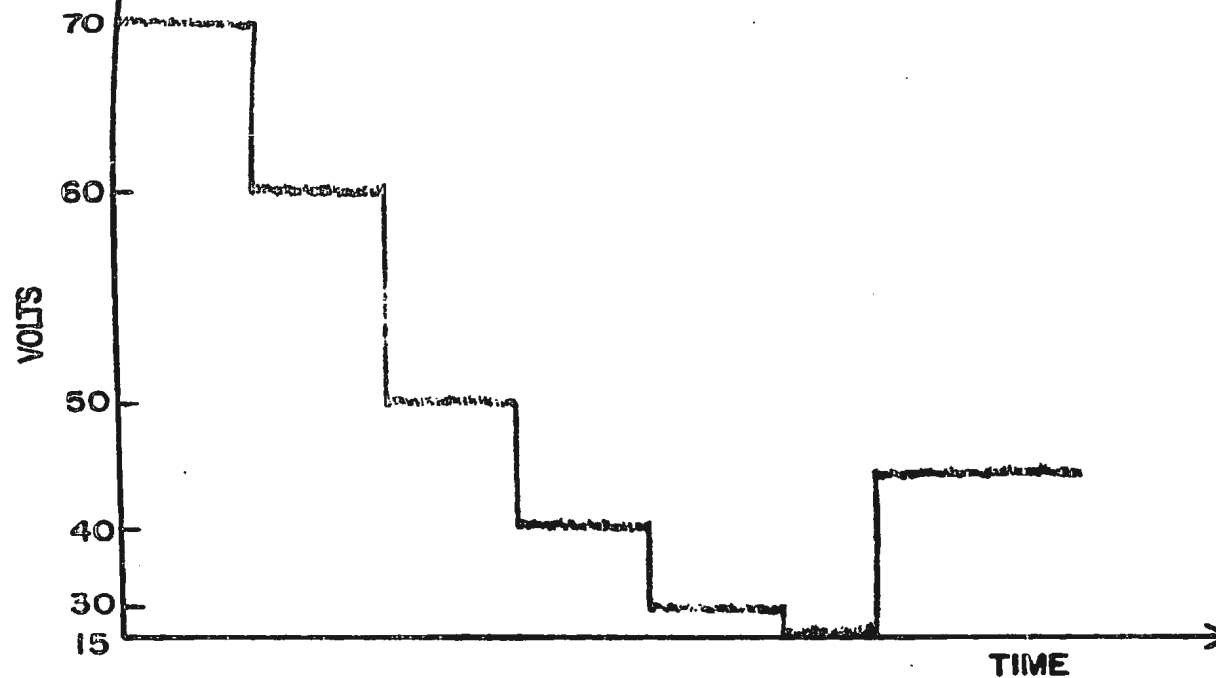


Fig. 22. RESPONSE TO EQUAL INCREMENTS OF + VOLTAGE ON COVER PLATE

RIGHT HAND TRACE SHOWS RESPONSE OF METER IN THE LAB WHEN COVER PLATE NOT IN POSITION. RESIDUAL VOLTAGE CANCELLED OUT BY COVER PLATE + VOLTAGE OF ABOUT 15 V.

the amplifying stages and the output displayed on a cathode ray screen. Recording of the trace was effected by photographing the screen. The polarity of the field was detected by additional studs which fed a "pip" which appeared either on the top or bottom of the waveform every ninth cycle according to the polarity of the field.

In the instrument described here, the output of the mill was amplified sufficiently to allow detection by tubes or crystals. The original results obtained are shown in diagrams 20, 21 and 22.

This method suffered from two disadvantages:

- (1) The rectified output showed a non-linear response either at the low or high signal levels.
- (2) The polarity of the field had to be determined by some other method.

In the final arrangement, a phase sensitive detector was designed and all circuits were transistorized to eliminate the need for cables carrying a.c. currents. The added advantage of a phase sensitive circuit is that it will also

- (1) give a linear response
- (2) record the polarity of the field
- (3) act as a narrow band-pass circuit.

The response of the mill using the transistorized phase sensitive detector for incremental voltage steps of 5 V is shown in Fig. (23a). This graph was obtained with minimum sensitivity of the recorder to prevent the readings going off scale. The response of the meter to

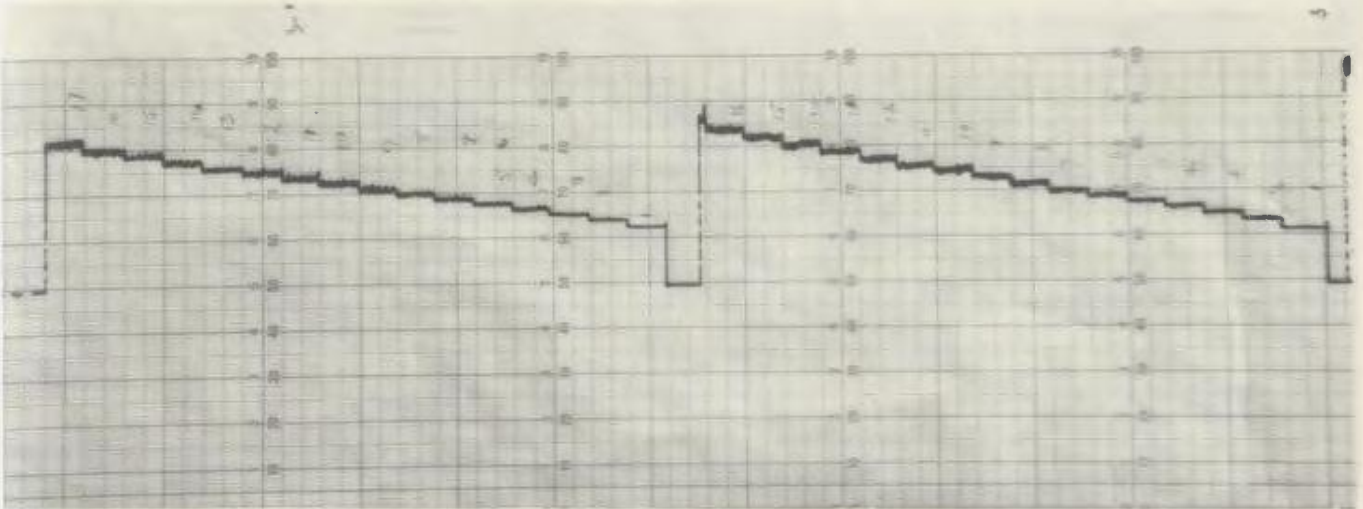


Fig. 23a. Response of Mill using Phase Sensitive Detector  
The Steps are Due to 5V Increments

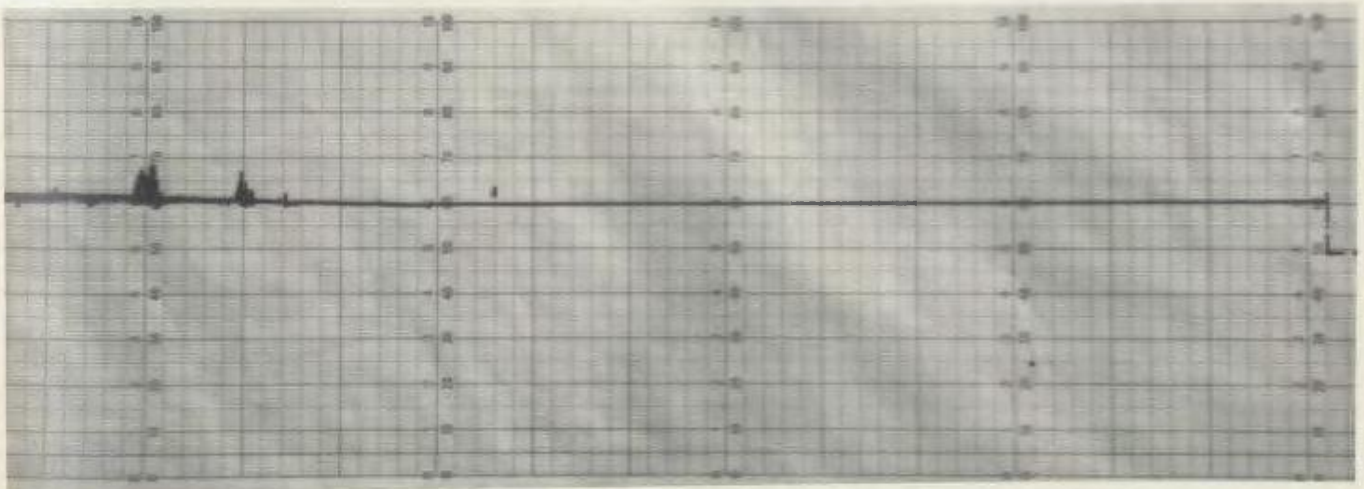


Fig. 23b. Response of Mill to Zero Signal

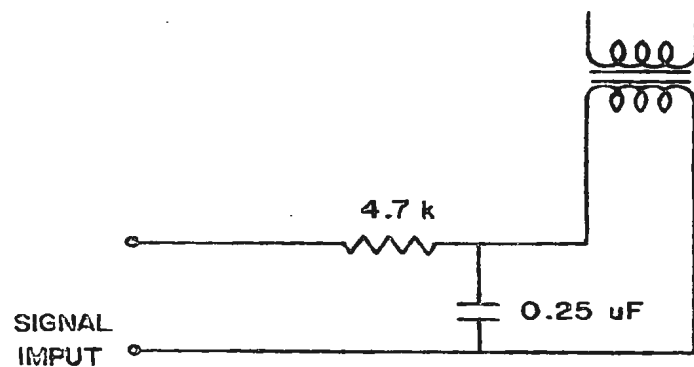


FIG. 24a. FILTER CIRCUIT INCORPORATED  
TO PREVENT FEEDBACK TO

AMPLIFYING CIRCUIT.

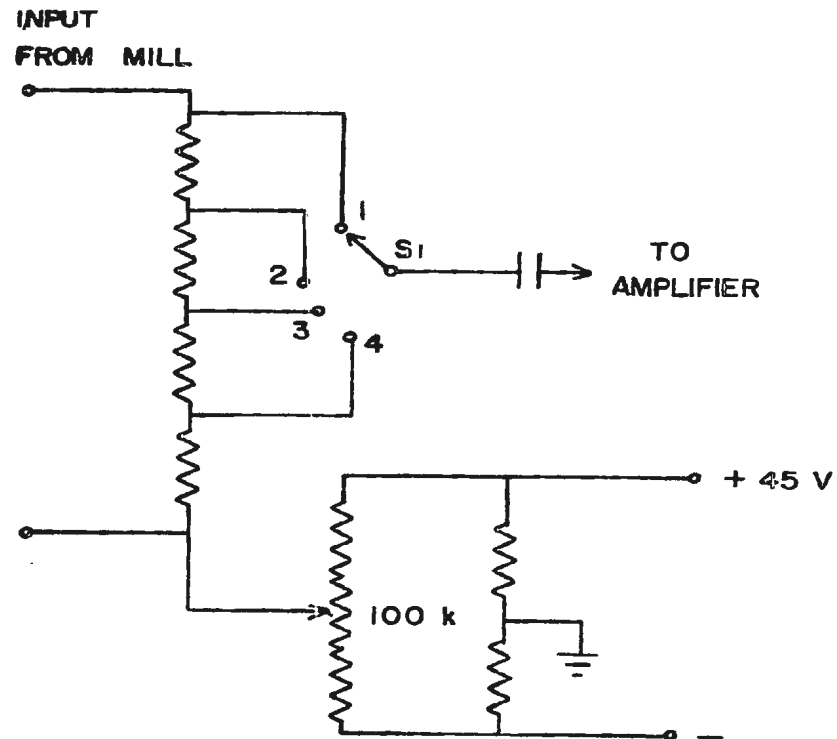


FIG. 24b. CIRCUIT MODIFICATION ADOPTED TO  
OFFSET THE RESIDUAL VOLTAGE.

zero signal (obtained by covering the mill with a well-grounded metal box) is shown in Fig. (23b). This shows the stability of the electronic circuits and the low noise level.

Initially, trouble was encountered in preventing feedback from the phase sensitive circuit to the amplifier. This was finally reduced to a workable level by using separate power supplies and incorporating a filter circuit shown in Fig. (24a).

As mentioned earlier, an inherent error of the field mill is the residual voltage generated by volta potentials in the rotating head of the mill. This shows a constant field value even when the signal input to the mill is zero. Its effect is most serious at high sensitivity level where the needle is liable to go off scale. The circuit finally adopted to overcome this residual field is shown in Fig. (24b), and consists simply of a backing-off voltage to reduce this signal to zero.

#### 6.19 The Amplifying Circuit

A block diagram of the amplifying and detection circuit is shown in Fig. (25). The circuit diagram is shown in Fig. (26).

#### 6.20 The Preamplifier

In order to eliminate the interference due to the a.c. power supply required for vacuum tube operation, recourse was made to a completely transistorized electronic circuitry. The disadvantage in the utilization of transistors is in their low input impedance which tends to load the previous stage.

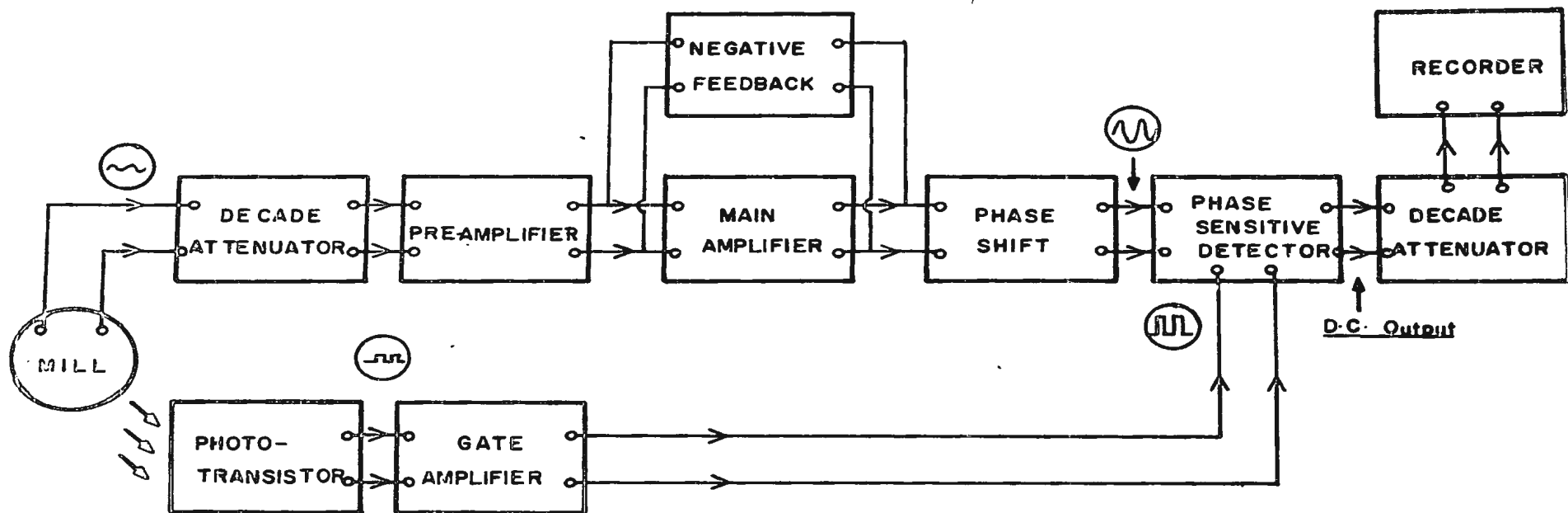


Fig. 25. Block Diagram of Electronic Circuits

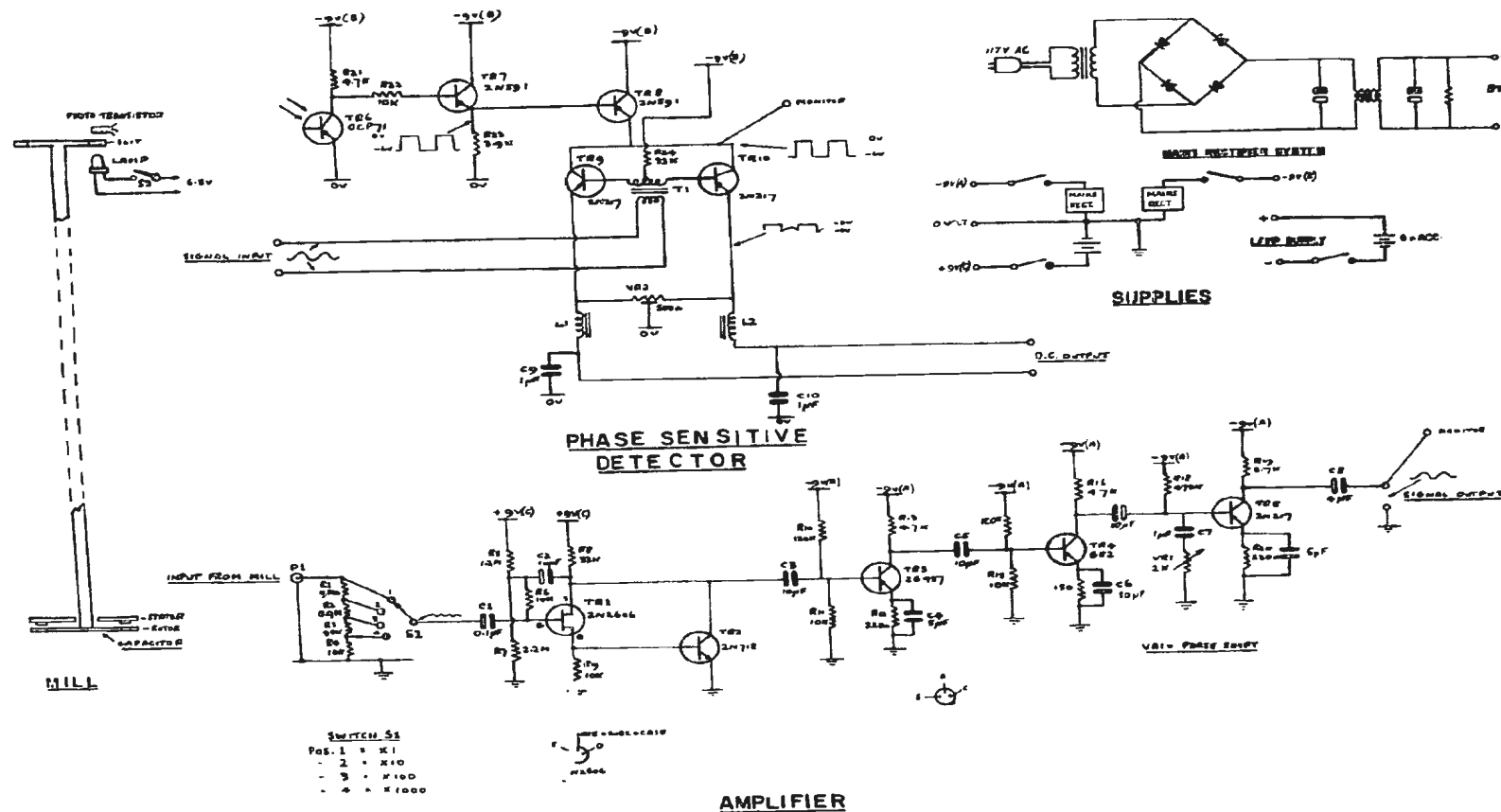


Fig. 26. Circuit Diagram of Electronic Circuits



The charge induced on the stator studs created an almost perfect sinusoidal waveform. This voltage developed to a value of 4 mV in amplitude in laboratory tests and before any amplification had been applied. This signal was due mostly to the residual voltage and the electrode effect. This signal voltage was developed across a capacitance of about 100 pf and a resistance of 75 megohms. Coupling to the amplifying stage was therefore achieved by a preamplifying stage employing a field effect transistor in cascade with an ordinary bipolar transistor. The main purpose of inserting the preamplifying stage was to provide the proper matching between the output of the mill and the input of the transistor amplifier.

The field effect transistor is a majority carrier controlled device wherein the resistance of a semiconductor channel is modulated by a transverse electric field. This offers a voltage controlled device which absorbs practically no current and therefore offers a high input impedance of the order of the value of the gate resistance  $R_g$  which, in this circuit, has a value of 22 megohms. The data for the 2N718 transistor is tabulated below.

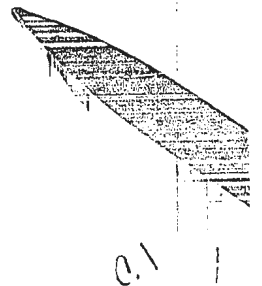
$$I_c = 125 \text{ uA}$$

$$h_{fe} = 30$$

$$h_{ie} = 5000 \text{ ohms.}$$

The current gain of this arrangement is given by the equation

$$(76) \quad h'_{fe} = h_{fe} \frac{R_d}{R_d + h_{ie}}$$



where  $R_d$  is the drain resistor and equals 15000 ohms.

$$h'_{fe} = 22.5$$

The voltage gain is given by

$$(77) \quad A_v = \frac{e_{out}}{e_{in}} = \frac{g_m h'_{fe} R_s}{1 + g_m h'_{fe} R_s}$$

$$= 0.98$$

The output resistance given by the formula

$$(78) \quad R_{out} = \frac{R_s}{1 + R_s g_m h'_{fe}}$$

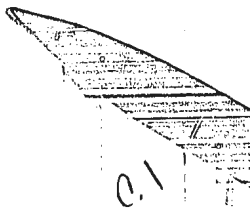
$$= 580 \text{ ohms (approximately).}$$

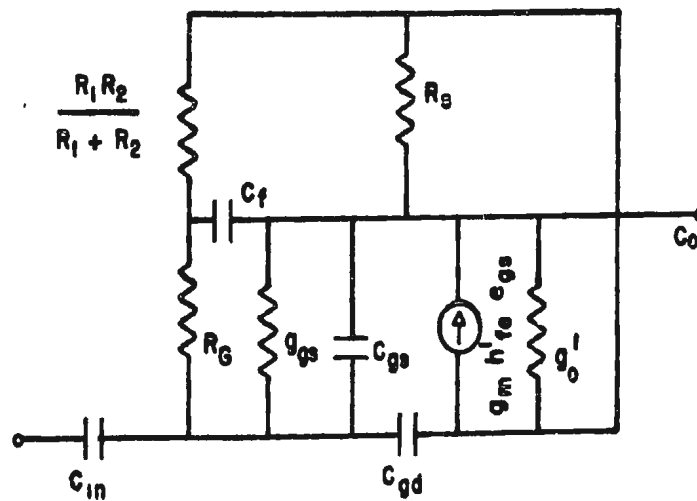
The 2N2606 is a low level, high input impedance device with a low capacitance.

The effective impedance of the circuit is considerably higher due to the boot strapping effect of  $C_f$ . If the reactance of  $C_f$  is small compared to the parallel resistance of the gate bias divider, the input resistance is given by

$$(79) \quad R_{in} = \frac{1}{(1-A_v)\left(\frac{1}{R_g} + \frac{1}{r_{gs}}\right) + \frac{1}{r_{gd}}}$$

This equation emphasizes the importance of maintaining a high value for  $R_g$  if high input resistance is to be maintained. The equivalent gate to drain  $r_{gd}$  and gate to source resistance  $r_{gs}$  are in excess of  $10^{10}$  ohms.

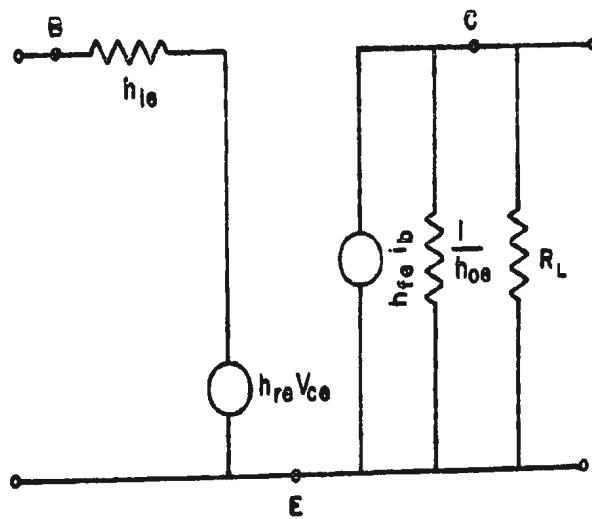




EQUIVALENT CIRCUIT OF THE PREAMPLIFIER

Fig. 27

0.1



EQUIVALENT CIRCUIT OF  
TRANSISTOR AMPLIFYING STAGE

Fig. 28

0.1

The calculated a.c. input resistance using equation (79) is approximately 1250 megohms.

The preamplifier thus provides a very high input impedance and a low output impedance thus providing the necessary coupling from the mill to the transistor amplifier. The gate current of the 2N2606 FET is less than  $10^{-9}$  amp. at room temperature. Furthermore, a blocking capacitor C isolates this current from the mill so that no interference to the signal from the mill is possible. The equivalent circuit of the preamplifier is shown in Fig. (27).

#### 6.21 The Main Amplifier

The equivalent circuit of the transistor amplifying stage is shown in Fig. (28).

$h_{ie}$  = input base resistance.

$h_{oe}$  = output conductance.

$h_{fe}$  = forward current gain for common emitter configuration.

$h_{re}$  = reverse voltage ratio.

$i_b$  = base current.

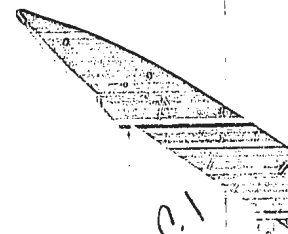
$R_1$  = load resistance in collector circuit.

From the equivalent circuit we can write

$$(80) \quad v_{in} = i_b h_{ie} + h_{re} v_{ce}$$

$$(81) \quad v_{out} = \frac{h_{fe} i_b R_1}{h_{oe} + 1}$$

$$(82) \quad \text{voltage gain} = \frac{v_{out}}{v_{in}} = \frac{\frac{h_{fe} i_b R_1}{h_{oe} + 1}}{h_{ie} i_b + h_{re} v_{ce}} \cdot$$

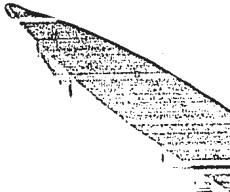


The voltage amplifying stages are provided by the transistors Tr3, Tr4 and Tr5. In the first of these stages,  $R_{10}$  and  $R_{11}$  provide a potential divider for bias and the emitter resistance  $R_{12}$  is incorporated for stability against thermal runaway. The values of the emitter resistors were chosen low values to allow maximum voltage gain through the voltage drop across the collector resistors. The emitter bypass capacitor was reduced from a normal value of 50 or 100  $\mu\text{F}$  to 5 or 10  $\mu\text{F}$ . At the frequency employed, this provides insufficient biasing of the emitter resistance and thus ensures a negative feedback loop from the output to the input circuit.

The gain of this circuit was experimentally found to be about 30. The second stage incorporating Tr4, which is essentially a similar circuit, was also found to have a similar gain.

Tr5 was biased through the series resistor R18. C7 and VR1 provide a phase shifting network capable of a phase change of up to  $5^\circ$ . A rough synchronization of phase relationship with the reference was achieved by mechanical setting of the rotating discs providing the signals, after which VR1 was used for finer control.

The collector load of Tr5 was reduced to 2.7 kilohms, thus affording a low input impedance for matching the output of this stage to the primary of the input transformer of the phase sensitive detector. The gain of this stage which was more of a power amplifying stage was thus reduced to less than 2. The total possible gain was thus around 50 db. Reducing the emitter bypass capacitors provided a negative feedback loop providing about 20 db.



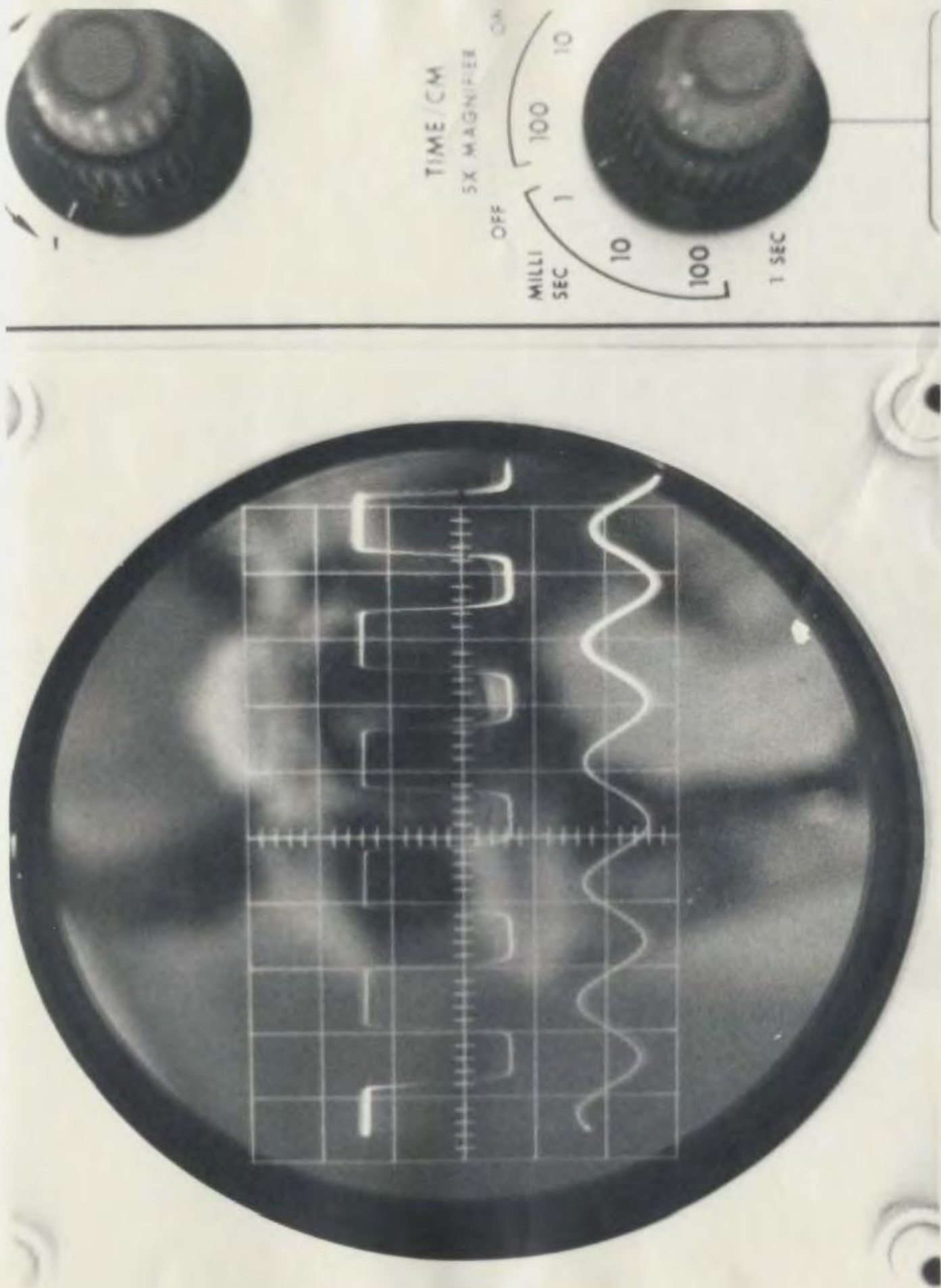


Fig. 29. Phase Relationship between Signal and Reference Voltages

## 6.22 The Phase Sensitive Detector

The signal required to act as a reference source was obtained by means of Tr6 - an OCPT1 photoelectric cell. A slotted wheel mounted on the same shaft as the rotor and having the same number of slots interrupted a light beam to the photoelectric cell. Tr7 wired as a DC amplifying stage switched the base of the transistor Tr8 such that the supply current to the pair of transistors Tr9 and Tr10 was in the form of a square pulse at the same frequency as the signal output from the mill. The phase relationship of the signal and reference signals is shown in Fig. (29). Depending on the polarity of the field, either Tr9 or Tr10 conducted producing a DC voltage output.

The filtering circuit  $L_1$ ,  $L_2$ ,  $C_9$  and  $C_{10}$  constituted a low pass filter. This has the added effect of improving the signal to noise ratio.

The DC output of the phase sensitive circuit is applied to a Westronics decade divider and then to a span and zero adjustable unit before entering the Westronics pen recorder.

## 6.23 Measurement Errors

The main errors to which a field mill is subjected to may be classified as follows:

- (1) the residual voltage.
- (2) drift.
- (3) noise.



The effect of the residual voltage is shown in Fig. (21).

This is a steady field which persists even when the field meter is completely shielded by a metallic screen. It is due to the development of contact potentials between the stator and adjacent surfaces, to volume and surface charges on insulators. Minimizing of this potential has been achieved by Nathan and Anderson (1965) by plating the exposed surfaces with highly polished chrome plating over a thin gold substrate. A more practical method has been to return the stator resistance to an adjustable d.c. bias voltage (Fig. 24b).

Drift is defined as the relatively slow variation in the residual voltage caused by changes in the responsible contact potential difference and charge distributions. Noise for the most part is due to electromagnetic radiation from sources such as arcing brushes, microphonics due to vibration, and to thermal noise in the input circuit.

For a bandwidth B cps and a parallel RC circuit at absolute temperature T, the mean square thermal noise voltage is given by

$$(83) \quad V_n^2 = 4 KTBR_\omega$$

where K = Boltzmann's constant

$Z_\omega$  = equivalent series impedance of the input circuit at angular frequency  $\omega$ .

The amplifier used has a flat bandwidth of about 20 KHZ ranging from the points where the response is down by 10 db. The signal to noise ratio could thus be reduced much further by designing a tuned amplifier with a very narrow response around the 480 C/S frequency.



## CHAPTER 7

### RESULTS AND DISCUSSION

#### 7.1 Measurements of the Potential Gradient

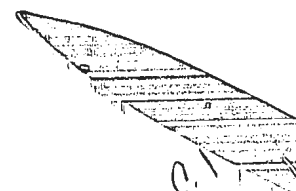
According to the Working Group of the IQSY of the joint committee of Atmospheric and Space Electricity, the atmospheric "fair weather" electrical condition was defined as follows:

"A fair weather period occurs when and where the influence of the atmospheric electrical local generators on the measured value is far less than the influence of global generators. This requires the exclusion of all periods with hydrometeors at the station ....."

Previously, the definition was more restrictive, in that a fair weather observation excluded the presence of low and mean clouds and any fresh winds. Thus, some observers restricted their observations to clear skies and winds at less than 5 mph. During the period that the following observations were conducted, the conditions for "fair weather" observations were rare. Consequently, the curves obtained show the effects of disturbed weather on the electric field.

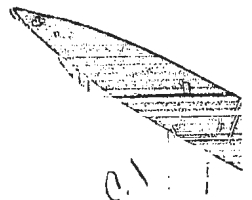
During the period 1957 - 1965, Gherzi made continuous recording of the electric field at Montreal. He reports from his observations that the potential gradient in those instances when maritime air was sweeping his locality was much less than when they were under the influence of Polar air masses. The reasons put forward for this difference were that:

In polar air, the minute particles suspended in the atmosphere are composed of rock and plant matter and are not hygroscopic. Maritime



air, on the other hand, contains suspended particles of chemical compounds such as chlorides, sulphides, bromides, etc., and these are hygroscopic. The resistivity of the air column is different according to the two types of aerosols. Continental polar air is also found to be more subsiding than the maritime air which is mostly convective. Maritime air would thus affect the columnar air resistance to a much higher altitude and, being more conductive, the effect would be to decrease the electric field whereas the polar air would increase the field.

Another aspect of the field found in these recordings was the number of sign reversals of the field. Confirmation of these reversals was given by the quadrant electrometer when connected heterostatically. These changes cannot be attributed to the changes in resistivity, nor to the changes in the dielectric constant of the atmosphere which is highly dependent on the humidity. Since 1956, many workers have reported the variations of the electric field and other basic electric parameters of the atmosphere. These were reported to occur about one to two hours before the onset and also before the dissipation of fog. The recordings made here show very strong agitation mostly during the duration of the fog and the extent of this variation varied with different observations. In some of the recordings made during the fog, strong negative spikes are observed. Positive going spikes are rare but did occur during a local thunderstorm.



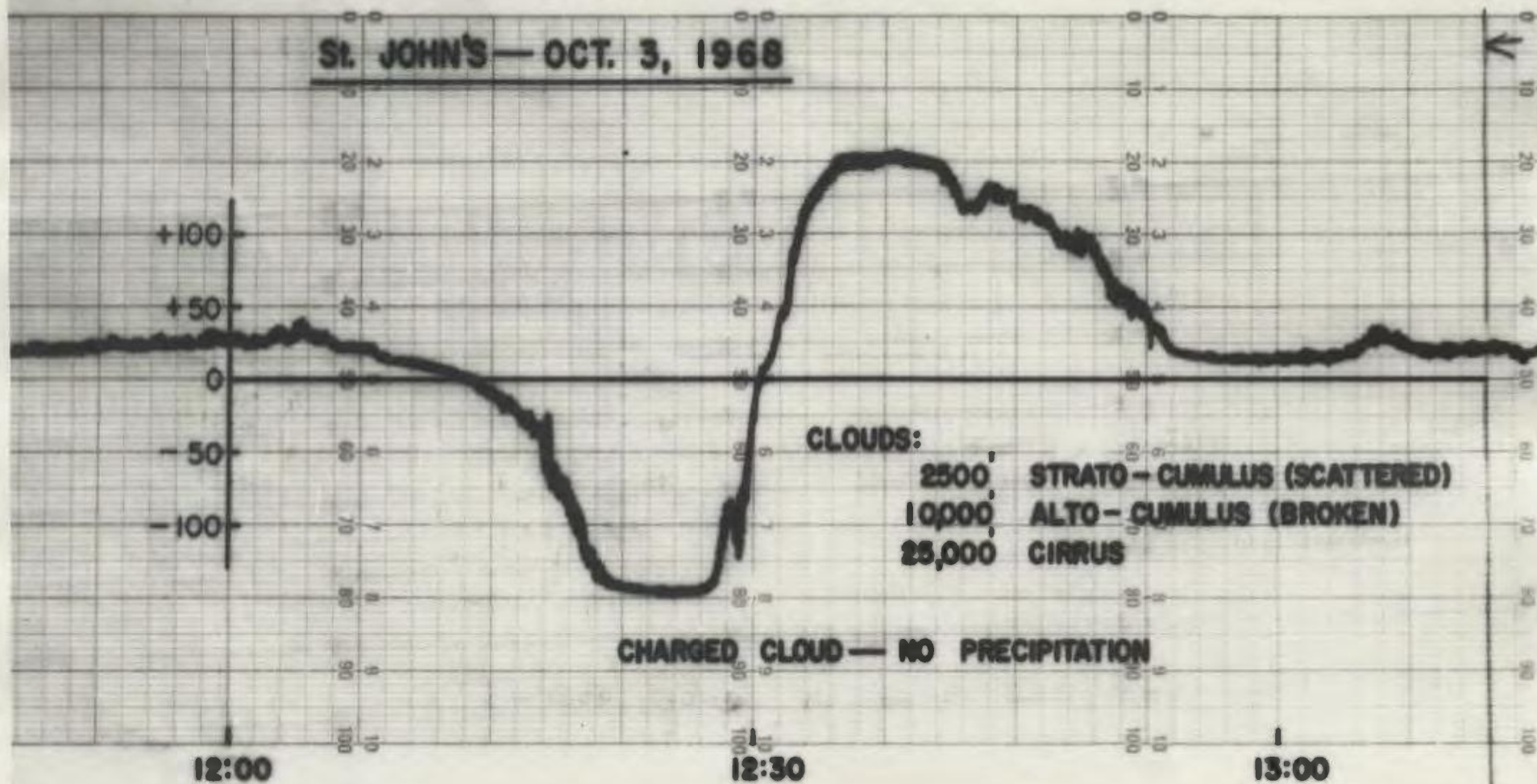


Fig. 30. Potential Gradient Due to Charged Cloud

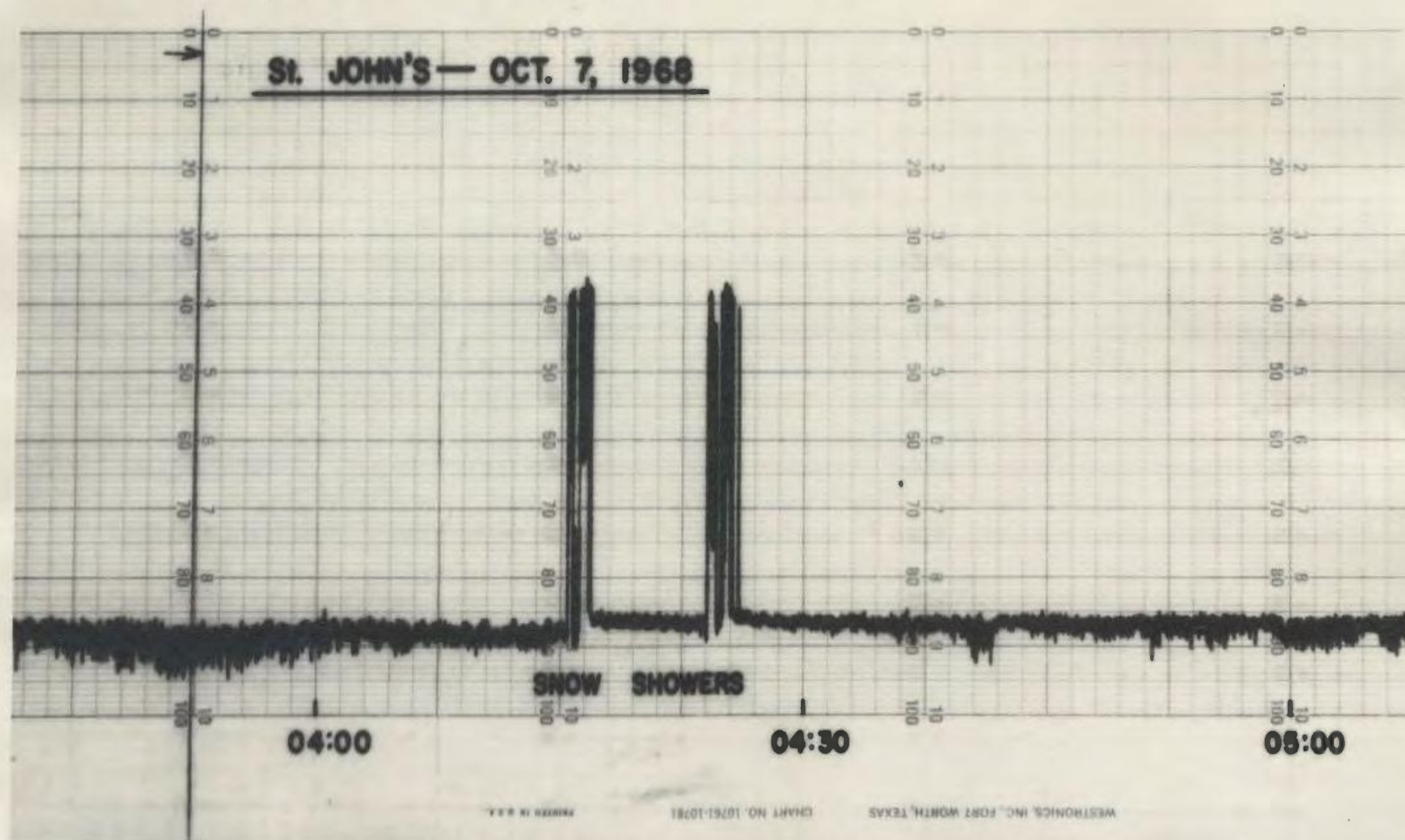


Fig. 31. Steep, Short Duration Positive Fields During Snow Showers

## 7.2 Discussion of Results

Fig. 30 shows the curve obtained when two banks of cumulus cloud were present over the station. The shape of the curve is assumed due to a bipolar cloud with a positive top and a negative base.

The potential at a point O distant D from cloud can be expressed by

$$(83) \quad V = \frac{2E}{4\pi\epsilon_0 (H^2 + D^2)^{3/2}} - \frac{2E}{4\pi\epsilon_0 (h^2 + D^2)^{3/2}}$$

where H = height of positive charge

h = height of negative charge.

Differentiating this equation, we get the potential gradient

$$(84) \quad \frac{dV}{dh} = \frac{-2EH}{4\pi\epsilon_0 (H^2 + D^2)^{3/2}} + \frac{2Eh}{4\pi\epsilon_0 (h^2 + D^2)^{3/2}}$$

The distance at which this changes sign is given by

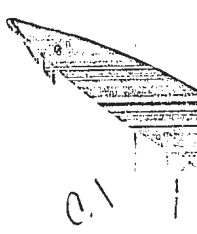
$$(85) \quad \frac{H}{(H^2 + D^2)^{3/2}} = \frac{h}{(h^2 + D^2)^{3/2}}$$

$$\therefore D^6 - 3h^2 H^2 D^2 - h^2 H^2 (h^2 + H^2) = 0$$

If h and H are nearly equal, the reversal distance is  $\sqrt{2H}$ .

If H = 2h, the value is about 1.2h.

Fig. 31 shows the field associated with the first snowfall of the season. The zero point had drifted here due to a faulty zeroing potentiometer which was later replaced by a smoother operating





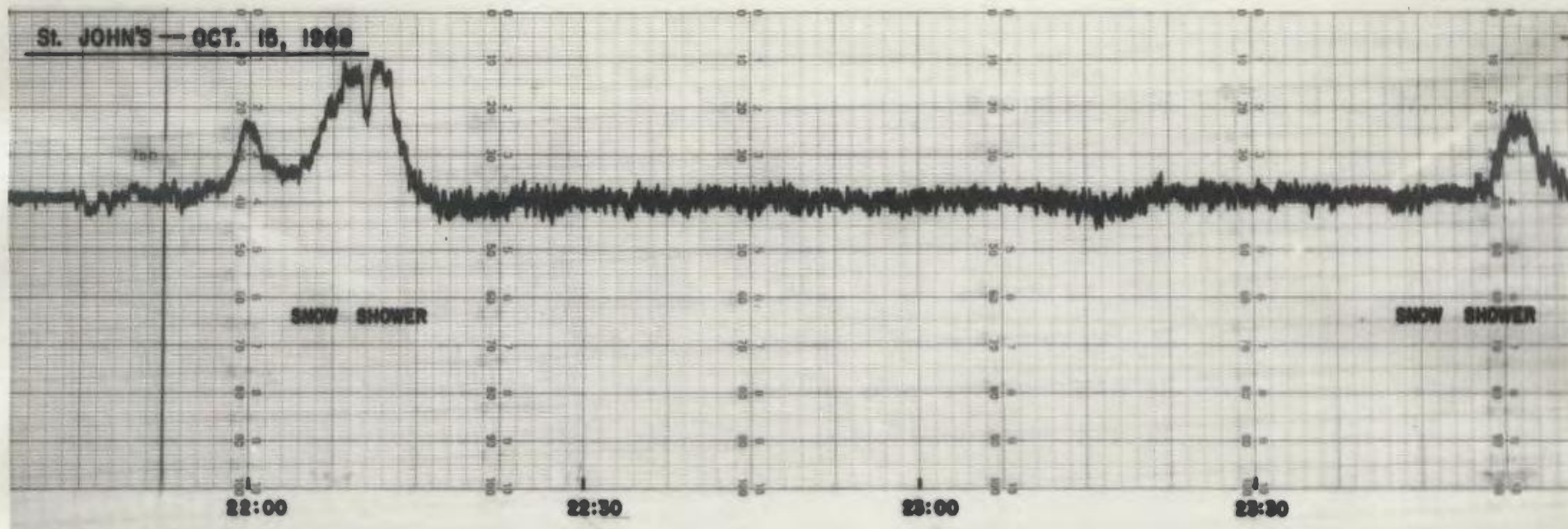


Fig. 32. Gradually Increasing Positive Fields During Snow Showers

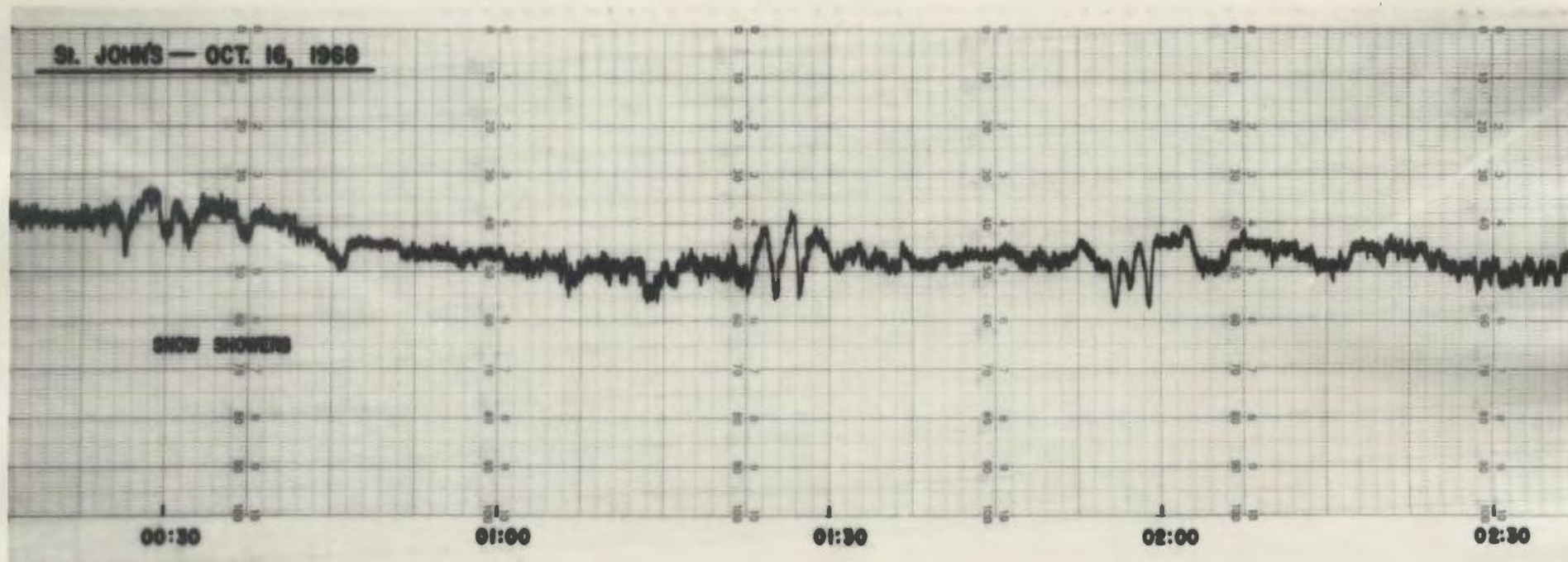


Fig. 33. Positive and Negative Fields During Snow Showers



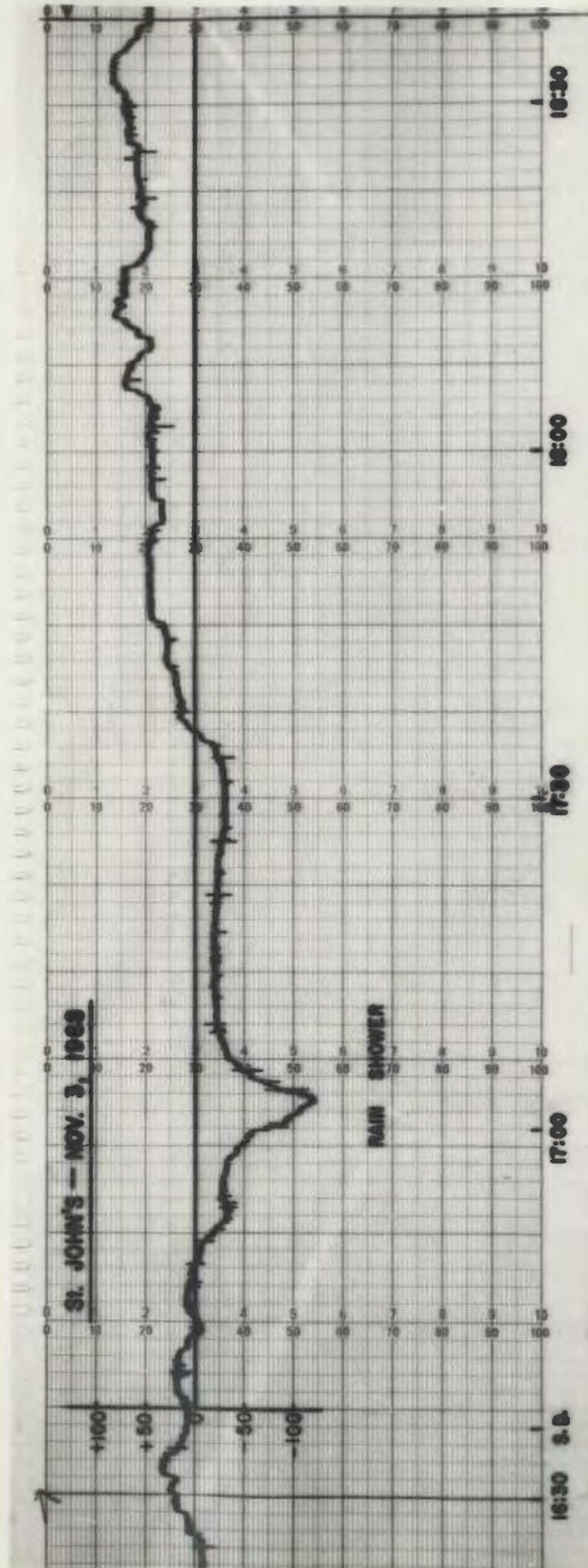


Fig. 34. Negative Field During Rain Showers

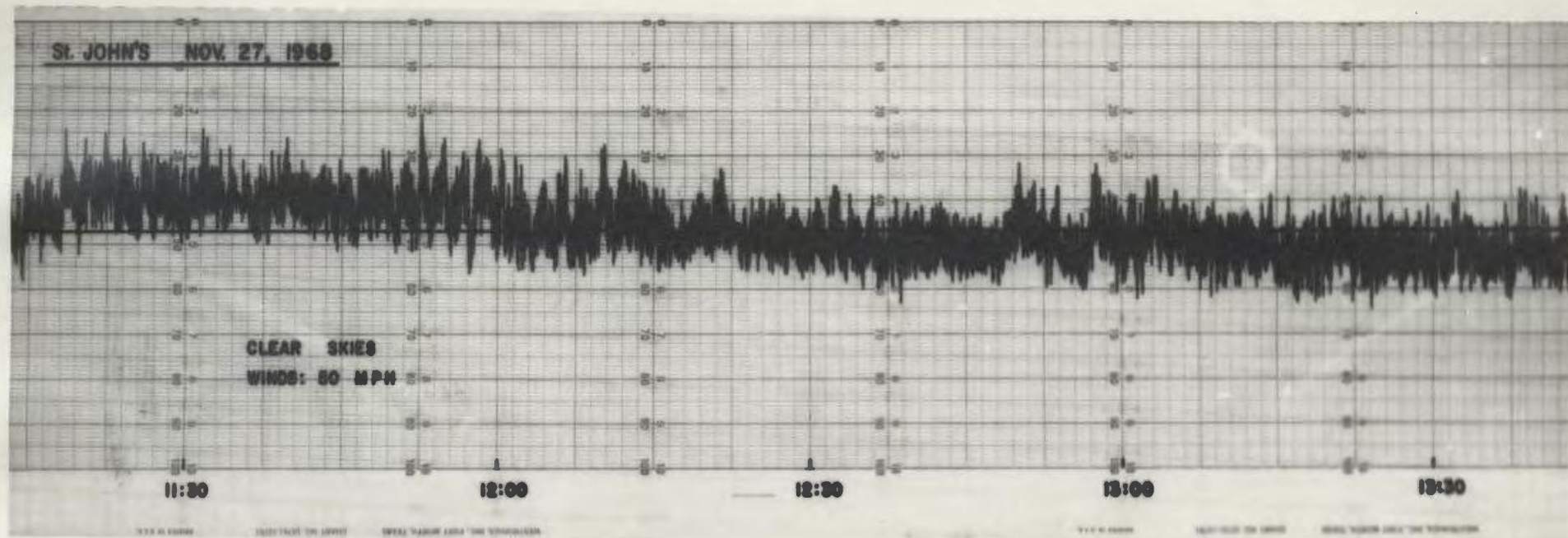


Fig. 35. Local Variations of Field During Period of High Wind Velocity

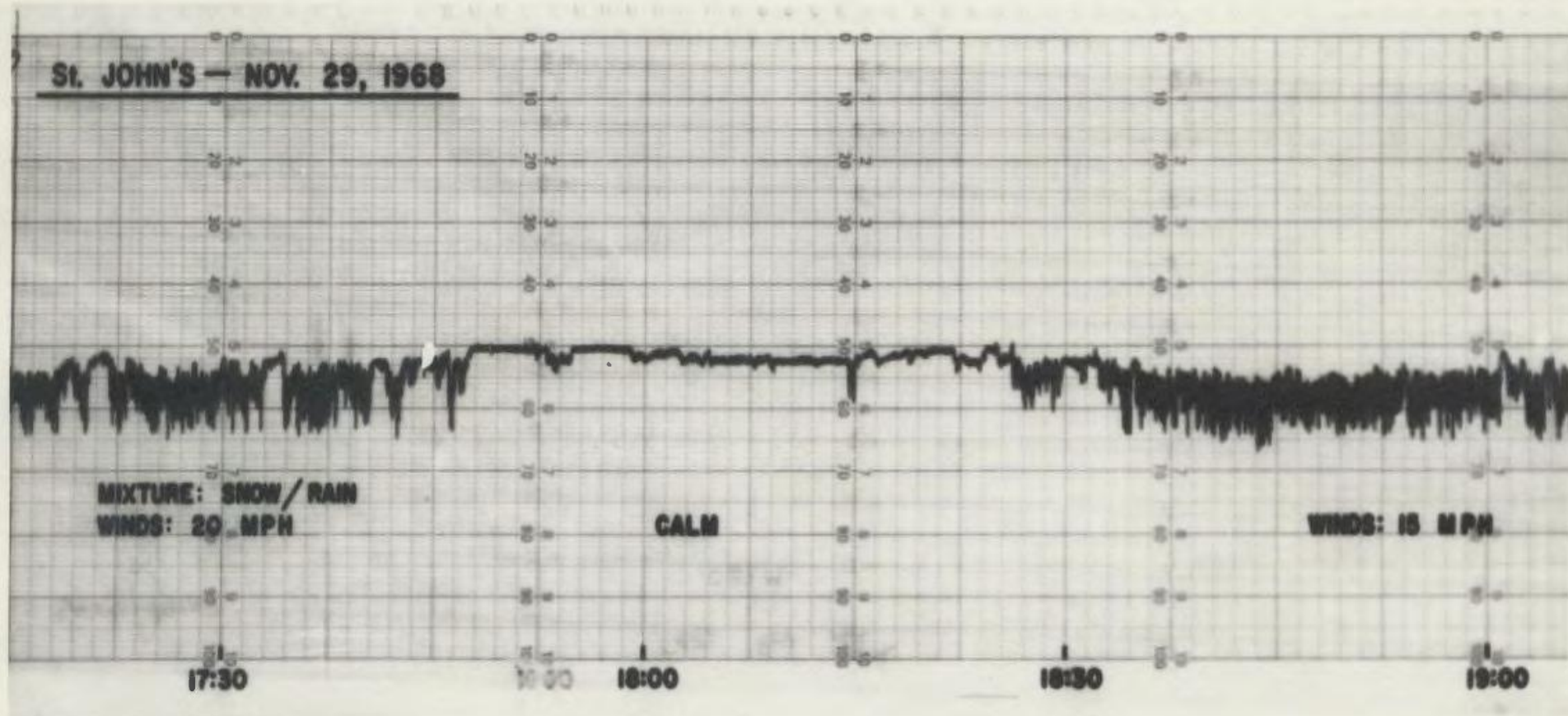


Fig. 36. Effect of Decreasing Wind Velocity on Electric Field



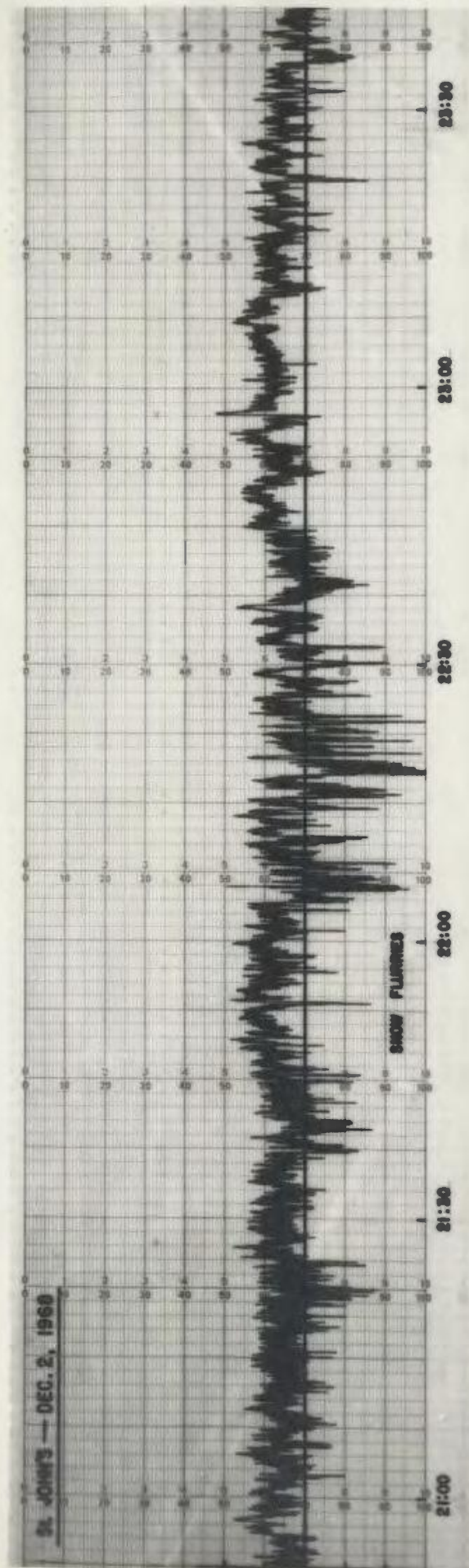



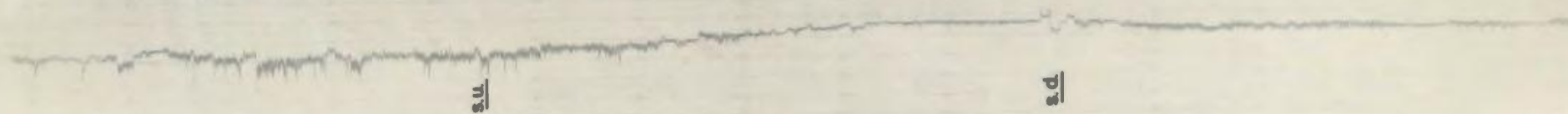
Fig. 37. Fluctuations During Snow Flurry Activity

potentiometer circuit. This was a short shower with dry snow and the sudden rise of the field as well as the sudden decrease is noticeable. The field also remained positive during the shower though there appears to have been some oscillations, though with no negative excursions.

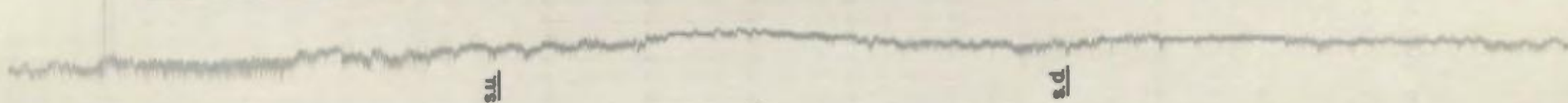
Fig. 32 shows the field during a snow shower of longer duration. The field in this case rose gradually and also remained positive for the duration of the shower. That the field associated with snow is not always positive is shown by the curve in Fig. 33 which shows negative excursions of the field. Large fluctuations occurred during snow flurry activity and a wind of about 20 miles per hour (Fig. 34). During rain, the field may be positive or negative also. In the curve of Fig. 35, there was a sustained negative field associated with the shower. Noticeable in this curve are positive and negative going spikes of short but equal lengths. Such spikes could be attributed to distant thunderstorms, but they are also reminiscent of the spikes that are associated with agitation due to fog. The effect of high winds on the electric field is evident from Fig. 36. As described in Chapter 4, this could be due to the convective currents in the atmosphere producing local anomalies. The decrease in fluctuations during a calm period is shown in Fig. 37. This would confirm the convective motion of the air particles producing the local anomalies shown. During the period of this recording, the cloud cover remained the same and the quietening down of the recording needle appears to have been due solely to the reduction of the wind velocity to zero.



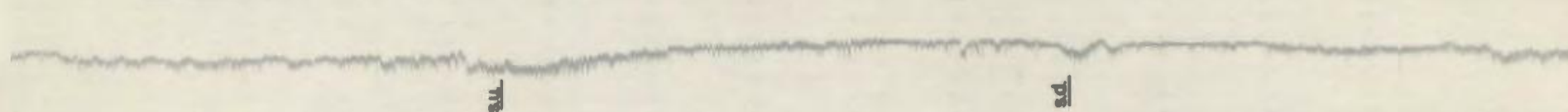
St. JOHN'S — DEC. 15, 1968



St. JOHN'S — DEC. 17, 1968



St. JOHN'S — DEC. 18, 1968



DEC. 19, 1968

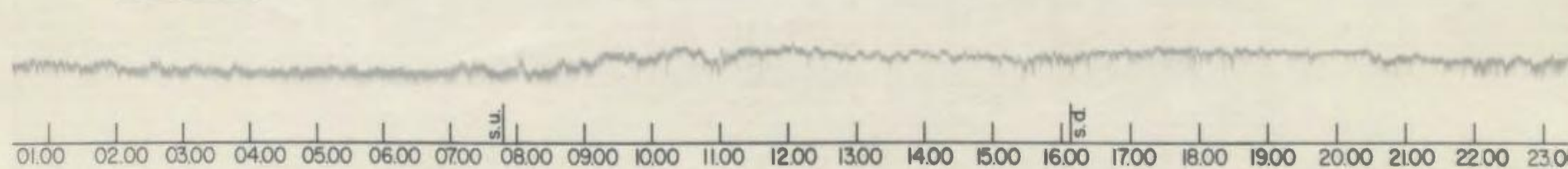


Fig. 38. Diurnal Variation of the Field


### 7.3 The Diurnal Variation

In order to carry out observations on the diurnal variation of the electric field, the speed of the graph paper was reduced to 2 in/hr.

The fair weather electric field over the whole earth (Fig. 1) shows a maximum and a minimum. The maximum occurs at about 18.00 hr and the minimum at about 04.00 G.M.T. There is also a small morning maximum at around 08.00 G.M.T. Over the oceans, the morning maximum is very small and the diurnal variation over the oceans may be considered as having one maximum around 19.00 and one minimum around 04.00 G.M.T.

According to Fig. 1, the N. American maximum occurs around 20.00 G.M.T. Gherzi reports the maximum at Montreal occurs around 14.00 G.M.T. During the same period of observation at Murchison Bay the maximum occurred at 19.00 G.M.T. Also, at Montreal, the minima were occurring at random, although there appeared to be a tendency to recur at night and also early in the morning.

Fig. 38 shows the daily variation of the field on four consecutive days. S.U. and S.D. denote sunrise and sunset times respectively. The graphs show a definite increase commencing about sunrise. The maxima, however, occur at different times, 19.00 and 15.00 respectively. Further observations are required in order to decide the actual times. These variations could be due to the local anomalies being superimposed on the fair weather field.



### DISCUSSION OF ERRORS

The main error involved the calibration of the field mill. The fluctuating field encountered during the calibration tests was by no means ideal and it was concluded that the only way to conduct calibration procedure was by means of variable artificial fields. However, during periods of calm and clear weather, calibration using the horizontal antenna and the quadrant electrometer was carried out. Errors inherent in the amplifiers or the phase sensitive detector are insignificant as long as the linear response of the circuits remains constant. Once a satisfactory calibration had been effected, all controls were locked and the only permitted variation was adjustment of the zero level for the residual field. Two other external sources of error are

- (1) air-earth current
- (2) the electrode effect.

The effect of the air-earth current was demonstrated by Mapleson and Whitlock (1955). The rotation of the rotor interrupts the flow of air-earth current, thus producing an alternating component of the same frequency as that due to the field. For a current density  $j$ , the alternating voltage across the resistor-capacitance circuit between stator and ground is given by

$$jAZ/2 \quad .$$

The signal voltage is given by

$$(66) \quad \epsilon_0 \omega EAZ/2 \quad .$$

0.1

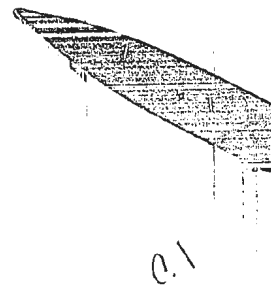


The former should be insignificant compared to the latter.

Thus  $j/\omega \ll \epsilon_0 E$ , in order that the effect of the air-earth current be insignificant compared to the effect of the electric field. The effect of the air-earth current is inversely proportional to the angular velocity of the rotor and for a value of  $10^{-10}$  amp. which is a maximum value for this current; the effect is less than that for a field of 1V/meter if the angular velocity of the rotor exceeds  $4\pi$ .

The electrode effect is mostly present for a few meters above the ground. Our field meter is located on top of the Physics/Chemistry Building at a height of 89.5 ft. above ground level. Thus, the electrode effect should not be affecting our readings.

Two other factors that may be affecting the readings, however, are the location of a substation at a distance of about 100 meters from the Physics/Chemistry Building, and the location of the outlets of the chemistry fume cupboards which were also located on the same roof. Chalmers and Little (1947) reported that, during fog and mist, negative air-earth currents were detected from measurements made at Aachen, Nurburg and Switzerland. Later, Wormell (1961) reported that these negative fields occurred downwind from power transmission lines. For accurate measurements, the "reduction factor" should also be taken into consideration. By means of this factor, it is possible to convert from the actual measurements of a collector to the absolute values that exist over level ground.



0.1


### SUGGESTED IMPROVEMENTS

The type of mill described here was designed for recordings of the potential gradient in S. Africa. The outside portion of the instrument contains an a.c. electric motor, a photoelectric device and a d.c. amplifying stage employing a transistor. These components exposed to the climate of Newfoundland are sure to deteriorate during long exposure periods. To improve matters, it was found necessary to protect the instrument by enclosing it in a wooden box. This had the effect of reducing the readings slightly and probably gave false readings during damp weather. Also, it was found necessary to include a small heater coil in the box.

To eliminate these disadvantages, this type of instrument should employ a radioactive probe completely protected from dampness and sufficiently storm proof to withstand the inclement weather. This device would be thus independent of the weather at the observing station.

To reduce the size and weight of the mill, the stator and rotor could be shaped in simple sector segments which would produce triangular waveform output. This type, called the S-type, by Mapleson and Whitlock, also yields a larger output current than do stator-rotor sectors designed to produce a sinusoidal variation. This type of mill would also operate with a smaller power motor.

The amplification of the amplifier is quite sufficient and the only improvement that is suggested here is that it could be



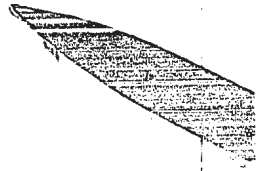
C.1

designed as a tuned circuit amplifier, thus cutting down even more on the noise level.

For further observations, the location of the measuring site should be taken into consideration. The present site suffers from the following disadvantages:

- (1) The metallic ventilation outlets are situated on the same roof as the meter.
- (2) Chemical fumes from the fume cupboards are also situated on the same roof.
- (3) The electrical transformers for the University supply are situated at a distance of only 300 ft. from the site of observations. This may produce negative space charge in the vicinity.
- (4) The room in which the recording instrument, final amplifier and phase sensitive detector is located is in close proximity to the electric fan systems for air ventilation of the building. This may cause spurious pick up by the amplifier and could be troublesome if picked up in the early stages of the amplifier.

An essential feature of potential gradient measurements is the provision of facilities for checking the calibration of the meter. In this case, the same method as used by Malan and Schonland was used. This did not prove satisfactory here due to the agitated nature of the atmospheric electric field. The only reliable source of calibration would be the construction of a variable artificial electric field.

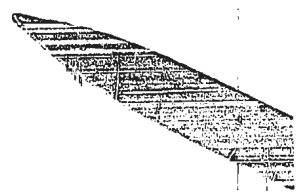


0.1

SUMMARY

The agitation of the electric field during fog, the diurnal variation, the sunrise effect and the relatively low atmospheric field have been demonstrated. Continuous recording of the electric field is now in progress and participation in a synoptic investigation of global, regional and local phenomena can be embarked upon. For a complete investigation, it is necessary that the other two basic elements - air-earth conduction current density and the two polar conductivities - be measured simultaneously. Access to meteorological data should also be available for correlation.

Further investigation could be devoted to variations of the sunrise effect, diurnal variation of the reduction factor and correlation to thunderstorm activity using radio receivers tuned to, say, 10 kc/s or 100 kc/s. The agitation of the electric field one or two hours before the onset and dispersal of fog has only recently been observed and the location of this station offers favourable conditions for this observation.



0.1

APPENDIX A

$$\text{SOLUTION OF THE EQUATION } K \frac{d^2 n}{dz^2} + q_1 e^{-\sqrt{\frac{1}{K}}(z-h)} + q_2 = \beta N n. \quad (1)$$


---

Boundary conditions for n are:

$$n = n_h \text{ for } z = h$$

$$n \text{ is finite at } z = \infty.$$

First of all, we find the special solution, i.e., the solution of

$$K \frac{d^2 n}{dz^2} = \beta N n$$

$$(2) \quad \text{i.e.} \quad \frac{d^2 n}{dz^2} = \frac{\beta N n}{K}.$$

The solution of this equation satisfying boundary conditions at  $z = 0$  is

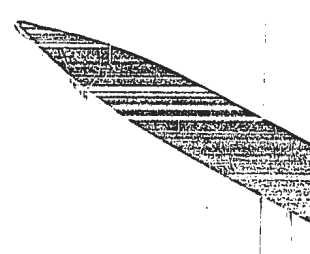
$$n_1 = e^{az} \quad \text{where} \quad a = -\sqrt{\frac{\beta N}{K}}.$$

Now set

$$n = e^{az} \cdot V$$

$$\frac{dn}{dz} = a e^{az} \cdot V + e^{az} \cdot \frac{dV}{dz}$$

$$\frac{d^2 n}{dz^2} = a^2 V e^{az} + 2a e^{az} \frac{dV}{dz} + e^{az} \frac{d^2 V}{dz^2}$$



c.1

Therefore, by substitution in equation (1), we get

$$Ka^2 Ve^{az} + 2a e^{az} \frac{dV}{dz} + e^{az} \frac{d^2V}{dz^2} + q_1 e^{-\sqrt{\frac{\tau}{K}}(z-h)} + q_2 = \beta NV e^{az}.$$

Since  $a^2 = \frac{\beta N}{K}$ , we get

$$\frac{d^2V}{dz^2} + 2a \frac{dV}{dz} = - \left\{ \frac{q_1}{K} e^{-\sqrt{\frac{\tau}{K}}(z-h)} + \frac{q_2}{K} \right\} e^{-az}.$$

Now let  $P = \frac{dV}{dz}$  and  $b = \frac{\tau}{K}$ . Then

$$\frac{dP}{dz} + 2aP = - \left\{ \frac{q_1}{K} e^{-b(z-h)} + \frac{q_2}{K} \right\} e^{-az}.$$

$$\begin{aligned} \therefore P = \frac{dV}{dz} &= e^{-\int 2adz} \left\{ - \int \left( \frac{q_1}{K} e^{-b(z-h)} + \frac{q_2}{K} \right) e^{-az} \cdot e^{\int 2adz} \cdot dz + C \right\} \\ &= e^{-2az} \left\{ - \int \left( \frac{q_1}{K} e^{-b(z-h)} + \frac{q_2}{K} \right) e^{az} dz + C \right\} \\ &= e^{-2az} \left\{ - \frac{q_1}{K} \int e^{(a-b)z+bh} dz - \frac{q_2}{K} \int e^{az} dz + C \right\} \\ &= e^{-2az} \left\{ - \frac{q_1}{K} \cdot \frac{1}{(a-b)} e^{(a-b)z+bh} - \frac{q_2}{Ka} e^{az} + C \right\} \\ &= - \frac{q_1}{K(a-b)} e^{-(a+b)z+bh} - \frac{q_2}{Ka} e^{-az} + C e^{-2az}. \end{aligned}$$

$$\begin{aligned} \therefore V &= - \frac{q_1}{K(a-b)} \int e^{-(a+b)z+bh} dz - \frac{q_2}{Ka} \int e^{-az} dz + C \int e^{-2az} dz \\ &= \frac{q_1}{K(a^2-b^2)} e^{-(a+b)z+bh} + \frac{q_2}{Ka^2} e^{-az} - \frac{C}{2a} e^{-2az} + C' \end{aligned}$$

$$= \frac{q_1}{\beta N - \tau} e^{-(a+b)z+bh} + \frac{q_2}{\beta N} e^{-az} - \frac{C}{2a} e^{-2az} + C' .$$

$$\therefore n = e^{az} \cdot V = \frac{q_1}{\beta N - \tau} e^{-b(z-h)} + \frac{q_2}{\beta N} - \frac{C}{2a} e^{-az} + C' e^{az} .$$

Since when  $z = \infty$ ,  $n$  is finite

$$\therefore C' = 0 .$$

$$\therefore n = \frac{q_1}{\beta N - \tau} e^{-b(z-a)} + \frac{q_2}{\beta N} - \frac{C}{2a} e^{-az} .$$

When  $z = h$ ,  $n = n_h$

$$\therefore n_h = \frac{q_1}{\beta N - \tau} + \frac{q_2}{\beta N} - \frac{C}{2a} e^{-ah} .$$

$$\therefore -\frac{C}{2a} = \left( n_h - \frac{q_1}{\beta N - \tau} - \frac{q_2}{\beta N} \right) e^{ah}$$

$$\begin{aligned} \therefore n &= \frac{q_1}{\beta N - \tau} e^{-b(z-a)} + \frac{q_2}{\beta N} + \left( n_h - \frac{q_1}{\beta N - \tau} - \frac{q_2}{\beta N} \right) e^{-a(z-h)} \\ &= \frac{q_1}{\beta N - \tau} e^{-\sqrt{\frac{\tau}{K}}(z-h)} + \frac{q_2}{\beta N} + \left( n_h - \frac{q_1}{\beta N - \tau} - \frac{q_2}{\beta N} \right) e^{-\sqrt{\frac{\beta N}{K}}(z-h)} . \end{aligned}$$

0.1

APPENDIX B

CALIBRATION OF THE POTENTIAL GRADIENT METER

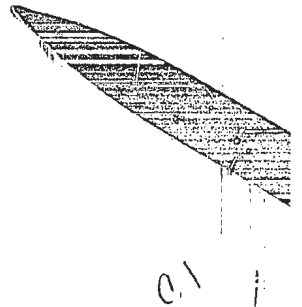
The requirements for an adequate calibration of the instrument are:

- (1) A measurable non-varying atmospheric electric field of sufficient duration to exceed the time constant of the antenna.
- (2) No zero drift of the needle for the duration of the calibration.

Both criteria are outside the control of the operator due to the vagaries of the atmospheric electric field and the ability of the instrument to pick up substantial electric static charges.

The method adopted for absolute calibration, namely an antenna in equilibrium with the potential at that location and an electrostatic electrometer to record the potential of the antenna, provided satisfactory calibration during periods of "quiet" electrical conditions. However, this method is not feasible during "disturbed" conditions.

The first requirement was to adjust the span range of the amplifier so that a division of one inch on the recording paper represented 100 volts. The sequence adopted in attaining this necessitated a long series of observations as follows:





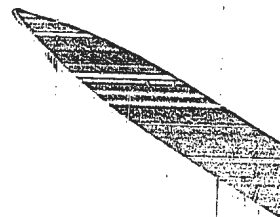
- (1) For a given change in the field value observed simultaneously on the quadrant electrometer and the mill, find the deflection of the recorder pen in inches per unit field change.
- (2) Ground output of mill to eliminate all static charges and adjust the zero level using the backing off voltage control.
- (3) Now adjust the gain to give a deflection of 1 inch for a field change of 100 volts per meter.
- (4) Repeat the procedure until the calibration is satisfactory.

This was satisfactorily accomplished during the "quiet" periods and the zero level also set to coincide with the central horizontal line on the graph paper, thus providing for equal excursions of positive and negative fields on either side of the centre line.

Fig. 30 obtained on October 3, 1968, was obtained soon after such a calibration had been performed. Between October 3 and October 7, the zero level drifted gradually while the field was in a continuous state of agitation. Fig. 31 shows the extent to which the zero level did drift. The range of the excursions which were positive, demonstrates the existence of an oscillating electric field extending to a value of about 250 volts for the duration of the showers.

A drift in the opposite direction is shown in Fig. 32. The range here shows a maximum positive excursion of 150 volts.

Ideal conditions for calibration were provided during the recording of the graph of Fig. 34. The recording of this graph was



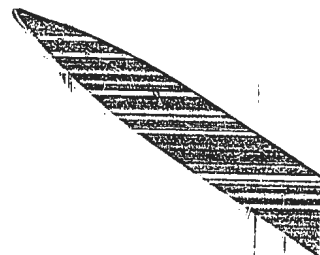
kept under observation and comparison maintained with the readings of the quadrant electrometer connected for heterostatic operation. There were long periods during which the needle of the quadrant electrometer remained constant and simultaneous readings of both instruments thus made possible. However, a positive zero shift is observed in this case also.

By this time, the linearity and the range of potential gradient of 50 volts per meter per one half inch division of graph paper had been satisfactorily established, and the zero shift had become the most troublesome factor.

In Fig. 35 and Fig. 37, the location of the actual zero line was located by shorting the output of the mill to ground, to eliminate all static charge, and then cover the mill with a grounded metal screen located about 5 cm above the collecting studs.

It has been suggested that further work using this mill be carried out using an artificial variable field. This method would ensure that calibration could be performed at any time, with a quick adjustment of the zero level and calibration of the meter as required.

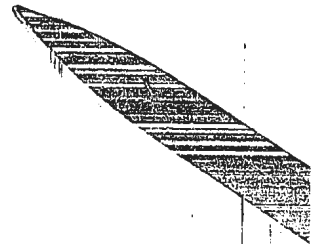
This would eliminate the reliance on the vagaries of the atmospheric electric field which is required to give a zero level and at least two definite distinct readings to set the calibration range span of the recording needle.



C.1

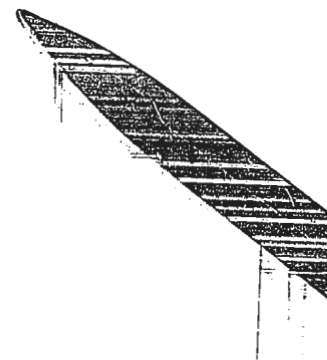
BIBLIOGRAPHY

- (1) Beccaria, G. B. 1775. Del electricitta terrestre atmosferica a cielo sereno turin.
- (2) Chalmers, J. A. 1954. Rep. Progr. Phys. 17, 101-134.
- (3) Chalmers, J. A. 1957. Atmospheric Electricity, Pergamon Press.
- (4) Clark, J. F. 1956. The fair weather atmospheric electric potential and its gradient Ph.D. thesis.
- (5) Coulomb, C. A. 1785. Mem. Acad. Sci. Paris, p. 616.
- (6) Dalibard, T. F. 1752. Mem. de l'acad. des Sci.
- (7) Dolezalek, H. 1963. Rev. Geophys. 1, 231-282.
- (8) Elster, J. and Geitel, H. 1899. Phy. Z. 1, 245-249.
- (9) Erman, P. 1804. J. Phys. 52, 95-105.
- (10) Franklin, B. 1750. Letter to Roy. Soc.
- (11) Gish, O. H. 1944. Terr. Mag. Atmos. Elect. 49, 159-168.
- (12) Gish, O. H. and Wait, G. R. 1950. J. Geophys. Res. 55, 473-484.
- (13) Gherzi, E. E. 1963. Bull. No. 13, College Brebeuf, Montreal.
- (14) Gherzi, E. E. 1967. Pure & Applied Geophys. 67, 239-259.
- (15) Groom, K. N. 1965. Jour. Atmos. Terr. Phys.
- (16) Hess, V. F. and Parkinson, W. D. 1954. Trans. Amer. Geophys. Un. 35, 869-871.
- (17) Hess, V. F. et al. 1953. Rep. No. 4, Fordham Univ.
- (18) Hoffman, K. 1923. Beitr. Phys. Frei. Atmos. 11, 1-19.
- (19) Hogg, A. R. 1950. Arch. Met. Wien. A3, 40-55.



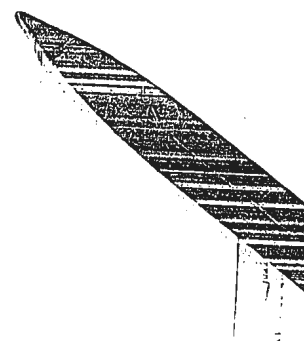
0.1

- (20) Israel, H. 1952. Astron. and Geophys. 3, 704-717.
- (21) Israel, H. 1953. Thunderstorm Electricity, 4-23.
- (22) Kawano, M. 1958. Recent Advances in Atmos. Electricity,  
Pergamon Press, 161-173.
- (23) Kelvin, Lord. 1860. Papers on Electrostatics & Magnetism,  
208-226.
- (24) Kraakevik, J. H. 1958. Recent Advances in Atmos. Electricity,  
Pergamon Press, 75-87.
- (25) Langevin, P. 1905. C. R. Acad. Sci. Paris, 140, 232-234.
- (26) Lemonnier, L. G. 1752. Observations sur l'electric de l'air.
- (27) Linss, F. 1887. Met. Z. 60, 340-351.
- (28) Malan, D. J. and Schonland, B. F. J. 1950. Proc. of the Phy.  
Soc. B. 63, 402-408.
- (29) Mapleson, W. W. and Whitlock, W. S. 1955. Jour. Atmos. Terr.  
Phys. 7, 61-72.
- (30) Mathias, A. 1926. Elektrizitatswirkschaft, 25, 297-308.
- (31) McClelland, J. A. and Kennedy, H. 1912. Proc. R. Irish Acad.  
A30, 72-91.
- (32) Muhleisen, R. 1956. J. Atmos. Terr. Phys. 8, 146-157.
- (33) Nolan, J. J. and Nolan, P. J. 1937. Proc. Roy. Irish Acad.  
A43, 79-93.
- (34) Nolan, J. J. and de Sachy, G. P. 1927. Proc. Roy. Irish Acad.  
A37, 71-94.
- (35) Peltier, A. 1842. Ann. Chim. Phys. 4, 389.

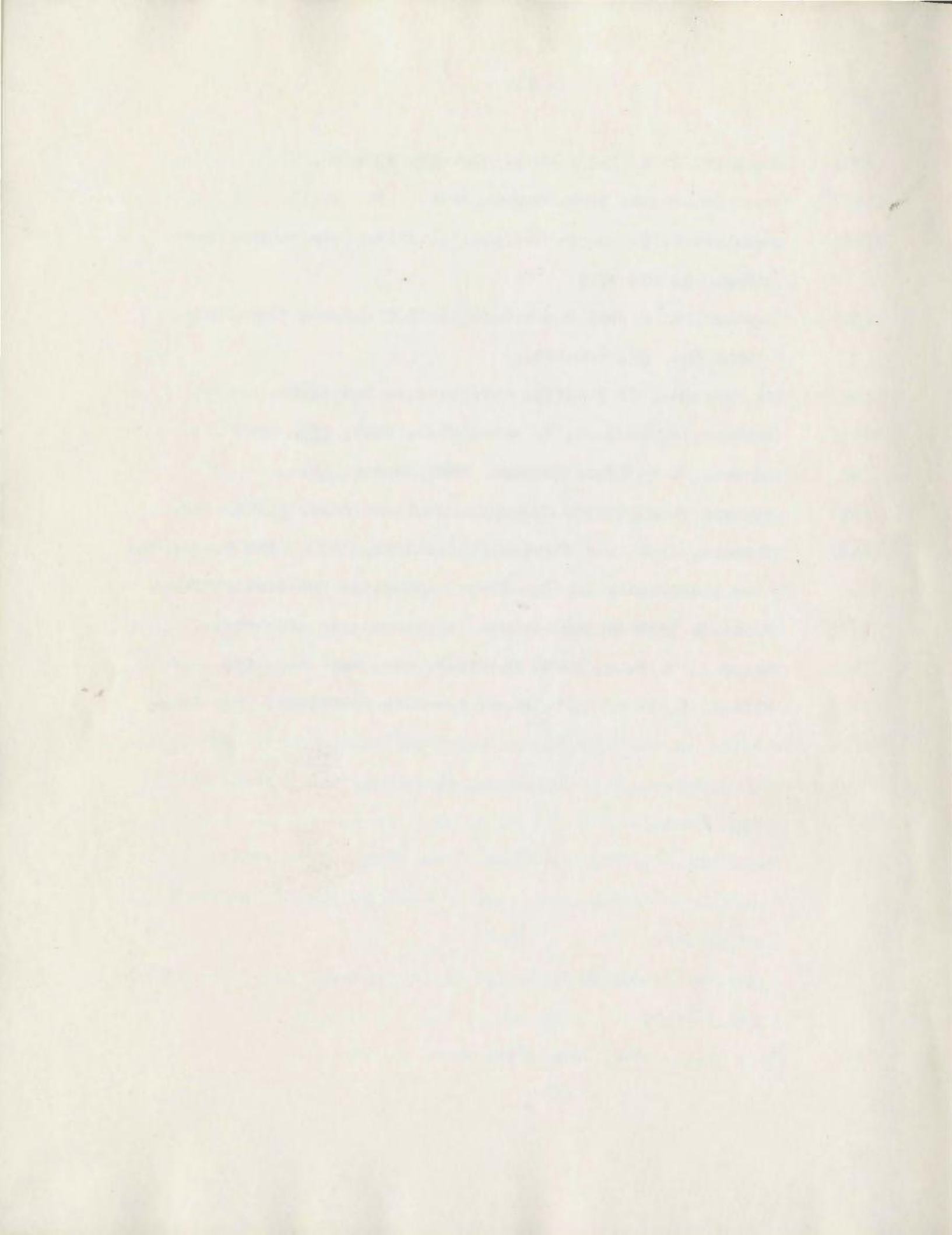


C.1  
1

- (36) Pollock, J. A. 1915. Phil. Mag. 29, 636-646.
- (37) Russelveldt, N. 1925. Norweg. Met. Inst. 11-15.
- (38) Sagalyn, R. C. and Faucher, G. A. 1954. Jour. Atmos. Terr. Phys. 5, 253-272.
- (39) Sagalyn, R. C. and Faucher, G. A. 1957. Quart. Jour. Roy. Met. Soc. 82, 428-445.
- (40) de Saussure, H. B. 1779. Voyages dans les Alpes.
- (41) Scholtz, J. 1931. S. B. Akad. Wiss. Wien, 140, 49-66.
- (42) Scrase, F. J. 1935. Geophys. Mem. London, 67.
- (43) Stergis et al. 1955. Jour. Atmos. Terr. Phys. 6, 233-242.
- (44) Thomson, J. J. and Thomson, G. P. 1928, 1933. The Conduction of Electricity through Gases, Cambridge University Press.
- (45) Volta, A. c1800. Lettres sur la meterologic electrique.
- (46) Whipple, F. W. J. 1929. Quart. J. Roy. Met. Soc. 55, 1-17.
- (47) Wilson, C. T. R. 1929. Jour. Franklin Institute, 208, 1-12.



0.1 /





MADE IN CANADA  
FRODO BAGGINS

FRODO BAGGINS  
MADE IN CANADA



